AN ABSTRACT OF THE DISSERTATION OF

Jed O. Eberly for the degree of Doctor of Philosophy in Biological and Ecological Engineering presented on October 21, 2010

Title: Analysis of the Thermophilic Cyanobacterium *Thermosynechococcus elongatus* as a Model Organism for Carbon Sequestration, Biofuel, and Biomaterial Production.

Abstract approved:

_____

Roger L. Ely

The thermophilic cyanobacterium *Thermosynechococcus elongatus* was examined for the ability to sequester CO_2 while producing hydrogen (H_2), polyhydroxybutyrate (PHB), lipids, and glycogen. H_2 was produced at a maximum rate of 188 nmol H_2 mg Chl a^{-1} hr^{-1}. Hydrogen production occurred in the presence of methyl viologen but the cells were not able to catalyze deuterium (D_2) exchange. Screening assay studies showed that the inhibitors DCMU, DBMIB, PCP, and malonate did not effect H_2 production while H_2 production was completely inhibited when KCN was present. The physiological response and genome analysis of *T. elongatus* indicates that the enzyme responsible for H_2 production may differ from the Fe-only or [NiFe] bidirectional H_2ase enzymes commonly found in green algae and in other species of cyanobacteria. *T. elongatus* was also analyzed for the ability to grow on 5-150 mM dissolved inorganic carbon (DIC) and 0-30% CO_2.

The effect of DIC and CO_2 concentrations on PHB, lipids, and glycogen was also measured. Glycogen and PHB were the primary carbon reserves depending on carbon availability. The highest glycogen concentration was 24.12% (w/w) with 150 mM DIC while the greatest PHB concentration was 14.5% (w/w) in cultures grown with 0% supplemental CO_2. Lipid content did not vary significantly with carbon concentrations and averaged around 15-20% (w/w) for all culture conditions. Cultures grown on CO_2 showed no difference in glycogen content over the range of CO_2 concentrations tested. Bioreactor experiments showed that *T. elongatus* was able to grow on up to 20% CO_2 while sequestering a maximum of 1.15 g L^{-1} over the 9 day experiment. The maximum productivity and CO_2 fixation rates were 0.09±0.01 mg d^{-1} and 0.17±0.01 mg ml^{-1} d^{-1}, respectively, for cultures grown on 20% CO_2.

Analysis of the Thermophilic Cyanobacterium *Thermosynechococcus elongatus* as a Model Organism for Carbon Sequestration, Biofuel, and Biomaterial Production.

by

Jed O. Eberly

A DISSERTATION

submitted to

Oregon State University

in partial fulfillment of

the requirements for the

degree of

Doctor of Philosophy

Presented October 21, 2010

Commencement June 2011

Doctor of Philosophy dissertation of Jed O. Eberly presented on October 21, 2010

APPROVED:

Major Professor, representing Biological and Ecological Engineering

---

Head of the Department of Biological and Ecological Engineering

---

Dean of the Graduate School

I understand that my dissertation will become part of the permanent collection of Oregon State University libraries. My signature below authorizes release of my dissertation to any reader upon request.

Jed O. Eberly, Author

ACKNOWLEDGEMENTS

I would like to express my appreciation to everyone who has supported and contributed to my graduate school experience. First of all, I would like to thank my advisor, Dr. Roger Ely for all of his support and assistance over the years. I would like to especially thank him for providing an environment that was intellectually stimulating and for challenging me in many ways to improve my skills and expand my knowledge. I would also like to thank my committee members, Dr. Frank Chaplen, Dr. Hong Liu, Dr. Mark E. Dolan, Dr. Bruce Geller, and Dr. Xiaoli Fern for their time and interest in my project.

I would also like to thank my many friends and colleagues in the Earth's Subsurface IGERT program. It was a great experience being able to interact with students and faculty is so many different fields. In particular I would like to thank Julie Cope for her many hours of tireless work in support of all the IGERT students. Her help was invaluable with planning seminars, scheduling speakers, arranging trips to Portland, and many other countless details. Thanks also to Rick Colwell for all of his help on our Group Process Training project and for making it an enjoyable experience.

I would also like to thank the Department of Biological and Ecological Engineering staff. Elena Maus and Susan Atkisson were always so helpful with ordering supplies and taking care of countless small details.

A big thank you to all of my fellow Ely lab grad students, Dr. Paul Schrader, Dr. SunHwa Park, Dr Liz Burrows, Dave Dickson, and Mark Luterra for your friendship, support, and encouragement over the years. A special thank you to Dr. Hatem Mohamed for all of his advice, help, and encouragement. I especially appreciate all the time he spent answering my questions and discussing ideas and also his brilliant insight into some of the problems and challenges I experienced in my project. I would also like to thank my undergraduate assistant Rebecca Miller for all of her hard work in the setup, operation, and maintenance of the bioreactors as well as her assistance on many other experiments. In addition, I would also like to thank the many high school and undergraduate students who helped out with a wide assortment of tasks.

I would also like to thank my family and all of my friends who have supported me over the years. In particular, I would like to thank my friends at Northwest Hills Community Church, Grad & Career group for their friendship, support, and encouragement. And finally and most importantly, I would like to thank Jesus Christ who has given me strength, hope, joy, and a sense of purpose in life.

CONTRIBUTION OF AUTHORS

In addition to the help of my advisor, Roger Ely, on all chapters, Dr. Hatem Mohamed provided help with designing the inhibitor experiments in Chapter 1 and was very helpful in analyzing the data.

TABLE OF CONTENTS

Page

CHAPTER 1: GENERAL INTRODUCTION....1
Introduction....1
Carbon Sequestration by Cyanobacteria....4
Regulation of carbon uptake....6
Chlorophyll fluorescence induction....8
Biofuel production from cyanobacteria....10
Biomaterials from cyanobacteria....18
Characteristics of Thermophiles....21
Thermosynechococcus elongatus as a platform for CO_2 sequestration, biofuels, and bioproducts production....24
Dissertation overview....26

CHAPTER 2: HYDROGEN PRODUCTION BY THE THERMOPHILIC CYANOBACTERIUM, *THERMOSYNECHOCOCCUS ELONGATUS*....28
Abstract....29
Introduction....29
Materials and Methods....31
Culturing conditions....31
GC vial tests and methyl viologen assay....32
Deuterium exchange and H_2 uptake assay....33
Effects of Inhibitors....34
Results....35
GC vial tests and methyl viologen assay....35
Deuterium exchange and H_2 uptake assay....37
Effects of Inhibitors....39
Discussion....41
Conclusion....46
Acknowledgements....48

CHAPTER 3: EFFECT OF DISSOLVED INORGANIC CARBON LEVELS ON GROWTH, FLUORESCENCE YIELDS, AND CARBON ACCUMULATION IN *THERMOSYNECOCCUS ELONGATUS*....49
Abstract....50
Introduction....51
Materials and Methods....55
Culturing conditions....55
Growth and biomass analysis....56
Results....58
Discussion....66
Conclusion....73

TABLE OF CONTENTS (Continued)

Page

Acknowledgements 74

CHAPTER 4: PHOTOSYNTHETIC ACCUMULATION OF CARBON STORAGE COMPOUNDS UNDER CO_2 ENRICHMENT BY THE THERMOPHILIC CYANOBACTERIUM *THERMOSYNECOCCUS ELONGATUS* 75
Introduction 76
Materials and Methods 80
Culturing conditions 80
Bioreactor Experiments 80
Biomass analysis 81
Carbon storage compounds 81
Results 83
Growth and biomass analysis 83
Carbon storage compounds 88
Discussion 90
Acknowledgements 96

CHAPTER 5: GENERAL CONCLUSION 97
Findings of the research 97
Impact of the research 98
Engineering implications 99
Future direction 100

BIBLIOGRAPHY 113

APPENDIX 114
Appendix A 115
Calculations 115
Headspace and aqueous CO_2 concentrations 115
Carbonate equilibrium calculations 116
Carbon assimilation rates 118
Modeling productivity 118
Photosynthetic efficiency 119
Bioreactor mass balance 120

LIST OF FIGURES

Figure Page

1.1. Process flow diagram of microbially mediated CO_2 sequestration and fuels and biomaterials production. 3

2.1. H_2 production from late log phase cells incubated in the dark.. 36

2.2. Headspace H_2 concentration 37

2.3. H_2 uptake assay 39

2.4. Effect of inhibitors on H_2 production in full light from *T. elongatus* 40

2.5. Schematic representation of photosynthetic/respiratory complexes. 43

3.1. Growth curves of *T. elongatus* on increasing levels of DIC 59

3.2. Monod model simulation 61

3.3. Chlorophyll content as a function of DIC concentration. 62

3.5. Variation in PHB content with increasing levels of DIC. 64

3.6. Maximum quantum efficiency of PSII 65

3.7. Photochemical and non-photochemical quenching of fluorescence in dark acclimated cultures 66

4.1. Growth curves of *T. elongatus* with gas bubbling with increasing CO_2 concentrations. 84

4.2. Monod model of maximum biomass accumulation with increasing

4.3. Glycogen, lipid, and PHB content in *T. elongatus* grown over a range of 0-20% CO_2. 89

4.4. Percent of total biomass carbon in lipids, PHB's, and glycogen 90

LIST OF TABLES

Table Page

4.1. Specific growth rates, productivity, CO_2 fixation rates, and percent CO_2 utilization of *T. elongatus* under increasing carbon concentrations. 84

A.1. Comparison of aqueous CO_2 concentrations at 30°C and 50°C at given headspace CO_2 concentrations. 116

A.2. Comparison of mass balance calculations based on total carbon analysis with calculations based on CO_2 fixation rates and carbonate equilibrium.. 122

A.3. Difference in CO_2 outlet concentrations based on GC measurements and calculated concentrations. 122

Analysis of the thermophilic cyanobacterium *Thermosynechococcus elongatus* as a model organism for carbon sequestration, biofuel, and biomaterial production.

CHAPTER 1: GENERAL INTRODUCTION

Introduction

Energy availability is one of the most pressing challenges facing the world today. While other problems such as clean water supply, food shortages, and disease are equally important, they all require energy to develop and implement any type of solution. Energy also figures prominently in the geopolitical situation today. As developing nations continue to grow and improve their standard of living, their demand for energy increases dramatically. In addition, the world's remaining petroleum reserves are located predominately in regions that are characterized by political and social instability, which makes the availability of these energy reserves tenuous at best. The dwindling energy supplies coupled with the commensurate increase in fuel costs have caused an increased awareness of the need to develop alternative sources of fuel. In addition to fuel, our society and economy are very dependent on many other products, such as plastics and fertilizer, which are also derived from or dependent on petroleum.

The pursuit of a renewable source of fuel and other materials has taken many directions. While abiotic processes such as solar, wind, geothermal, wave, and nuclear offer many benefits, they are generally limited to producing

electricity rather than liquid or gaseous energy storage forms and they do not provide a solution for production of other materials that are currently derived from petroleum.

In contrast, biological systems offer the potential of producing liquid or gaseous fuels, and biomass has the potential to function as a feedstock for many products that are currently derived from petroleum. Biologically based fuel sources are ideal because they are renewable and have the potential to achieve high efficiencies and are generally well distributed geographically. Any biological energy system must ultimately be solar based, either through direct solar energy-to-fuel conversion or by indirect means that rely on accumulated biomass. Currently much effort is focused on hydrogen (H_2), ethanol, and lipid production. Additional work has focused on biomass production, which can then be used in fermentative processes or abiotic processes, such as gasification and pyrolysis, for generating fuel [55]. In addition to fuels, many other commonly used materials are based on petroleum. Plastics, fertilizers, asphalt, cosmetics, and dyes are just a few of the many products that rely on petroleum. Interest in finding renewable feedstocks for many of these products is rising for many of the same reasons that are motivating the pursuit of renewable fuels. Ultimately a bio-based system that incorporates CO_2 sequestration with production of fuels and other bioproducts will provide the most comprehensive solution. A proposed process flow schematic that incorporates many of these features is shown in Figure 1.1.

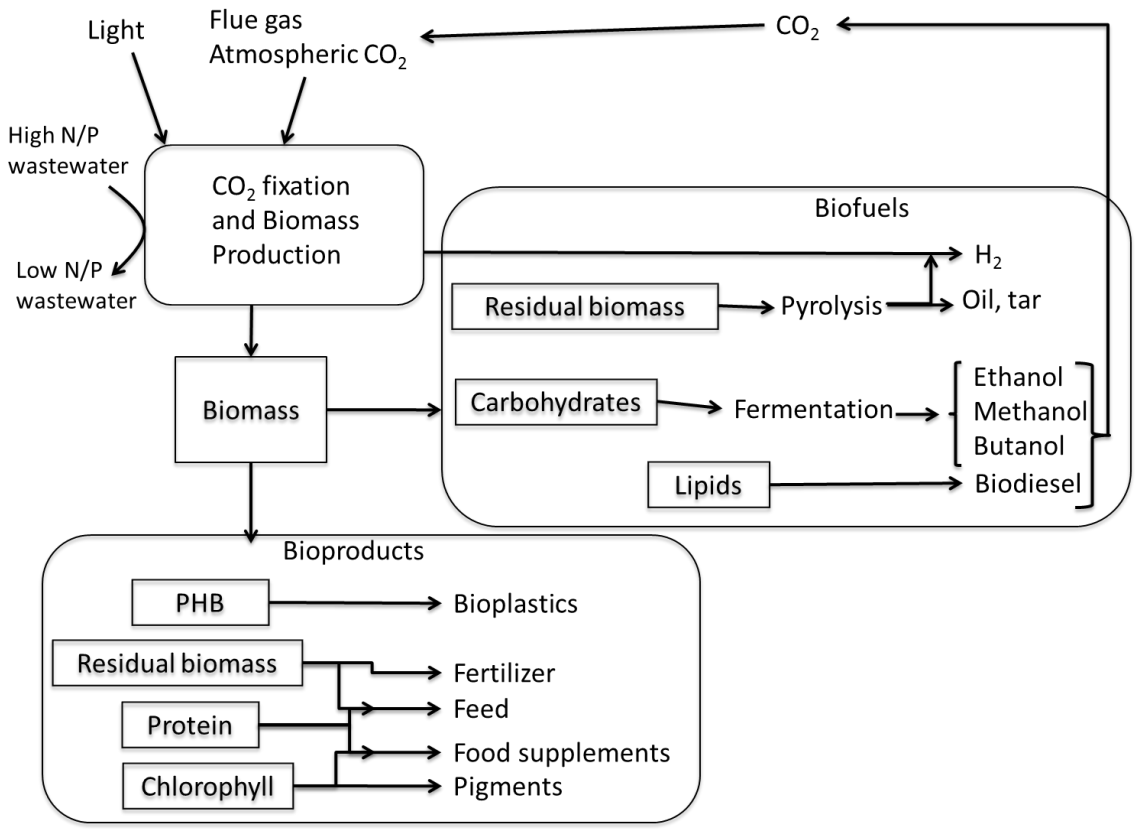

Figure 1.1. Process flow diagram of microbially mediated CO_2 sequestration and fuels and biomaterials production.

Microbially based systems are the most promising approach to bio-based fuels and materials. Biomass production per unit area from microorganisms has the potential to be much higher than from plants because of rapid growth rates. The ease of genetically manipulating microorganisms is an additional advantage as it allows enzymatic pathways to be modified in order to produce specific products and to improve productivity. Cyanobacteria in particular are well suited to the production of fuel and materials because of their ability to convert solar energy to biomass directly.

Carbon Sequestration by Cyanobacteria

Cyanobacteria are photosynthetic prokaryotes belonging to the kingdom Monera, division Cyanophyta. Cyanobacteria have very diverse morphology that includes unicellular, filamentous, branched filamentous, and heterocystis [138]. Cyanobacteria are photosynthetic bacteria containing photosystems I and II (PSI and PSII) and the associated antennae that enable them to harvest light in a manner similar to plants. They are capable of fixing carbon through the reductive pentose phosphate pathway (Calvin Cycle) and some species are also capable of fixing N_2.

Cyanobacteria are ubiquitous throughout nature and are found in aquatic environments from lakes and streams to hot springs, marine environments, and in terrestrial environs from arctic to deserts [19]. Cyanobacteria are also responsible for producing nearly 30% of the earth's O_2 and play an important role in global carbon and nitrogen cycling [65]. Cyanobacteria represent one of the most promising sources of renewable, bio-based fuels and other bioproducts.

Biological CO_2 mitigation strategies have attracted much attention in recent years as a way to sequester anthropogenic CO_2. While chemical mitigation strategies, such as cyclic carbonation/de-carbonation reactions and washing in aqueous amine solutions are well developed [152], bio-based systems have the potential to operate much more efficiently and economically. Biological CO_2 mitigation has the additional advantage of producing biomass, which can then be used to generate fuels or other valuable bioproducts. The potential for increased

CO_2 capture by relatively slow growing terrestrial plants is only about 3-6% of fossil fuel emissions [139] with a photosynthetic efficiency of only around 0.5% [76]. In contrast, cyanobacteria can achieve a photosynthetic efficiency of 10-20% [76] and are able to tolerate high CO_2 concentrations [64]. Cyanobacteria are also effective at nitrogen and phosphorous removal [85] and aid in metal ion depletion [152], benefits not necessarily provided by chemical CO_2 sequestration strategies. While extensive work has focused on establishing CO_2 uptake rates of cyanobacteria in bioreactors [39, 62, 68], very little research has focused on establishing global carbon sequestration rates [61].

The ability of cyanobacteria to grow under high levels of CO_2 has stimulated interest as a means of sequestering CO_2 from industrial flue gas. The higher CO_2 concentrations found in flue gas could contribute to improved growth rates since growth is often carbon limited under standard atmospheric conditions where the CO_2 concentration is only 0.03-0.06% [152]. Increasing CO_2 levels above 5% contributes to greater photosynthetic activity and correspondingly higher growth rates. Some species, such as *Synechococcus* PCC 7942, are capable of growing at CO_2 concentrations as high as 30% [64]. Industrial CO_2 sequestration can be coupled with the production of feedstocks for biofuels or other bioproducts thus providing additional benefits from the sequestered carbon.

Cyanobacteria sequester inorganic carbon through an inorganic carbon concentrating mechanism (CCM), which enables them to maintain localized high

carbon concentrations in carboxysomes. The CCM enables cells to maintain an internal carbon concentration that is 1000-fold greater than external concentrations [68]. This high inorganic carbon gradient is necessary for ribulose 1,5-bisphosphate carboxylase/oxygenase (RubisCO), the primary enzyme in carbon fixation, to function. The CCM relies on several energy dependent transport systems. Direct uptake of CO_2 is facilitated by a NDH-1 complex [120] while bicarbonate (HCO_3^-) uptake is mediated by an extracellular carboanhydrase that converts carbonate to CO_2, which is then assimilated into the cell [58], or by direct transfer of carbonate through an active transport system [89]. While at least some species of cyanobacteria are capable of taking up both CO_2 and HCO_3^-, the rate of CO_2 transport is significantly higher [96]. Regardless of the form of carbon that is transported, HCO_3^- is the predominant species in the cytoplasm. HCO_3^- is then transported to the carboxysome where carbonic anhydrase converts it to CO_2 [68]. RubisCO, located in the carboxysome, catalyzes the reaction between ribulose 1,5-bisphosphate and CO_2, which is the first step in carbon fixation.

Regulation of carbon uptake

The regulation of inorganic carbon uptake is very complex and relies in part on the concentration of carbon. Studies have shown that some species, such as *Synechocystis* sp. PCC 6803, have two mechanisms of CO_2 uptake; a constitutive system and one that is activated under low CO_2 conditions [135]. The inducible

CO_2 mechanism has greater affinity for CO_2 and much higher transport rates but both systems involve NDH-1 complexes [96]. Carbonic anhydrase and CCM activity are also regulated by a photosynthesis-dependent step. Although not completely understood, light intensity and photorespiratory carbon metabolism both play a role in the induction of the photosynthesis dependent carbon uptake step [96]. In addition to activating CO_2 transport systems, a decrease in the level of CO_2 can induce gene expression leading to an increase in the number of carboxysomes, thus increasing the level of CO_2 uptake [68].

A significant amount of research [7, 68, 96] has focused on understanding the tolerance of cyanobacteria to high concentrations of CO_2. While microorganisms are naturally adapted to the relatively low atmospheric concentrations of CO_2 (0.036%), some have the ability to grow quite readily on concentrations as high as 40% while others are very intolerant of such conditions [156]. The sensitivity to high CO_2 concentrations is due in part to the internal pH value. RubisCO and the Calvin cycle are both rapidly inactivated by low pH and several studies have shown that growth inhibition at high CO_2 levels is associated with cytoplasmic acidification [96].

Cyanobacteria also have the ability to adapt to transitions from low to high CO_2 or from high to low CO_2. A number of significant changes have been identified following the transition from high to low CO_2. The amount of RubisCO and number of carboxysomes increases, purine biosynthesis increases, and the cells have an increased ability to accumulate inorganic carbon coupled with a

higher photosynthetic affinity for carbon [68]. In spite of the progress that has been made in understanding the adaptation process, the signal responsible for the response to CO_2 levels remains unknown. Several candidates have been proposed, including the total inorganic carbon concentration, ratio of CO_2/O_2, and the aqueous CO_2 concentration [67]. The availability of inorganic carbon also affects the photosynthetic electron transport system. Changes in chlorophyll fluorescence caused by shifts in the photosynthetic electron flow have provided insight into the cellular response to inorganic carbon levels.

Chlorophyll fluorescence induction

Chlorophyll fluorescence has become a valuable tool for noninvasive and rapid measurement of photosynthetic light harvesting and electron transfer. Chlorophyll fluorescence was first described by Kautsky et al. [69] when they observed that the transfer of photosynthetic material from the dark to light caused chlorophyll fluorescence to increase rapidly for about 1 s. Research since then has provided insight into the mechanism that causes the fluorescence increase and this has formed the basis for chlorophyll fluorescence theory.

Light energy absorbed by chlorophyll may be used to drive photosynthesis, dissipated as heat, or re-emitted as fluorescence. When PSII has absorbed light energy and excited an electron it is unable to accept another photon until the excited electron is passed on to downstream electron acceptors in the photosynthetic pathway. During this brief time the reaction center is

considered closed. When a photosystem is dark-acclimated all the reaction centers are open and ready to receive photons. As soon as they are exposed to light, the reaction centers are rapidly closed as photons are absorbed. This causes a rapid increase in fluorescence followed by a return to baseline levels as fluorescence quenching is initiated. Fluorescence quenching is caused by several factors. First, after the photosynthetic pathways are activated, electron transport rates are increased which allows the reaction centers to open more quickly. This process is known as photochemical quenching (qP). Second, excess energy is converted to heat and the efficiency of this process increases until a steady state is reached [87]. This process is known as non-photochemical quenching (NPQ). Quenching parameters are one way of measuring stress due to environmental factors, information that is not easily determined by other methods [87]. Fluorescence quenching analysis assumes the change in fluorescence is proportional to changes in competing processes such as photochemistry and heat dissipation. [17].

Most of the work in the area of chlorophyll fluorescence has focused on plants. Because the key photosynthetic complexes, PSII and PSI, are very similar in cyanobacteria and plants, many of the methods are mutually applicable. However, there are key differences that must be taken into account when interpreting fluorescence data from cyanobacteria. The primary light harvesting complexes in cyanobacteria are phycobilisomes, while in plants the chlorophyll-a/b binding proteins are responsible for most of the light harvesting [17].

Cyanobacteria also have a very high PSI to PSII ratio [104] and consequently PSII accounts for very little of the total chlorophyll. The abundance of PSI means that electrons are rapidly transferred away from PSII, making it challenging to saturate the photosystems and make an accurate measurement of the maximum fluorescence yield (Fm). In particular this can make it difficult to calculate Fv/Fm. In cyanobacteria, 3-(3,4-dichlorophenyl)-1,1-dimethylurea (DCMU), an inhibitor that prevents electrons from being transferred from PSII to the plastoquinone (PQ) pool [92, 117], is often used to determine Fm accurately [145]. By blocking electron flow from PSII, all reaction centers can be effectively closed, thus yielding an accurate measurement of maximum fluorescence.

Chlorophyll fluorescence is influenced by carbon accumulation and can even be used to estimate CO_2 fixation rates [17], thus making it a valuable technique for the carbon accumulation experiments done for this dissertation. Miller et al. [95] documented the effects of inorganic carbon accumulation on fluorescence. They found that the addition of inorganic carbon caused an increase in the nonphotochemical quenching due to the increased oxidation of Q_A.

Biofuel production from cyanobacteria

In recent years, considerable research has focused on the production of fuels such as hydrogen and biodiesel from cyanobacteria [24, 49]. Additional research has examined biomass production for use in gasification and pyrolysis [55]. Cyanobacteria are ideal organisms for fuel production because of their rapid

growth and photosynthetic efficiency. In addition, they can be grown in ponds or bioreactors, thus eliminating the competition for agricultural land that has emerged with biofuel crops.

One potential fuel produced by cyanobacteria is hydrogen (H_2). H_2 production is mediated by a class of enzymes known as hydrogenases (H_2ases), which catalyze the oxidation or reduction of H_2 according to the reaction:

$$2H^+ + 2e^- \leftrightarrow H_2$$

These enzymes are found primarily in Archaea and Bacteria, although several have been identified in Eucarya as well. H_2 redox enzymes are a diverse group of enzymes that are divided into three categories based on their catalytic activity and active site composition. First, nitrogenases produce hydrogen as a byproduct of nitrogen fixation. Second, uptake H_2ases are capable only of oxidizing molecular hydrogen. Third, bidirectional H_2ases are capable of catalyzing both the oxidation and reduction of protons. Bidirectional H_2ases have specific activities about 1000 times higher than nitrogenases and are not ATP dependent [11]. Most H_2ases are metalloproteins that contain either two Fe atoms or a Ni and Fe atom in the catalytic site [151].

Several physiological roles have been postulated for H_2ases. H_2 production provides a mechanism for removing excess reductant in anaerobic environments [66]. H_2 redox cycling across the cytoplasmic membrane may also play a role in maintaining transmembrane proton gradients in sulfate reducing bacteria [110]. Some H_2ases are also capable of catalyzing the reduction of sulfur to H_2S, which is

believed to be an energy conservation process. This idea is supported by the observation that the accumulation of hydrogen can cause a metabolic shift to a fermentative pathway, which is less efficient [127]. Therefore, by removing hydrogen cells can maintain the most efficient fermentative pathway for maximum ATP production.

Although the advantages of photobiological H_2 production are well known there are several major challenges that must be overcome. Oxygen sensitivity of the H_2ase is one of the greatest challenges to biological H_2 production. Oxygen can bind to the enzyme active site causing reversible inhibition of the bidirectional [Ni-Fe] H_2ases found in many cyanobacteria [121]. Several approaches are being taken to overcome this problem. One approach is through genetic engineering of the H_2ase to modify the gas channels or active site to minimize O_2 sensitivity [151]. Other strategies include spatially or temporally separating H_2ases from oxygenic photosynthesis in heterocystous N_2 fixing cyanobacteria [125].

Another strategy that merits further research is the development of photochemical cells that incorporate photosystems and H_2ases either in solution or immobilized. Immobilization of H_2ases on a solid support matrix is of particular interest since it is known to improve protein stability [18]. Recently Badura et al. [8] proposed a model for an electrochemical cell that uses PSII attached to the anode and PSI attached to the cathode. Electrons would be transported from the water-splitting PSII attached to the anode, to PSI where

they would be raised to a higher energy state before being transferred to the H_2ase [8]. This concept has been investigated since the late 1970's when Haehnel and Hochheimer [47] developed a photosynthesis driven galvanic cell and proposed a model system containing PSII in solution in an anode half cell and PSI and H_2ase in the cathode half cell. Chief advantages of using an electrochemical cell are that the reduction potential of both photosystems can be used and oxygenic photosynthesis can be physically separated from the H_2ase, which eliminates the problem of inactivation by oxygen.

Another limitation to photobiological H_2 production is the availability of reduced electron carriers to mediate the transfer of electrons between PSI and H_2ase. In microbial cells, H_2ases must compete with other metabolic processes for electron carrier molecules such as NADPH or ferredoxin. Recently Ihara et al. [59] developed a novel system for photobiological H_2 production that addresses this problem. They fused the psaE subunit of PSI from *Thermosynechococcus elongatus* to the membrane bound H_2ase from *Ralstonia eutropha*. The fusion protein was then combined with psaE-free mutant PSI from *Synechocystis* sp. PCC 6803 resulting in a purified H_2ase-PSI complex capable of producing H_2 through direct transfer of electrons from PSI to the attached H_2ase. The complex exhibited a 5-fold increase in electron transfer between PSI and H_2ase [59]. This hybrid complex appears to be an important breakthrough in developing methods for improving the efficiency of energy transfer between the light harvesting

complexes and H_2ases and holds great potential both in whole cell H_2 production and in cell-free enzyme based systems.

H_2ases have gained considerable interest in recent years because of their ability to generate molecular hydrogen, which is an attractive source of clean renewable energy. They also have potential applications in biosynthesis, bioremediation, and other biotechnological processes. A number of comprehensive reviews [42, 78, 90, 122, 125, 144, 151] have described and classified H_2ases and their potential biotechnological applications.

Another potential fuel from cyanobacteria is biodiesel. Biodiesel is made by the transesterification of triacylglycerols (TAG's). TAG's are non-polar triesters of glycerol with fatty acids that serve as a carbon and energy reserve compound [46]. The synthesis of biodiesel begins with the reaction of sodium hydroxide with an alcohol, forming sodium methoxide. In the second step the sodium methoxide reacts with the fatty acid by attacking the carbonyl carbon and forming a tetrahedral intermediate. Finally, the methyl esters are separated from the glycerol backbone, thus forming biodiesel.

One of the primary advantages of biodiesel is that it is compatible with the current energy infrastructure and can quickly supplement or replace petroleum. In addition, biodiesel production from algae can produce substantial quantities of fuel on far less land than is needed for growing oil crops. The fastest growing crops, such as switchgrass, have a solar energy to biomass conversion rate of only 1 W/m^2 annually, which is less than 0.5% of the incident solar energy [76].

Microalgae have a photosynthetic efficiency of 10-20% or greater and a biomass productivity 50 times greater than switchgrass [76]. Water use is also far less in an enclosed bioreactor compared to oil crops, which require up to 1000 L of water per kg of biodiesel [50]. Potential oil yields from microalgae are much higher, with estimates ranging from 58,700-136,000 L ha^{-1} while the highest yield from an oil crop is 5,950 L ha^{-1} from oil palm [137]. Growing cyanobacteria or algae for biodiesel also has the potential to provide many value-added byproducts, thereby improving the economic viability of the system.

Decades of research have focused on producing oil from algae. Efforts such as the US Department of Energy's Aquatic Species Program (ASP) focused on biodiesel from algae for nearly 20 years [134] and yet a viable system has not yet been produced. However, studies such as these have greatly increased our understanding of algae biochemistry and physiology and have enabled researchers to identify key problems that must be addressed. Although projects such as ASP have contributed greatly to our understanding, they were hindered by a lack of many of the molecular techniques and genetic tools available today. Recent advances in molecular biology and genetic engineering, as well as advances in materials science and bioreactor design, indicate that a successful, comprehensive solution for biodiesel production from algae may now be within reach. Much less effort has focused on lipid production from cyanobacteria and a more comprehensive analysis, like the ASP program, is needed to explore new species and strains.

The type of fatty acids used in the transesterification process determines the properties of biodiesel. Saturated fat acids produce biodiesel with high oxidative stability and cetane number but poor cold-flow properties while polyunsaturated fatty acids are more susceptible to oxidation but better cold-flow properties [57]. Recently efforts have focused on genetically modifying organisms to produce "designer" fuels that have specific properties for a given application or location. For example, a strain that produces only saturated fatty acids would yield a more stable and higher energy fuel but in colder climates it would be advantageous to use organisms that produce polyunsaturated fatty acids so that the biodiesel would have better cold-flow properties. In addition, modifying the lipid production pathways may make it possible to produce biodiesel with hydrocarbon chains that closely match diesel produced from petroleum. Petroleum diesel consists primarily of C_{10}-C_{15} hydrocarbons while the fatty acids found in algae vary from C_{10}-C_{24} [57]. Therefore. by genetically modifying lipid pathways it may be possible to shorten the hydrocarbon chain length and produce biodiesel with properties similar to petroleum based diesel.

Recently, a great deal of research has focused on enzymatic production of biodiesel as an alternative to the artificially catalyzed process. Several classes of enzymes including lipases, esterases, and phospholipases are being considered as biocatalysts. Enzymes have the advantage of specific fatty acid selectivity thus enabling the selection of fatty acids with the properties that are desired for a

specific application [129]. However, these reactions still require the addition of a solvent such as ethanol or methanol.

Cyanobacteria can also provide a source of biomass for gasification, pryrolysis, liquefaction, and combustion [152]. Syn-gas (H_2/CO) produced by gasification can be used to produce liquid fuels, such as methanol and dimethyl ether [83]. Pyrolysis of microalgae biomass has been demonstrated to produce high quality fuel oils that can be used directly in internal combustion engines. However the quality and chemical instability limit their usability [76]. Pyrolysis of biomass can achieve conversion efficiencies of up to 95.5% [76], making this a much better option than biomass combustion.

Cyanobacteria can also be used as a source of biomass for fermentation. Fermentation can be used to produce ethanol, methane, and butanol [52, 80]. Cyanobacteria are a better source of biomass than higher plants because of their low cellulose and lignin content [52], thus rendering them more readily degradable.

The cost of cultivation is one of the greatest limitations to biofuel production from cyanobacteria [24]. Most of this cost is due to the complexity and expense of setting up bioreactors and maintaining sterile conditions. Another one of the major limitations is the low biomass concentrations of cultures due to the limited ability of light to penetrate the culture. Typical biomass yields are from 1-5 g/L [76]. While pilot scale demonstrations have shown the feasibility of algal biodiesel production, overall efficiency and the economies of scale have

prevented commercial success. For example, estimated biodiesel production costs in 1995 was $1.40-$4.40 per gallon [134], which must be decreased for the process to become economically viable.

Complete biochemical characterization of fatty acid and TAG synthesis pathway's is still lacking with many of the key structural and regulatory genes still unknown [57]. Future progress in improving growth and lipid content will not be possible without advances in our understanding on the genomic level. The efficiency of lipid production is also hindered by the efficiency of photosynthesis. Photosynthetic organisms typically have large antennae systems in order to capture the maximum amount of energy under low light conditions. However under high light intensity much of this energy is lost as heat or fluorescence. By engineering smaller antennae it may be possible to reduce this energy loss by 85-90% [50].

Biomaterials from cyanobacteria

Cyanobacteria have significant potential for producing a wide range of products including glycogen, carotenoids such as astaxanthin and β-carotene, cyanophycin, lutien, vitamins B and C, and aromatic compounds [101], [31, 52, 76, 129]. The production of carotenoids is of particular interest because of their antioxidant properties and provitamin A activity [129]. They are also used extensively as a source of pigments. Currently, β-carotene, lycopene, and astaxanthin are produced commercially as health supplements [129]. A

significant number of bioactive compounds with antiviral, anti-tumor, and antibacterial properties have also been identified in cyanobacteria [138]. The production of vitamins from microorganisms is especially attractive because it eliminates energy intensive chemical synthesis and the associated high costs of waste disposal [143]. However, in biological systems, yields are often low and the process of harvesting biomass and extracting the desired compound can be complex and cost prohibitive [100]. In spite of these limitations some species such as *Spirulina* and *Chlorella* have been successfully grown on a commercial scale [4, 12].

Biopolymers also have significant potential for bioproducts production. Recent discoveries in the field of biopolymer synthesis have opened new horizons for the development of novel compounds for many industrial and medical applications. Microorganisms are capable of synthesizing four main classes of polymers: polysaccharides, polyesters, polyamides, and polyanhydrides, all of which have potential industrial applications [123]. Polymers in microorganisms function primarily as storage compounds or play a structural role in the cell. The majority of polymers are extracellular while some, such as glycogen and PHA are located internally [123].

Polyhydroxyalkanoates (PHA's) are biodegradable biopolyesters that many microorganisms synthesize as a storage molecule from the condensation of two molecules of acetyl-CoA [82], [116]. PHA's, such as polyhydroxybutyrate (PHB), are of particular interest for their potential in the bioplastics industry

[23]. PHB is used as the raw material for biodegradable plastic production [98], and is thus a much more environmentally amenable alternative to petrochemical plastics.

Polythioesters (PTE's) are another type of biopolymers synthesized by microorganisms. PTE's have different physical and chemical properties than PHA's, such as improved thermal stability and elasticity [82]. Several other biopolymers are currently being commercially produced. Dextran, which has several medical and laboratory applications, and xanthan, used as a food additive, are currently produced on the order of 2, 000 and 100,000 tons, respectively, on an annual basis [123]. The biocompatible and biodegradable nature of biopolymers makes them ideal replacements for many of the petroleum-derived polymers in use today. However, several technological challenges relating to production and harvest remain before they can provide an economically viable alternative to the current polymer industry, and current production costs are 5-10 times higher than for petroleum based plastics [123]. Several recent reviews have provided a comprehensive description of the different classes of biopolymers and their characteristics and potential applications [52, 123, 142].

Microbial biomass also has potential in applications such as fertilizer, soil conditioner, and feed [61], all of which are useful end products that can be utilized after other valuable products have been extracted. A more complete summary of compounds that can be produced from biomass has been compiled in several DOE reports [55, 154].

Characteristics of Thermophiles

The group of organisms known as thermophiles consists of microorganisms from a variety of archaeal and bacterial genera that are unique in their ability to thrive at high temperatures. Organisms that can tolerate temperatures above 50°C are classified as thermophiles and those that can live in temperatures above 80°C are classified as hyperthermophiles [10]. Over 75 species of thermophilic microbes have been discovered, living at temperatures ranging from 50-110°C [148] and thermophilic enzymes, known as thermozymes, can be active up to 130°C [37].

Despite years of effort to elucidate the factors responsible for thermotolerance, no systematic method of determining thermalstability based on protein structure has yet been demonstrated. With the complete sequencing of thermophilic genomes it is now possible to do sequence comparisons to correlate structural features and specific sequence with improved thermal stability. By comparing thermophilic and mesophilic protein sequence and structure it is now possible to identify some of the factors that enable proteins to remain stable in high temperatures.

The ability of organisms to tolerate high temperatures is largely attributed to the thermostability of proteins, which is defined in terms of thermodynamic and chemical properties. The thermodynamic stability is determined by the Gibbs free energy change between the native and denatured state of the protein,

$$\Delta G = \Delta H - T\Delta S$$

where T is the temperature, ΔH is the change in enthalpy and ΔS is the change in entropy. The changes in enthalpy and entropy between the unfolded and folded states are temperature-dependent [73]. Thermodynamic studies using native hydrogen exchange have identified protein residues that confer thermo stability in *Thermus thermophilus*. These studies indicate that properties that increase stability are distributed throughout the protein rather than at a specific site [73], consistent with the idea that there are many factors involved in maintaining thermostability

Some of the features common to thermophiles, and which are believed to confer greater thermostability, include surface loop deletions, fewer cavities, increased numbers of α-helixes, greater hydrogen bonding, higher levels of hydrophobic residues with branched side chains, reduction of conformational strain and entropy of unfolding, loop stabilization, resistance to covalent destruction, and more charged residues [13, 147, 149]. Increased atomic packing and a higher number of salt bridges is also believed to confer greater thermal stability [73].

A recent study by Beeby, et al., [10] compared the number of salt bridges in homologous proteins from over 100 prokaryotic genomes by three-dimensional mapping of protein sequences. The results showed a marked increase in the number of disulfide bonds in thermophiles compared to mesophilic organisms. They also described protein disulfide oxidoreductase

(PDO) that is believed to play a role in forming and maintaining disulfide bonds in thermophiles. While disulfide bonds are generally considered unstable in the reducing environment of the cytosol, thermophiles appear to have a mechanism for stably maintaining these bonds [10]. Genome sequence analysis showed that these proteins are exclusive to thermophiles and are associated with increased disulfide levels [10], which supports the idea that they play a crucial role in thermostability. Sequence analysis has identified an N-terminal redox site with a CxxC motif, and *in vitro* experiments have shown that this site is primarily oxidized in the native protein, lending further evidence to the idea that it is involved in disulfide bond formation [10].

In addition to disulfide bonds, the physical and chemical properties of individual amino acids also contribute to thermostability. Gromiha et al, [44] found that thermostability is correlated to the position of branch points in amino acids and that β and γ-branched amino acids increase stability. Thermophilic proteins are also rich in charged Arg, Lys, His, Asp, and Glu residues and have fewer uncharged Cys, Ser, Gln, Asn, and Thr residues relative to mesophilic proteins [73].

Pressure also plays a role in stabilizing proteins in marine thermophiles found in deep-sea hydrothermal vents. While high pressure is typically considered a denaturant in mesophilic organisms, studies indicate it may play a role in stabilizing proteins at high temperatures. Activity assays of H_2ases isolated from *Methanococcus jannaschii* showed an increase in half-life of 400%

at 90°C when pressure was raised from 1 to 50.7 MPa [53]. The authors proposed that the pressure stabilization was due to increased hydrophobicity of the protein. A more in-depth analysis of the structural features, characteristics, and potential applications of thermophilic enzymes can be found in a number of reviews [37, 73, 147, 149].

Thermosynechococcus elongatus as a platform for CO_2 sequestration, biofuels, and bioproducts production

Thermosynechococcus elongatus is a unicellular cyanobacterium that grows in hot springs at an optimal temperature of 55°C and is an obligate autotroph [107]. The photosystems of *T. elongatus* have served as models for extensive structural studies due to their extraordinary stability [63, 77], however very little is known about the metabolic pathways in this organism. This is due in part to the fact that it is an obligate autotroph and thus is not amenable to significant knockout mutations that are often needed to analyze metabolic pathways.

T. elongatus was chosen as a model for this research for several reasons. It is thermophilic, which is a significant advantage in the operation of a photobioreactor. Elevated temperatures are detrimental to the growth of most cyanobacteria. Studies have show that *Synechocystis* sp. PCC 6803 grow optimally at a temperature of 30°C and stop growing at 45°C [60]. While many organisms can tolerate temperatures up to 15°C cooler than their physiological optimum,

temperature increases as little as 2-4°C above their optimum can be detrimental [86]. Temperatures in photobioreactors in direct sunlight can reach 55°C [86]. In order to avoid such temperature increases, which could inhibit growth or kill the cyanobacteria, photobioreactors are cooled with mechanical, energy-consuming circulation systems, which lowers the overall efficiency [34]. By using thermophilic organisms, cooling systems could be minimized or even eliminated which would make bioreactors more energy efficient. It has also been postulated that in addition to harvesting light energy with thermophilic microbes, thermal energy could also be captured from the bioreactor thus improving the overall energy production of the system [99]. Another advantage of operating bioreactors at higher temperatures is that the risk of contamination is minimized since the majority of microorganisms including many pathogens, cannot live at these temperatures.

T. elongatus is also an obligate autotroph and cannot grow on any organic carbon source. Although this has historically been a limitation for metabolic and genetic studies, it is an advantage for carbon sequestration and storage experiments since no additional organic carbon needs to be supplied. In contrast, many other carbon storage (e.g. lipids, PHB, glycogen) studies have relied on an organic carbon supplement [30, 105] to achieve maximum production.

Although the genome of *T. elongatus* has been sequenced and the species is the focus of extensive photosynthesis research, no effort has been made to analyze it for the sequestration of storage compounds such as glycogen, PHB, and

lipids. In addition, no work up until now has examined the ability of *T. elongatus* to tolerate high concentrations of CO_2 and dissolved inorganic carbon (DIC).

Dissertation overview

The purpose of this dissertation is to provide a comprehensive analysis of the ability of *T. elongatus* to sequester carbon and produce H_2 and storage compounds with potential as biofuels and bioproducts. Very little data is available comparing the utilization of DIC vs. CO_2 [56] and even less data is available regarding the effect of the carbon source and concentration on internal carbon reserves.

In the first paper *T. elongatus* was examined for H_2 production under a range of conditions. H_2 production was monitored by gas chromatography (GC) analysis and by using a screening assay recently developed by Schrader et al., [130]. Several electron transport chain inhibitors were used to identify the possible mechanism of H_2 production.

In the second paper, the growth of *T. elongatus* under high levels of DIC is investigated. The effect of DIC concentration on growth, photosynthetic activity, and accumulation of glycogen, lipids, and PHB's was examined. Chlorophyll fluorescence was used to measure photosynthetic parameters to provide insight into photosynthetic activity and also potential stress caused by high carbon concentrations or by carbon deprivation.

The third paper explore's the growth of *T. elongatus* in bioreactors with increasing concentrations of CO_2. The effect of CO_2 concentration on growth, photosynthetic activity, and accumulation of glycogen, lipids, and PHB's was investigated. Biomass productivity, carbon uptake rates, and the efficiency of CO_2 utilization were calculated.

CHAPTER 2: HYDROGEN PRODUCTION BY THE THERMOPHILIC CYANOBACTERIUM, *THERMOSYNECHOCOCCUS ELONGATUS*

Jed O. Eberly, Hatem Mohamed, and Roger L. Ely

To be submitted for publication

International Journal of Hydrogen Energy

Abstract

The ability of *Thermosynechococcus elongatus* to produce molecular hydrogen (H_2) was investigated. Cultures incubated in the dark produced H_2 at a maximum rate of 188 nmol H_2 mg Chl a^{-1} hr^{-1}. Hydrogen production was induced in the presence of methyl viologen but the cells were not able to catalyze deuterium (D_2) exchange. Screening assay studies showed that the inhibitors DCMU, DBMIB, PCP, and malonate did not effect H_2 production while H_2 production was completely inhibited when KCN was present. The inhibitor results suggest that the electron flow to the putative hydrogenase (H_2ase) in *T. elongatus* does not follow the same scheme as with the bidirectional [NiFe] H_2ase found in species such as *Synechocystis* sp. PCC 6803. The physiological response and genome analysis of *T. elongatus* indicates that this H_2ase may differ from the Fe-only or [NiFe] bidirectional H_2ase enzymes commonly found in green algae and in other species of cyanobacteria. Here we report evidence of H_2 production by *T. elongatus* from a potentially novel H_2 production pathway.

Introduction

Rising energy costs have led to heightened interest in biological hydrogen (H_2) production. Cyanobacteria in particular are an attractive organism for biological H_2 production because they are capable of directly harvesting solar energy. The H_2 producing capabilities of cyanobacteria are well known and have been studied in species such as *Synechocystis* sp. PCC 6803 [3, 27, 132] and *Anabaena variabilis* [128].

H_2 redox enzymes comprise a diverse group that is divided into three categories based on catalytic activity and active site composition. Nitrogenases produce H_2 as a byproduct of nitrogen fixation. Bidirectional hydrogenases (H_2ases) catalyze both the oxidation of H_2 and the reduction of protons, while uptake H_2ases primarily catalyze the oxidation of molecular H_2. Most bidirectional H_2ases contain two Fe atoms or a Ni and Fe atom in the catalytic site [151]. Most bidirectional H_2ases are sensitive to O_2, with [NiFe]-H_2ases being reversibly inhibited by O_2 while [FeFe]-H_2ases are irreversibly inhibited. A third type of H_2ase, H_2-forming methylene-tetrahydromethanopterin dehydrogenase (Hmd) has also been described. This H_2ase is Fe-S cluster-free with a single [Fe]-center and is O_2 tolerant [136].

The H_2ases of many heterotrophic thermophiles have also been extensively studied and recent reviews have described their potential applications in H_2 production, biosynthesis, bioremediation, biosensors, coenzyme regeneration, and other biotechnological applications [35, 42, 125]. While much effort has been made in understanding H_2 production in mesophilic cyanobacteria and thermophilic heterotrophs, virtually no research has examined H_2 production by thermophilic cyanobacteria.

T. elongatus is a unicellular cyanobacterium that grows in hot springs at an optimal temperature of 55°C and is an obligate autotroph [108]. The photosystems of *T. elongatus* have served as models for extensive structural studies due to their extraordinary stability [63, 77], however very little is known

about the metabolic pathways in this organism. This is due in part to the fact that it is an obligate autotroph and thus is not amenable to significant knockout mutations that are often needed to analyze metabolic pathways. Although the genome of *T. elongatus* has been sequenced and the species is the focus of extensive photosynthesis research, it has not been analyzed for H_2 production to date. In addition, no sequences with significant homology to nitrogenases or [NiFe]-H_2ases have been identified. Here we report evidence of H_2 production by *T. elongatus* from a potentially novel H_2 production pathway.

Materials and Methods

Culturing conditions

Thermosynechococcus elongatus BP-1 was cultured in modified BG-11 media [20] designated Thermo BG-11, pH 7.8, at 48°C under continuous lighting (30-50 μE m^{-2} s^{-1}). Cultures were incubated in 500 ml Erlenmeyer flasks on an orbital shaker table at 180 rpm. Cell growth was monitored by measuring the optical density of the cultures at 730 nm. Cells were also counted in a hemacytometer over a range of optical densities to establish a standard curve correlating optical density to cells ml^{-1}. The resulting equation, $(OD_{730}+0.0001)/1x10^{-9}$ = cells ml^{-1}, was used to determine the cell concentration throughout the course of the experiments. The amount of H_2 produced was quantified per mg of chlorophyll. Chlorophyll concentrations were determined

using methanol extraction followed by spectrophotometric measurement at 665 nm, with concentrations calculated by the method of Porra, 2002 [119].

GC vial tests and methyl viologen assay

Cells were tested for H_2 production by harvesting cultures at early, mid, and late log phase by centrifuging at 2000 x g for 5 minutes (Beckman centrifuge, model J2-21M, JA-10 rotor, GMI Inc., Ramsey, Minnesota, USA) and resuspending them in fresh media to a final concentration of 2 x 10^9 cells ml^{-1}. Cells were grown and incubated in either Thermo BG-11 or in media containing reduced levels of sulfur and nitrogen (0.52 mM NH_4^+, 20.1 μM SO_4^{2-}) [16]. 1 mL of culture was placed in 4 mL GC vials and the vials were degassed in a hypoxic glove bag (Coy Laboratory Products, Grass Lake, Michigan, USA) under a nitrogen atmosphere for 1.5 hours. The vials were capped with screw caps with PTFE lined septa, inverted, and incubated at 48°C with either continuous light at 50 μE m^{-2} s^{-1} or in the dark on an orbital shaker at 180 rpm. Headspace samples were collected after 1, 3, 6, 12, 24, and 48 hours and analyzed on a gas chromatograph (GC) with a thermal conductivity detector (Agilent Technologies Series 6890N Santa Clara, CA, USA) and GS-CARBONPLOT 30 m x 0.32 mm x 3.0 mm column using argon as the carrier gas at 1.6 mL min^{-1}. The oven temperature was 35°C and the detector temperature was 150°C. 100 μL gas samples were injected using a glass, gas-tight syringe (VICI Valco Instruments Inc., Houston, TX, USA).

Methyl viologen/dithionite assays were also carried out with 1 mL cells at a concentration of $1x10^9$ cells mL^{-1} in 4 mL GC vials. The vials were degassed in a hypoxic glove bag (Coy Laboratory Products, Grass Lake, Michigan, USA) under a nitrogen atmosphere for 1.5 hours. Methyl viologen and dithionite were added to a final concentration of 10 mM. The vials were capped with screw caps with PTFE lined septa, inverted, and incubated at 48°C with either continuous light at 50 μE m^{-2} s^{-1} or in the dark on an orbital shaker at 180 rpm. Controls consisted of media without cells. Headspace samples were collected after 15 and 30 minutes then again at 2, 4, 6, and 20 hours. H_2 was measured by gas chromatograph as described above.

Deuterium exchange and H_2 uptake assay

Cells were grown to a concentration of 1 x 10^9 cells ml^{-1} for the D_2 exchange assay. The culture was analyzed in a Hansatech® chamber (Hansatech, Norfolk, England) attached to a membrane inlet mass spectrometer (Pfeiffer Vacuum, Nashua, NH, USA). A circulating water bath was used to maintain the chamber at 45°C. A l mL sample of culture was loaded in the chamber and 5 mM glucose and 80 U ml^{-1} glucose oxidase were added to remove O_2. The culture was kept in the dark throughout the experiment to maintain anaerobic conditions. D_2 was then injected into the chamber until a steady state concentration was reached. D_2 and HD signals were monitored until they returned to baseline levels.

T. elongatus was also assayed for H_2 uptake ability. Cells were harvested in early exponential phase and concentrated to 1 x 10^{10} cells ml^{-1}. The sample size was 1 ml of cells in 4 ml GC vials. Samples were degassed for 1.5 hours and then incubated in full light or dark. Vials with media but without cells were used as controls. After injecting 200 µl of H_2 the headspace was immediately sampled and measured by GC. H_2 concentrations were measured at 1 hr and then every 24 hrs throughout the course of the experiment.

Effects of Inhibitors

The effect of well-known photosynthetic/respiratory electron transport inhibitors on H_2 production was also examined. The inhibitors used were dibromomethylisopropyl benzoquinone (DBMIB), 3-(3,4-dichlorophenyl)-1,1-dimethylurea (DCMU), pentachlorophenol (PCP), potassium cyanide (KCN), and malonate. Cells were assayed for H_2 production with inhibitors added to concentrations of 10 mM DBMIB, 10 mM DCMU, 10 mM PCP, 1 mM KCN, 10 mM malonate, and 10 mM malonate + 1 mM KCN. Cultures were grown to mid log phase then concentrated to 3 x 10^9 cells ml^{-1}. Effects of inhibitors were evaluated using a high throughput-screening assay that determines relative H_2 production based on the color change of an indicator dye [130]. The screening assay plates were degassed in a hypoxic glove bag (Coy Laboratory Products, Grass Lake, Michigan, USA) under a nitrogen atmosphere for 5 hours, then sealed and incubated at 45°C in full light (120 µE m^{-2} s^{-1}) for 7 days.

Results

GC vial tests and methyl viologen assay

Initial H_2 tests in GC vials showed no H_2 production after 1 hour of incubation in any of the samples. Between 3 and 12 hours incubation time, the H_2 concentration increased to about 0.2 μmol H_2 mg Chl^{-1} in cultures that were in late exponential phase, but after 24 hours no detectable H_2 remained (Figure 2.1 A). Cultures harvested in early to mid exponential phase had measurable concentrations of H_2 at 24 and 48 hours in both light and dark and the amount of H_2 produced was nearly double the amount produced from late exponential phase cells (Figure 2.1B). H_2 production appeared to be very sensitive to pH and culture age. At pH 7, which is close to the physiological optimum, H_2 production was about 50% higher than at other pH values (data not shown). The maximum rate of H_2 production from cells incubated in the dark was 146 nmol H_2 mg Chl^{-1} hr^{-1}.

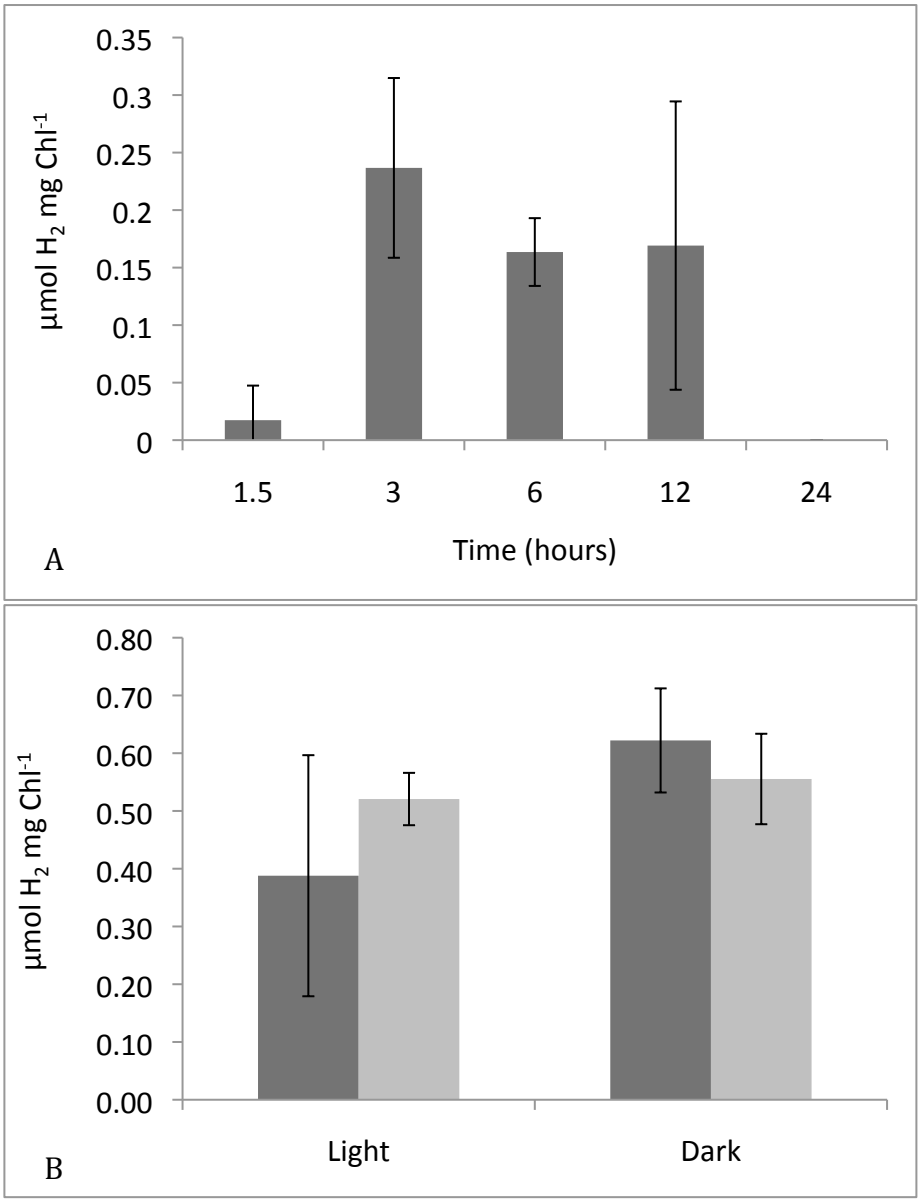

Figure 2.1. A: H_2 production from late exponential phase cells incubated in the dark. B: H_2 production from early exponential phase cells in the light and dark. ■ 24 hours, ■ 48 hours.

H_2 production was also seen in the methyl viologen/dithionite assay. No H_2 was seen until after 4 hours of incubation and the concentration of H_2 reached a maximum of 0.16 umol H_2 mg Chl^{-1} after 6 hours in culture incubated in the dark (Figure 2. 2). By 20 hours no H_2 remained in the headspace. Controls showed no H_2 (data not shown).

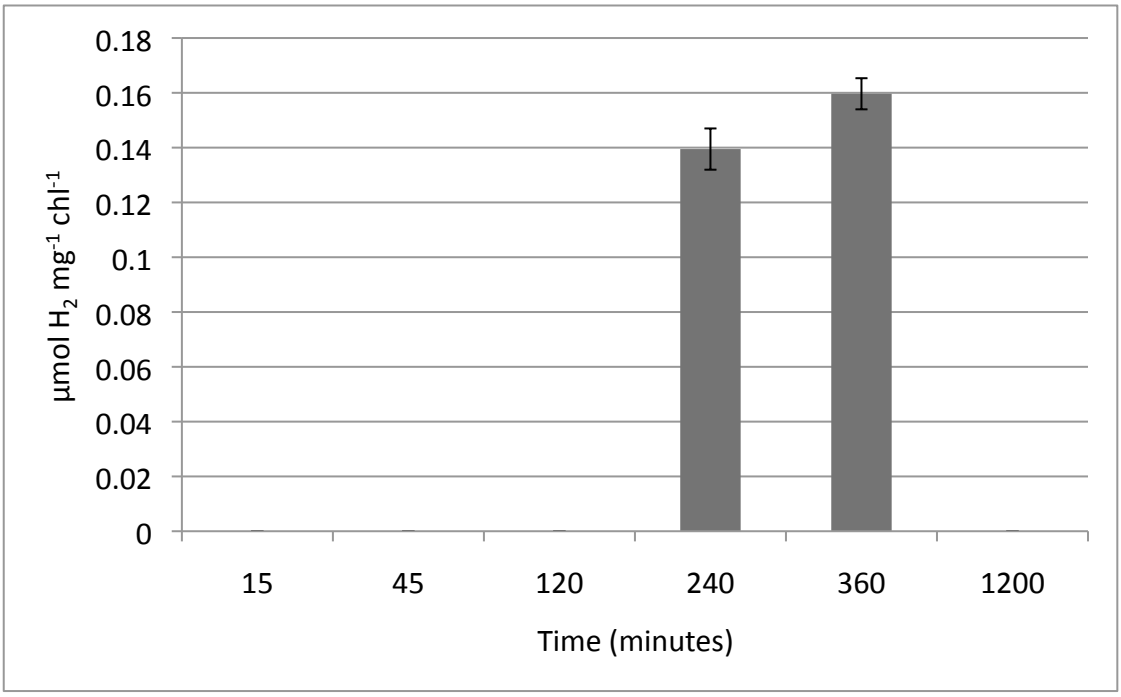

Figure 2. 2. Headspace H_2 concentration in 4 mL GC vials following treatment with dithionite and methyl viologen.

Deuterium exchange and H_2 uptake assay

Analysis of *T. elongatus* for D_2 exchange showed no activity. Upon the addition of D_2, the level of HD present did not rise above the control, indicating that no H-D exchange was occurring. A low level of H_2 was seen, indicating that

the H_2-producing enzyme was active during the assay. *Synechocystis* sp. PCC 6803 is known to catalyze D_2 exchange [27] and was used as a positive control to ensure that the sensitivity of the system was sufficient to observe changes in the level of HD.

In the H_2 uptake assay, the cell-free controls lost about 20% of the total H_2 that was injected most likely due to leakage, compared to a loss of only 8.7% for the cells incubated in the dark (Figure 2. 3) suggesting that the cells were actively producing H_2. Cells incubated in the light showed a rate of loss the same as the control (data not shown), indicating that H_2 was not produced. The average rates of loss were 5.27 μM hr^{-1} and 1.89 μM hr^{-1} for the controls and for cells in the dark, respectively. The difference between these rates of loss was used to calculate an average rate of H_2 production in the dark. From these data the calculated average rate of H_2 production was 188 nmol H_2 mg Chl a^{-1} hr^{-1}.

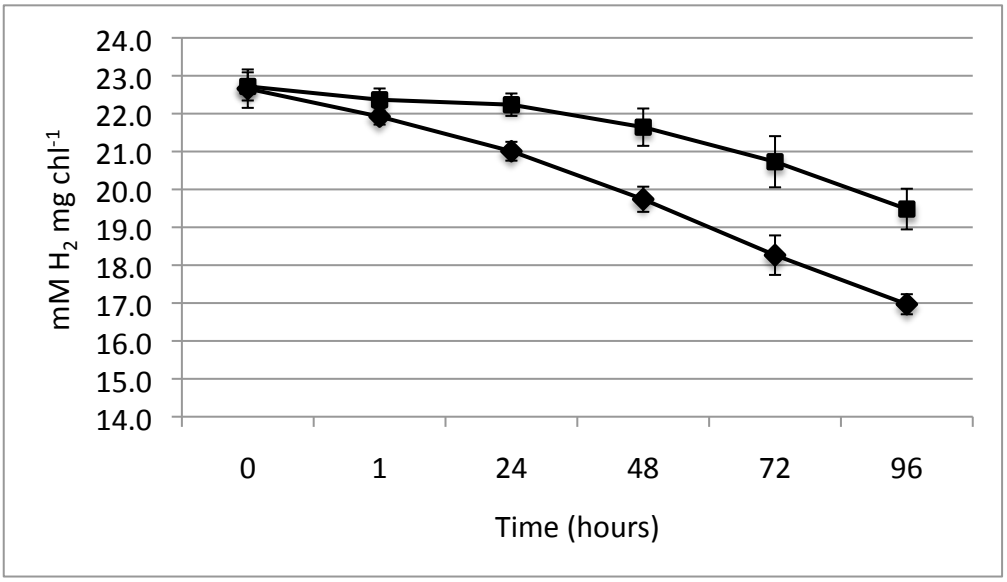

Figure 2. 3. H_2 uptake assay: ■ cells in the dark, ◆ media only control.

Effects of Inhibitors

Several well-known respiratory inhibitors were used in order to gain insight into how H_2 production observed in *T. elongatus* is related to components of the photosynthetic/respiratory electron transport chains. In general, the inhibitors did not cause increases in H_2 production and in some cases the presence of inhibitors resulted in no H_2 production. Cells treated with DCMU, DBMIB, PCP, and malonate showed no difference in H_2 production when compared to untreated cells. However, cells treated with KCN showed no H_2 production (Figure 2. 4 A). In addition, the presence of KCN and malonate appeared to have a negative effect on the assay response. This in part, is an

artifact of the assay, which shows slightly lower responses in the presence of acids.

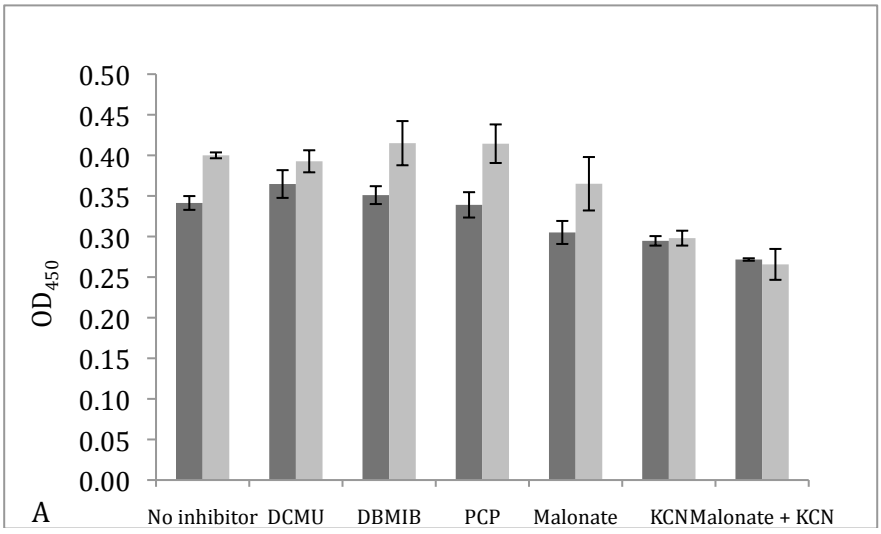

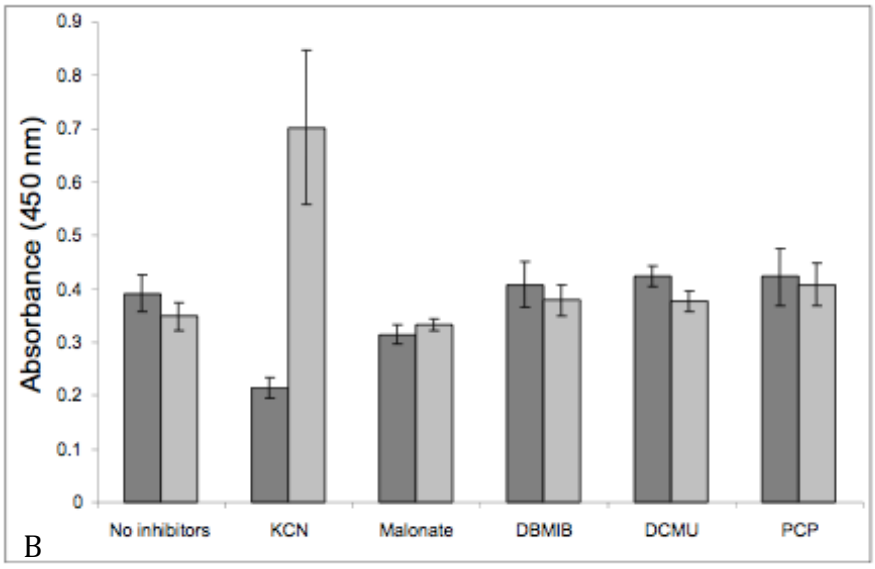

Figure 2. 4. Effect of inhibitors on H_2 production in full light from *T. elongatus* (a) and Synechocystis PCC 6803 (b). ■ cell-free control, ■ cells. Figure b from Burrows et al (2010) with permission of the publisher[1].

[1] This article was published in Bioresource Technology, 2010, Burrows, E., Chaplen, F., and Ely, R. Effects of Selected Electron Transport Chain Inhibitors on 24-hour Hydrogen Production by *Synechocystis* sp. PCC 6803, doi:10.1016/j.biortech.2010.10.042. Copyright Elsevier (2010).

Discussion

Previously, there have been no reports of H_2 production from *T. elongatus*, although H_2ases are common in mesophilic cyanobacteria and in many other mesophilic and thermophilic heterotrophic microorganisms [35, 42, 150]. Most research to date has focused on identifying novel H_2 producing mesophilic cyanobacteria and elucidating the metabolic role of the various types of H_2ases. Very little effort has focused on identifying and characterizing H_2ases in thermophilic cyanobacteria. However the occurrence of H_2ases in thermophilic cyanobacteria would seem probable given their prevalence in mesophilic strains. Also, even though several N_2 fixing thermophilic cyanobacteria strains have been found [99, 131], there have been no reports of N_2 fixation in *T. elongatus*, and our sequence analysis showed no genes with significant homology to known nitrogenases, suggesting that H_2 was not being produced from a nitrogenase.

The presence of a H_2ase or H_2 producing pathway in *T. elongatus* has not been previously investigated in the literature. This is not surprising given the fact that the entire genome has been annotated and no gene sequences for a typical cyanobacterial bidirectional or uptake H_2ase have been identified.

H_2 production from early log phase cells was nearly double the amount produced by late log phase cells, which is opposite of what has been reported in other cyanobacteria. Studies of *Synechocystis* sp. PCC 6803 have shown that H_2 production is greatest from late log phase cells [16] and similar results have been

seen in *Arthrospira maxima* [1]. This provides additional evidence that H_2 may be produced via a novel pathway in *T. elongatus*.

The maximum rate of H_2 production from *T. elongatus* was 188 nmol H_2 mg Chl a^{-1} hr^{-1}, which is comparable to reported production levels from *Anabaena* sp. 7120 (260 nmol H_2 mg Chl a^{-1} hr^{-1}) [118, 132]. However, unlike *Anabaena*, which catalyzed tritium exchange, the *T. elongatus* enzyme lacks the ability to catalyze deuterium exchange.

The inhibitors used in this study are known to interrupt electron flow (Figure 2. 5) in the photosynthetic/respiratory electron transport chain in many organisms, from plants to cyanobacteria. DCMU is a very specific inhibitor of photosynthesis that prevents electrons from being transferred from PSII to the PQ pool in both plants and microorganisms [92, 117] while DBMIB inhibits electron transfer from the PQ pool to cytochrome b6/f [38]. PCP inhibits electron transfer from the PQ pool to terminal oxidases while KCN inhibits cytochrome oxidase activity [126]. Malonate inhibits the succinate dehydrogenase complex (SDH), and prevents electron transfer to the PQ pool via succinate oxidation [26].

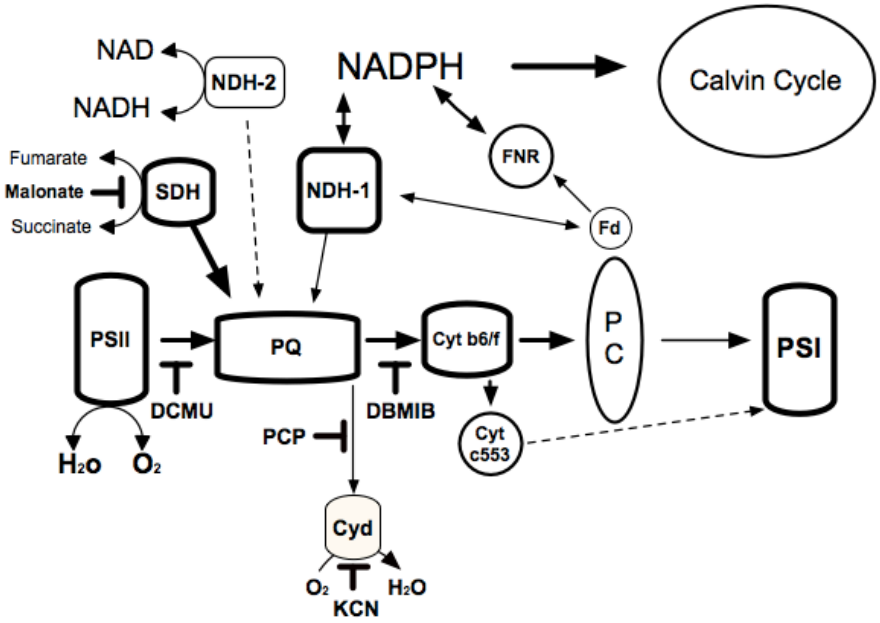

Figure 2. 5. Schematic representation of photosynthetic/respiratory complexes: photosystem I (PSI), photosystem II (PSII), succinate dehydrogenase (SDH), plastoquinone (PQ), cytochrome b6/f complex (cyt b6/f), cytochrome c553 (cyt c553) quinol oxidase (cyd), NADPH-quinone oxidoreductase type 1 and 2 (NDH-1 and NDH-2), Ferredoxin--NADP reductase (FNR), and ferredoxin (Fd). Dashed lines indicate presumable path of electron flow. The presumable sites of inhibition for the inhibitors DCMU, DBMIB, PCP, KCN, and malonate are also shown based on their confirmed role in other species of cyanobacteria [45, 126].

It is difficult to predict the result of any given inhibitor because many different metabolic pathways can be altered. In addition, the precise effects of all these inhibitors have not been elucidated for *T. elongatus*. However, some of the key enzyme complexes, including both NDH-1 and -2 have been identified in the

genome of *T. elongatus* [108] and a fumarate nitrate reductase FNR complex has also been described [106], and a cyd type cytochrome oxidase has been annotated in the genome (www.ncbi.nlm.nih.gov). The presence of these, and other related enzyme complexes, suggests that the photosynthetic pathways may be similar to other cyanobacteria such as *Synechocystis* sp. PCC 6803 and *Synechococcus elongatus* PCC 7942.

Although the presence of these enzymes does not conclusively determine the metabolic pathways or the mechanism of inhibition, they do suggest that inhibitor effects may be similar to the responses seen in other cyanobacteria.

The inhibitors DBMIB, PCP, and malonate all caused the cultures to bleach out over the course of the 7-day experiment. However H_2 production was not affected (Figure 2. 4A), which suggests that these inhibitors may not have interfered with H_2 production, or that H_2 production occurred prior to chlorosis. In contrast, other experiments have shown that *Synechocystis* sp. PCC 6803 does not produce H_2 in the presence of DBMIB, PCP, and malonate (Figure 2. 4B). The fact that H_2 production occurred in the presence of DBMIB, PCP, and malonate indicates that electron flows through SDH, b6/f, and cyd are not essential to the H_2 production process, in contrast to the [NiFe] bidirectional H_2ases found in species such as *Synechocystis* sp. PCC 6803 [15]. KCN was expected to increase electron availability to the H_2-evolving enzyme by limiting activity of the terminal oxidases [126], leading to an increase in H_2 production. Such an increase in H_2 production has been demonstrated in *Synechocystis* sp. PCC 6803 where the

addition of KCN results in significant H_2 production (Figure 2. 4B). However, in *T. elongatus* no H_2 production was observed in the presence of KCN (Figure 2. 4A). This suggests that the oxidases are not in direct competition with the enzyme for electrons as in *Synechocystis* sp. PCC 6803 and that inhibiting oxidases is not an effective way of redirecting electron flow toward the H_2-evolving enzyme. The results of this inhibitor test provide additional evidence that electron flow to the unknown H_2-evolving enzyme in *T. elongatus* does not follow the same scheme as to the bidirectional [NiFe]-H_2ase found in other species such as *Synechocystis* sp. PCC 6803.

The inhibitor responses, coupled with the delayed response (4+ hours) to dithionite and methyl viologen addition, raises the possibility that H_2 may be produced indirectly from an enzyme that is primarily involved in another redox reaction. This could potentially be through an associated enzyme that is capable of producing H_2 as a byproduct of a reaction involving dihydrolipoamide dehydrogenase (LPD). This would provide one possible explanation for the anomalous inhibitor results. For example KCN, a respiratory inhibitor, caused a decrease in H_2, which would be expected if the H_2 production were linked to respiration. An LPD gene (tll0868) has been annotated in *T. elongatus* although it has very low sequence similarity with the LPD in *Synechocystis* sp. PCC 6803 and to date this enzyme has not been isolated and characterized. Another potential candidate for the source of H_2 is a formate hydrogen lyase (FHL) complex. In this system, FHL catalyzes the conversion of formate to CO_2 and H_2 [70]. *T. elongatus*, has

a sequence (tlr0226) that has been annotated as a pyruvate formate lyase-activating enzyme and another (tlr0227) that is annotated as a pyruvate-formate-lyase deactivase but no genes with significant homology to the FHL complex.

Overall, the results indicate that the activity of this unknown H_2-evolving enzyme might not be closely associated with photosynthesis as it is in some species such as *Synechocystis* sp. PCC 6803 [45]. Since *T. elongatus* is an obligate autotrophic cyanobacterium, this unknown enzyme is likely associated with another metabolic pathway that indirectly uses reductant from photosynthesis in the form of reserved carbon such as glycogen and/or poly-hydroxybutyric acid polymers. The ability of *T. elongatus* to produce H_2 under certain physiological conditions raises the possibility of the existence of a novel type of H_2ase or another enzyme that is also capable of producing H_2. More work is needed to identify the responsible genes and to characterize this H_2-evolving enzyme.

Conclusion

This research provides evidence of H_2 production from thermophilic cyanobacteria by means of an unknown H_2-evolving enzyme that appears to be at least somewhat O_2 tolerant and that does not appear to be directly linked to photosynthesis.

H_2 production from thermophilic cyanobacteria represents a previously unexplored area of biohydrogen research and may open the door to new biotechnological applications that can take advantage of the unique capabilities

these organisms offer. Many applications for organisms with thermophilic H_2ases are currently being explored [35] but these applications require an organic carbon source. Thermophilic cyanobacteria capable of using solar energy would be advantageous in some of these applications and could lead to the development of other novel applications.

Thermophilic cyanobacteria may eventually play a critical role in commercializing biological hydrogen production due to their ability to withstand higher temperatures. It has been documented that photovoltaic cells can reach temperatures as much as 20°C warmer than ambient temperature when operated in direct sunlight [84] and similar results may be anticipated in bioreactors designed for H_2 production. This necessitates either the use of cooling systems, which lower the overall efficiency of the reactor, or thermophilic strains that can survive higher temperatures. In addition to H_2 production, thermophilic H_2ases may play an important role in many other industrial processes [35]. More work is needed to explore the diversity of H_2ases in thermophilic H_2ases and ongoing discoveries will undoubtedly provide insight into the range and function of these enzymes.

Acknowledgements

This work was supported in part by the Earth's Subsurface Biosphere IGERT program at Oregon State University, NSF grant number 0114427. *T. elongatus* was a gift from the Wim Vermaas lab at Arizona State University

Tempe, Arizona. We would also like to thank Elizabeth Burrows for her technical assistance with the screening assays and Markel Luterra for his review of this manuscript.

CHAPTER 3: EFFECT OF DISSOLVED INORGANIC CARBON LEVELS ON GROWTH, FLUORESCENCE YIELDS, AND CARBON ACCUMULATION IN *THERMOSYNECOCCUS ELONGATUS*

Jed O. Eberly and Roger L. Ely

To be submitted for publication

Abstract

The ability of cyanobacteria to sequester carbon and produce storage compounds with potential biofuel and bioproduct uses is of great interest. Previous studies in this area have focused primarily on mesophilic organisms. The objective of this study was to characterize the growth of *Thermosynechococcus elongatus* on increasing levels of dissolved inorganic carbon and analyze the major carbon storage pools and the effects on growth. *T. elongatus* was grown on 5-150 mM dissolved inorganic carbon (DIC). Growth rates, glycogen, lipid and polyhydroxybutyrate concentrations, and fluorescence parameters were determined in order to ascertain the effect of carbon availability on the primary carbon storage pools. The highest specific growth rate and cell density was 0.42 d^{-1} and 0.87 mg dry wt ml^{-1}, respectively, achieved with culture supplemented with 80 mM dissolved inorganic carbon. Glycogen content increased with increasing concentrations of inorganic carbon while PHB content was greatest under low carbon concentrations. The highest glycogen concentration was 16.1% (w/w) with 150 mM DIC, while the greatest PHB concentration was 10.8% (w/w) at 5 mM DIC. Lipid content did not vary significantly with carbon concentrations and averaged 10-15% (w/w) for all cultures. Chlorophyll fluorescence measurements were also used to analyze carbon uptake. Cultures with 40-100 mM and higher DIC showed increasing non-photochemical quenching which indicates a state 1 to state 2 transition likely caused by high rates of carbon accumulation.

Abbreviations: F_o, Base line fluorescence yield following dark adaptation; Fm, maximum fluorescence yield; F_v, variable fluorescence; F_v/F_m, maximum quantum efficiency of PSII; ΦPS2, Quantum efficiency of PSII; qP, photochemical quenching; NPQ; non-photochemical quenching; ETR, electron transport rate; F_m', light adapted maximum fluorescence; F_v'/F_m', light adapted quantum efficiency

Introduction

Cyanobacteria are photosynthetic bacteria that are ubiquitous in aquatic ecosystems and are found in a diverse range of environments from artic climes to hot springs, deserts, and permafrost zones. Cyanobacteria are responsible for nearly 30% of the earth's annual O_2 production and play an important role in global carbon and nitrogen cycling [65]. The ability of cyanobacteria to harvest solar energy and fix CO_2 has evoked considerable interest in them as a source of renewable bio-based fuels and other bioproducts. Considerable research has focused on the production of fuels such as hydrogen and biodiesel from cyanobacteria [24, 49]. Polyhydroxyalkanoates (PHA), such as polyhydroxybutyrate (PHB), are also found in cyanobacteria and have potential as biofuel and other products such as bioplastics [23, 98]. Additional research has examined biomass production for use in gasification and pyrolysis [55].

Cyanobacteria have mechanisms for the active transport of HCO_3^- and CO_2 that lead to the accumulation of large internal reservoirs of dissolved inorganic carbon (DIC). DIC is the largest nutrient flux that occurs in cyanobacteria [120].

The CO_2 concentrating mechanism (CCM) functions to provide inorganic carbon to the carboxysome where energy derived from photosynthesis is used to make reduced forms of organic carbon that can be utilized by the cell [7]. The CCM enables cells to overcome the low affinity of ribulose bisphosphate caboxylase/oxygenase (Rubisco) for CO_2 by greatly increasing the local CO_2 concentration, in some cases up to 1000 fold above ambient levels [111]. Direct uptake of CO_2 is facilitated by the NDH-1 complex [120] while uptake of HCO_3^- is carried out by several processes. Transfer of HCO_3^- is accomplished either by an extracellular carboanhydrase that converts bicarbonate to CO_2 which is then assimilated into the cell [58] or by direct transfer of carbonate through an active transport system [89].

One tool for evaluating carbon accumulation is chlorophyll fluorescence. Chlorophyll fluorescence has become a valuable technique for simple, non-destructive, real-time analysis of photosynthetic activity. It also provides direct insight into the efficiency of photosynthesis, which has a linear correlation to carbon fixation [88]. Fluorescence also provides an estimate of the rate of electron transport, which can be used to calculate photorespiration rates and corresponding CO_2 uptake and O_2 production rates.

The basic theory of fluorescence is that light energy absorbed by chlorophyll can be used to drive photosynthesis, dissipated as heat, or re-emitted as fluorescence. The amount of fluorescence can then be used to determine the redox state of the photosynthetic electron transport chain [114] and to provide insight into stress responses, including those caused by excess carbon or carbon limitation [88].

The level of inorganic carbon is known to affect the response of fluorescence quenching and the quantum yield of PSII [7]. Fluorescence quenching can indicate a state transition due to a change in electron flow through the photosynthetic pathway. State transitions are defined as a shift in the energy distribution between PSII and PSI. There are several theories regarding the cause of this transition from state 1 to state 2. One possibility is that the transition from state 1 to state 2 occurs when the energy distribution is shifted from PSII to PSI due to the reduced state of intermediate electron carriers [54]. Another possibility is that the state transition occurs due to increased cyclic electron flow around PSI [102] caused by another metabolic process such as increased carbon accumulation [112]. While fluorescence response has been linked to carbon accumulation, to date there has been no correlation established between the fluorescence response and metabolic activities that lead to the accumulation of specific storage compounds such as glycogen or PHB. Even less is known about fluorescence responses in thermophilic cyanobacteria.

Cyanobacteria store reduced carbon as glycogen, PHB, and lipids [98, 109, 155]. PHB were initially believed to play a relatively minor role as a carbon storage compound in cyanobacteria [141]. Initial findings of PHB in cyanobacteria were unexpected because cyanobacteria lack a complete citric acid cycle and thus the metabolism of PHB can provide products of only limited use in the cell [30]. In spite of this, more recent data have shown that some species sequester large reserves of PHB, up to 30% cell dry weight [98]. Lipids and PHB are of particular interest because of their potential as precursors for biofuels and bioplastics. Much effort in recent years has focused on identifying organisms with the ability to produce high concentrations of these compounds and to optimize their production [24, 81, 134].

The species used in this study, *Thermosynechococcus elongatus*, is a unicellular thermophilic cyanobacterium found in hot springs at an optimal temperature of 55°C and is an obligate autotroph [108]. It is naturally transformable and has been fully sequenced. The photosystems of *T. elongatus* have served as models for extensive structural studies due to their extraordinary stability [63, 77], however very little is known about the metabolic pathways in this organism. This is due in part to the fact that it is an obligate autotroph and thus is not amenable to significant knockout mutations that are often needed to analyze metabolic pathways.

The aim of this study was to characterize the growth and major carbon stores of *T. elongatus* grown on increasing concentrations of dissolved inorganic

carbon (DIC) and to identify compounds of potential interest for biofuels and bioproducts. The effect of carbon accumulation on fluorescence parameters was also determined. Chlorophyll fluorescence was used to measure photosynthetic efficiency and quenching parameters and to identify potential stress responses and state 1 to state 2 transitions due to high carbon concentrations or carbon limitation. We also demonstrate that chlorophyll fluorescence is an effective method of monitoring inorganic carbon assimilation, as previously proposed [93].

Materials and Methods

Culturing conditions

Thermosynechococcus elongatus BP-1 was cultured in BG-11 media [20] supplemented with TES-KOH, pH 7.8, at 48°C under continuous lighting (30-50 $\mu E\ m^{-2}\ s^{-1}$). Cultures were incubated in 500 ml Erlenmeyer flasks containing 150 ml media on an orbital shaker table at 120 rpm and cell growth was monitored by measuring the optical density at 730 nm. An equimolar mixture of $NaHCO_3$ and Na_2CO_3 was used as a dissolved inorganic carbon (DIC) source and the cultures were supplemented with 5, 10, 20, 40, 60, 80, 100, and 150 mM concentrations with pH maintained at 7.8. Growth rate data were also collected from cultures grown on 0.8 mM DIC and used for establishing kinetic parameters, however the biomass at this concentration was not sufficient to do the other

analyses. The determination of the growth kinetics of *T. elongatus* were calculated using the Monod model, relating growth to the concentration of DIC. All experiments were done in triplicate.

Growth and biomass analysis

Chlorophyll concentrations were determined using methanol extraction followed by spectrophotometric measurement at 665 nm, with concentrations calculated by the method of Porra, 2002 [119]. Biomass yield was measured by filtering the cells on Whatman filter paper and drying them overnight in a drying oven at 60°C.

Glycogen was measured based on the method of Ernst [40]. Cells were concentrated to 600 μg Chl ml^{-1} in a final volume of 50 μl, and 200 μl of 30% w/v KOH was added prior to incubating 90 minutes at 100°C. Samples were cooled and 600 μl of ethanol was added followed by incubation on ice for 2 hours to precipitate the glycogen, which was then collected by centrifugation and washed twice with ethanol. The pellets were then resuspended in 300 μl of 100mM sodium acetate at pH 4.75, and 10μl each of amyloglucosidase (1U/μl) and amylase (2U/μl) were added, followed by incubation for 1 hour at room temperature to convert the glycogen to glucose. A glycogen standard was run to ensure the enzymatic digest was complete during the incubation time and was also used to correlate glucose concentration to the initial glycogen concentration.

The glucose concentration was then determined with a Sigma glucose assay kit (GAGO20-1KT, Sigma-Aldrich, St. Louis, MO, USA).

Lipids were extracted following the method of Bligh and Dyer (Bligh, 1959). 50 ml of cell culture were centrifuged and resuspended in 20X the wet pellet weight of 2:1 methanol (50 µg BHT/ml): chloroform, bead beat 2 minutes, and incubated shaking at 160 rpm at room temperature. The lipids were then extracted with chloroform and dried at 50°C for 2 hours prior to measuring.

PHB extraction was done following the method of Law and Slepecky using heat and H_2SO_4 to convert PHB's quantitatively to crotonic acid [75]. PHB was extracted by boiling the samples in chloroform at 60°C for 6 hours after incubating the sample in methanol overnight to remove pigments. The samples were filtered through a glass filter while hot. A 0.5 ml aliquot was then evaporated and 4 ml H_2SO_4 was added and the sample was boiled at 100°C for 10 min. and the absorbance was measured at 230 nm. A standard curve was made using 10 mg PHB granules (GoodFellow Oakdale PA, USA) dissolved in 10 ml H_2SO_4. Additional cultures grown with 5 and 100 mM DIC were also nitrogen deprived for 24 hours prior to extracting PHB's.

Chorophyll fluorescence parameters were measured using a Hansatech FMS1 fluorescence monitoring system (Hansatech Instruments LTD, Norfolk, England). Measurements were made in a Hansatech liquid phase electrode chamber (Hansatech Instruments LTD, Norfolk, England) after 3 days of growth at approximately mid exponential phase. Temperature during the measurement

was maintained at 45°C with a circulating water bath. Cells were dark acclimated for 5 minutes prior to measuring. Cultures were measured with chlorophyll content between 8-12 μg/ml to ensure consistent quenching analysis [145] [17]. F_m was also measured in the presence of 50 μM DCMU, an inhibitor of photosynthetic electron flow; to ensure complete closure of PSII reaction centers and verify that the initially recorded F_m was saturating. Fluorescence quenching parameters were determined with samples exposed to the same level of light they were acclimated to under standard growing conditions (50 μE m^{-2} s^{-1}). Fluorescence parameters were calculated using the equations from Campbell et al. [17] and Maxwell and Johnson [88] and standard nomenclature from van Kooten and Snell [71].

Results

A maximum cell density of OD_{730} = 1.04 was achieved with 100 mM DIC concentration (Figure 3. 1) while cultures grown on 150 mM DIC only doubled in density.

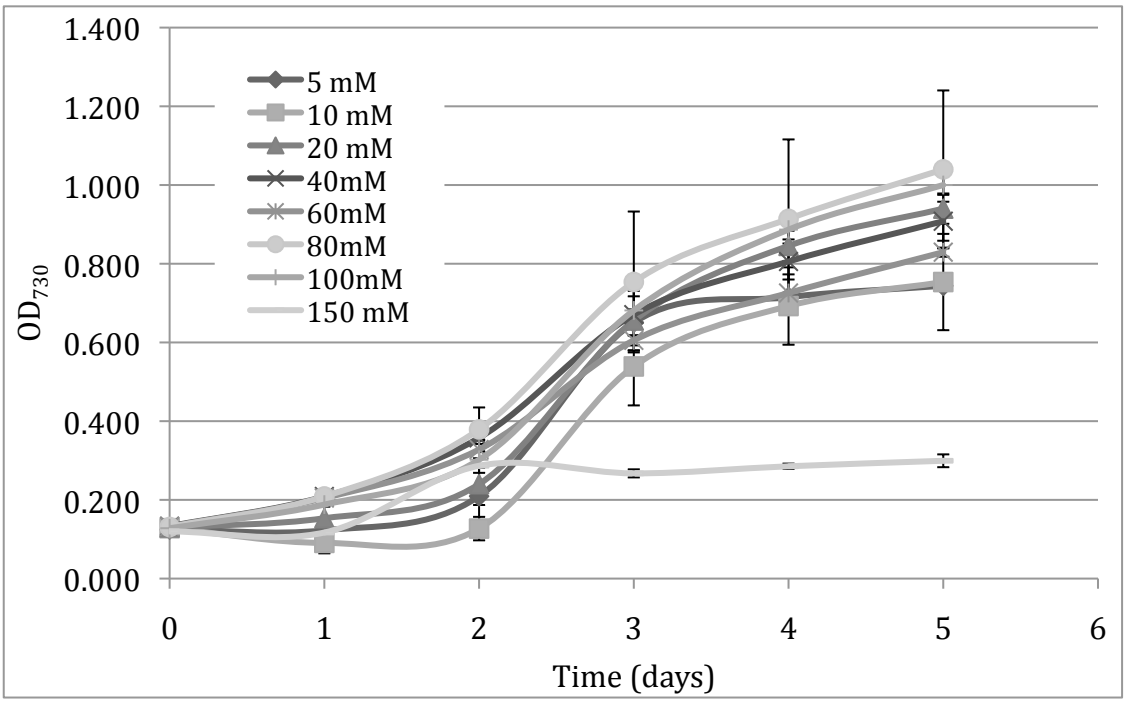

Figure 3. 1. Growth curves of *T. elongatus* on increasing levels of DIC. Data points represent mean (n = 3). Error bars indicate standard deviation from the mean.

Cell density was still increasing through day 5, indicating that stationary phase was not yet reached with DIC concentrations above 20 mM while cultures growing on 5 and 10 mM DIC had entered stationary phase. Cultures grown on 150 mM DIC achieved less than half the density of the other cultures. The average specific growth rate for cultures grown on each DIC level was calculated by the following equation:

$$\mu = \frac{\mathrm{Ln}(\mathrm{OD}_{730}/\mathrm{OD}_{730\mathrm{o}})}{\Delta \mathrm{t}} \qquad (3.1)$$

Where μ is the specific growth rate (d^{-1}), OD_{730o} is the initial and OD_{730} is the final optical density at 730 nm, and Δt is the time period in days. The specific growth rate increased with increasing DIC concentration and reached a maximum rate of 0.414 d^{-1} for cultures growing on 80 mM DIC (Figure 3. 2). The growth kinetics were modeled using the Monod equation [14]:

$$\mu = \frac{\mu_{max} S}{K_S + S} \tag{3.2}$$

The nonlinear Monod model-fitting parameters were fit using the sum of the squared weighted errors [140]. The values of the fitting parameters were: μ_{max} 0.416 d^{-1}, K_s 0.868 mM.

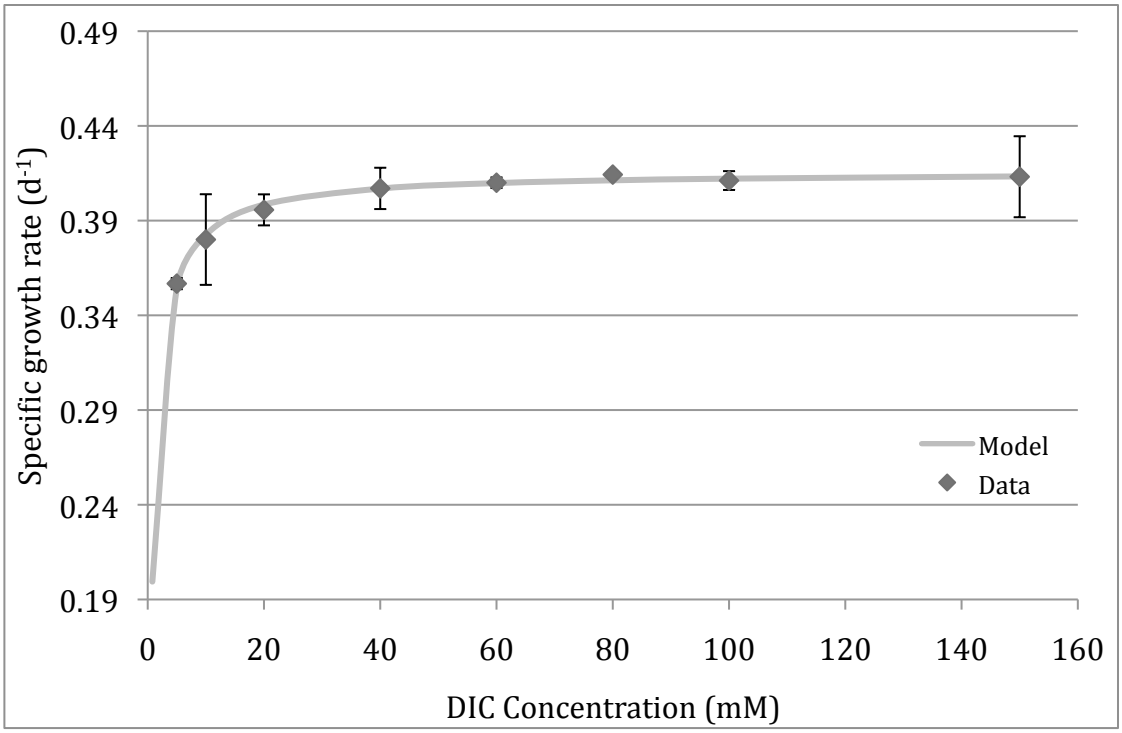

Figure 3. 2. Monod model simulation of the data from figure 1 showing the specific growth rates as a function of DIC concentration.

The highest biomass concentration was 0.869 mg dry wt/ml in cultures grown on 80 mM DIC. Chlorophyll content was approximately 17.0 μg/mg dry cell weight at 5 mM DIC and reached a maximum of 40.0 μg/mg dry cell weight at 60 mM DIC (Figure 3. 3). Carbon concentrations between 20-80 mM did not significantly affect chlorophyll content. At 150 mM DIC, chlorophyll content decreased to only 20 μg/mg dry cell weight, which was 34% less than at 40 and 60 mM DIC.

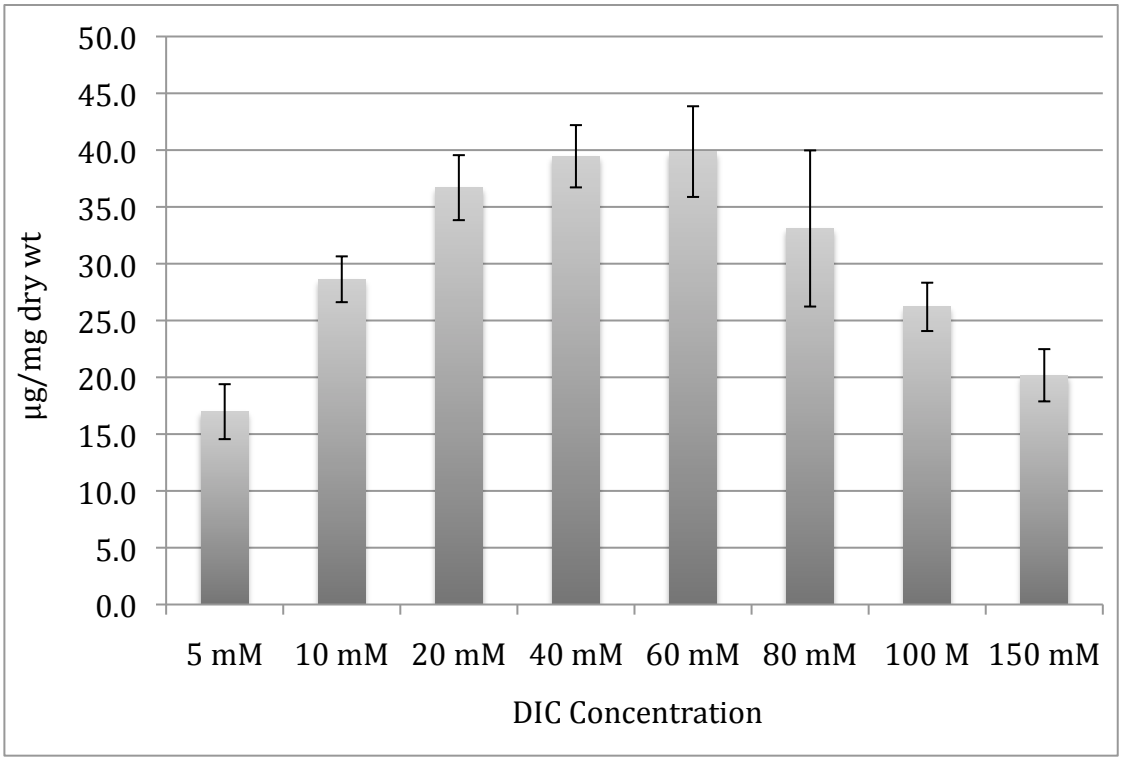

Figure 3. 3. Chlorophyll content as a function of DIC concentration. Data points represent mean (n = 3). Error bars indicate standard deviation from the mean.

Glycogen content was not statistically different between cultures grown on 5-60 mM DIC, remaining around 20-25 µg/mg dry wt. However cultures supplemented with 80 and 100 mM DIC showed a 3.5 and 5 fold increase in glycogen respectively and a maximum glycogen content of 16.12% (w/w) was achieved in cultures grown on 150 mM DIC (Figure 3. 4). Lipid content did not vary substantially at any level of DIC and was around 12% (w/w) for all samples. (data not shown).

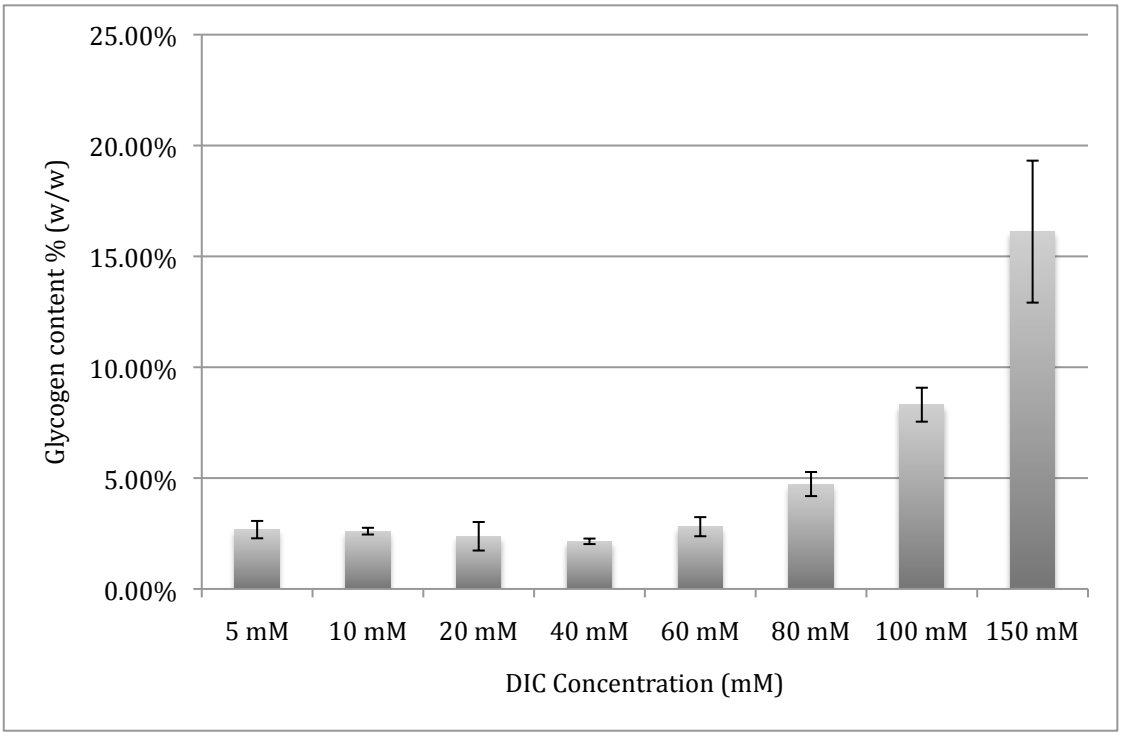

Figure 3. 4. Glycogen concentration as a function of DIC concentration. Data points represent mean (n = 3). Error bars indicate standard deviation from the mean.

PHB content decreased with increasing levels of DIC. The highest content was around 10.8% (w/w) in cultures grown on 5 mM DIC (Figure 3. 5). At 80 and 100 mM DIC concentrations, PHB content decreased to around 2% (w/w). Nitrogen deprivation also affected PHB accumulation. At 5 mM DIC, incubating the cultures for 24 hours without nitrogen decreased the PHB content to 8.75% (w/w) while cultures grown on 100 mM DIC increased 3–fold to 7% (w/w) when incubated without nitrogen (Figure 3. 5, inset).

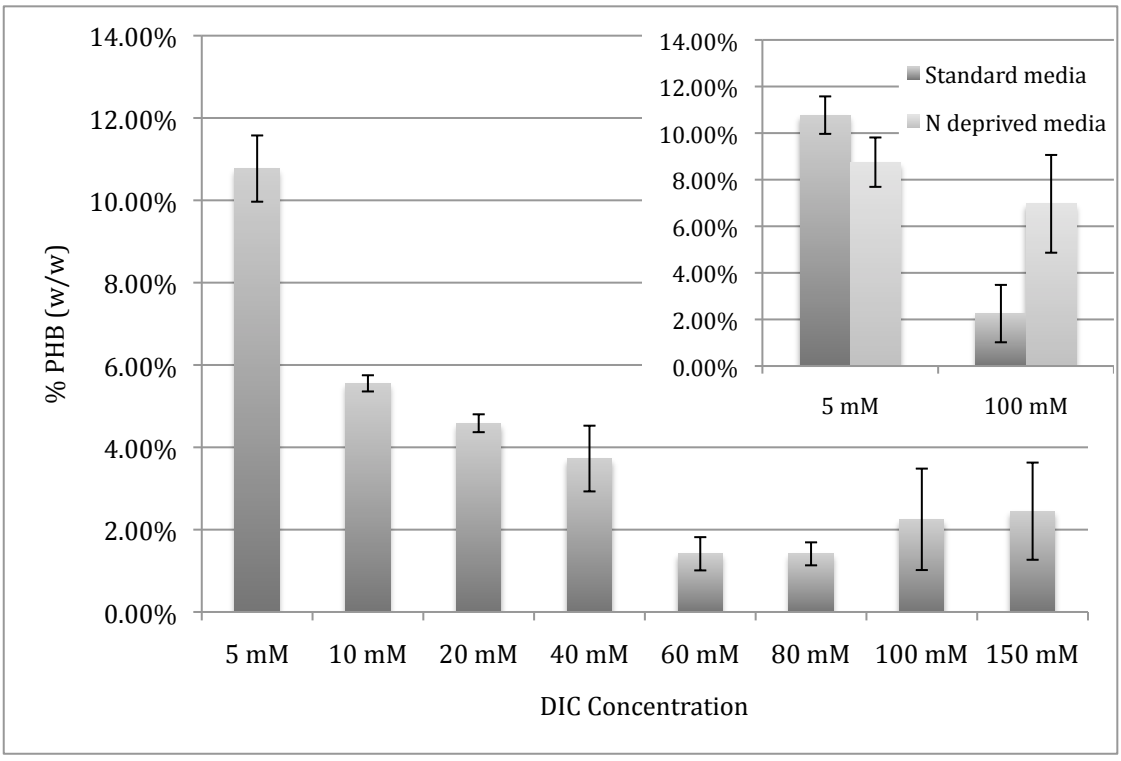

Figure 3. 5. Variation in PHB content with increasing levels of DIC. Inset shows samples grown on 5 and 100 mM DIC followed by 24 hours N deprivation. Data points represent mean (n = 3). Error bars indicate standard deviation from the mean.

Fluorescence analysis showed that maximum quantum efficiency was achieved between 40-80 mM DIC (Figure 3. 6). At 100 and 150 mM DIC, quantum efficiency was 20% less than the maximum at 60 mM DIC. From 5-20 mM DIC, the maximum quantum efficiency was only 60% of the efficiency of cells grown on 40-80 mM. The addition of DCMU did not result in an increase in F_m, demonstrating that saturation of PSII was possible without the addition of an electron inhibitor (data not shown).

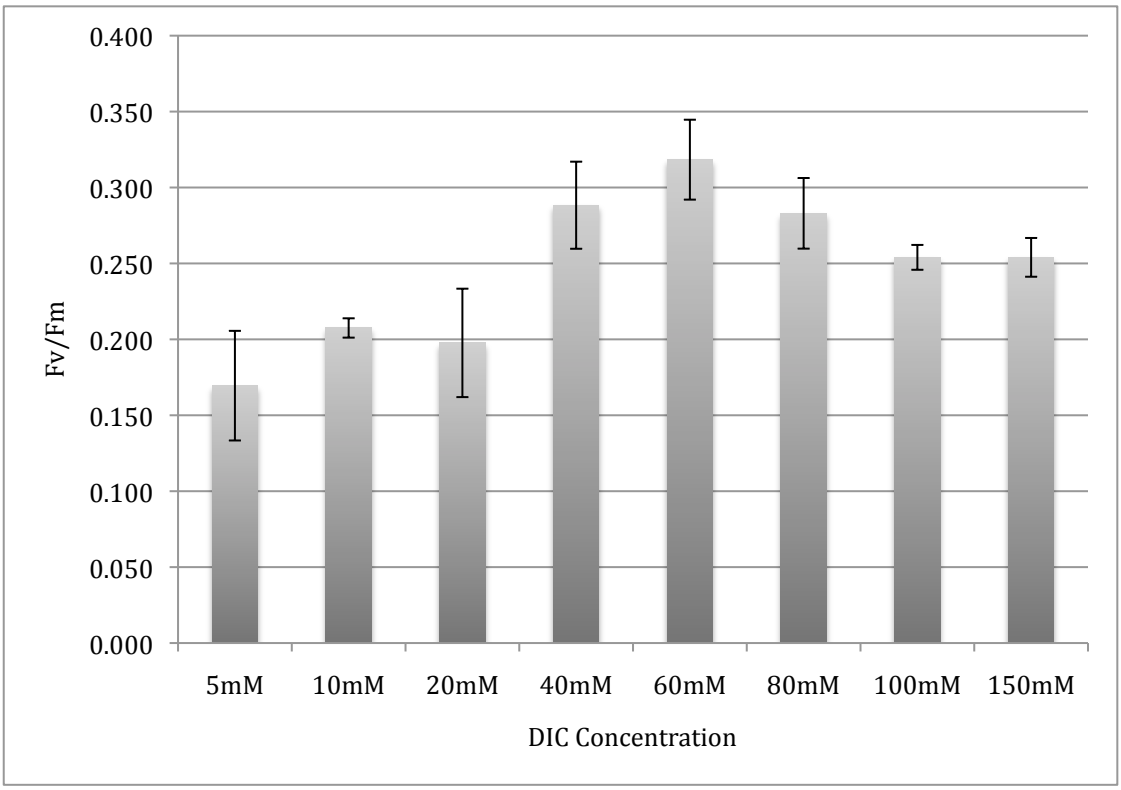

Figure 3. 6. Maximum quantum efficiency of PSII. Data points represent mean (n = 3). Error bars indicate standard deviation from the mean.

Analysis of quenching parameters showed very little change in qP with a decrease from 0.94-0.73 over the range from 5 mM to 150 mM DIC. NPQ was not detectable from 5-20 and 150 mM DIC but increased to 0.14 in cultures with 80 and 100 mM DIC (Figure 3. 7).

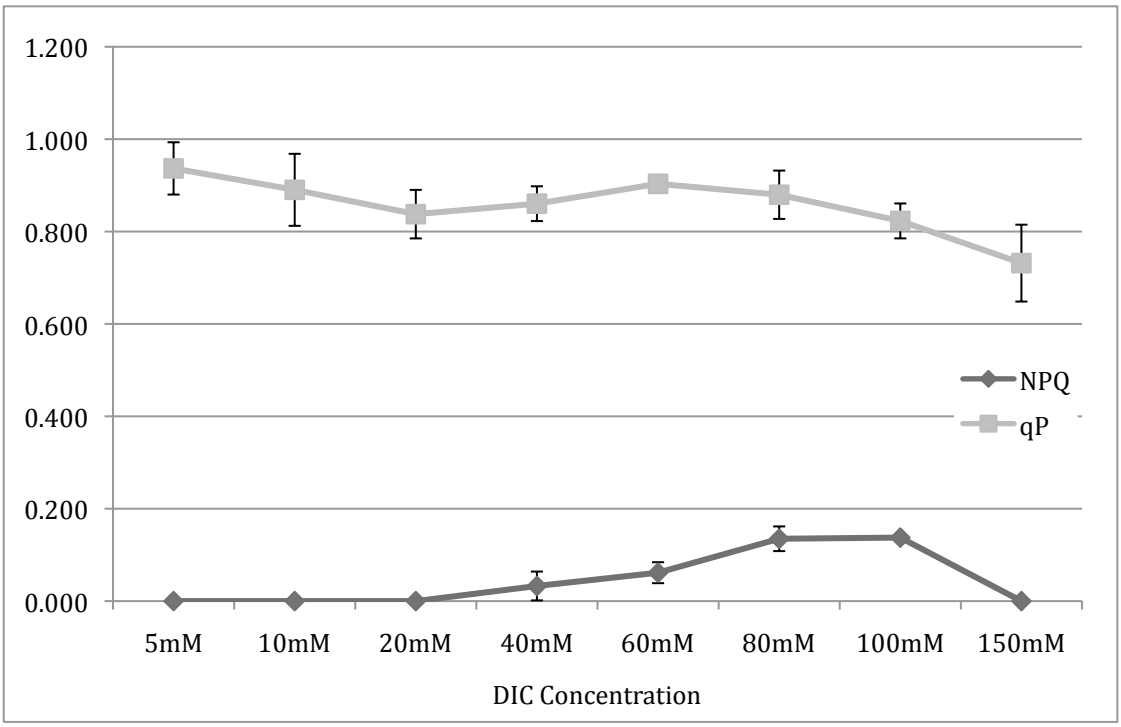

Figure 3. 7. Photochemical and non-photochemical quenching of fluorescence in dark acclimated cultures. Data points represent mean (n = 3). Error bars indicate standard deviation from the mean.

Discussion

Direct uptake of CO_2 and HCO_3^- has been reported in cyanobacteria and sequence analysis has indicated that *T. elongatus* has *cmpABCD*, which encodes for a high affinity ATPase that has been implicated in HCO_3^- transport [6]. However it does not have homologues of the *sbtA* gene that encodes a Na^+/HCO_3^- symporter in *Synechococcus* PCC 7942 and *Synechocystis* PCC 6803 [6]. *T. elongatus* also contains a NDH-1 complex, which is involved in CO_2 uptake [9]. The ability of *T. elongatus* to grow to high densities and sequester high levels of

glycogen when grown on 80 mM and higher DIC concentrations (Figure 3. 4) indicates that they have the ability to take up HCO_3^- directly, likely by a c*mpABCD* type transporter.

The specific growth rate did not increase significantly above 40 mM DIC, which indicates that at this concentration and above, the CCM is operating at its maximum capacity and increasing the carbon concentration above this point cannot stimulate higher growth rates and may only cause an inhibitory effect which became apparent based on the much lower cell density at 150 mM DIC (Figure 3. 1).

Cyanobacteria fix CO_2 through the reductive pentose phosphate pathway (Calvin cycle) and store the reduced carbon as glycogen. Glycogen stores are then oxidized in the dark by the oxidative pentose phosphate pathway to generate energy when sunlight is not available [141]. Glycogen concentration reached a maximum of around 16.12% (w/w) in *T. elongatus* at 150 mM DIC. This was 6-fold higher than the concentration of glycogen in cells grown on 5-60 mM DIC (Figure 3. 4) but significantly less than values reported for other species, such as *Spirulina maxima*, which can accumulate up to 70% (w/w) glycogen when grown in nitrogen-limited conditions [30]. A DIC concentration of at least 80 mM was needed to stimulate glycogen accumulation above baseline levels.

PHB accumulation appeared to be the inverse of glycogen accumulation as carbonate concentrations were increased. PHB levels were comparable to values reported for other cyanobacteria. Under standard conditions *Synechocystis* sp.

PCC 6803 accumulates around 6% (w/w) PHB [29] and *Spirulina* strains can accumulate from 0.10-6.0% (w/w) [30]. One exceptionally high PHB producer is the thermophilic cyanobacterium *Synechococcus* sp. MA19 where PHB content up to 27% (w/w) has been reported under nitrogen-depleted conditions [97]. This is significantly higher than maximum PHB yield of around 11% (w/w) that was observed in *T. elongatus* without nitrogen deprivation.

Nitrogen limitation is known to cause a stress response that leads to increased PHB accumulation [97]. It is also possible that a similar stress response is initiated under carbon-limiting conditions, causing cells to accumulate PHB. PHB is also known to accumulate as cells enter stationary phase [141], which is consistent with what was observed in this experiment. Cells grown on 5 and 10 mM DIC had entered stationary phase (Figure 3. 1) due to carbon limitation, since other nutrient levels were the same with the exception of DIC concentration. Nitrogen deprivation in carbon-limited cultures did not lead to PHB accumulation as high as was observed with carbon limitation alone. However, in cultures that had abundant carbon, nitrogen deprivation did lead to a 3-fold increase in PHB (Figure 3. 5). The effects of carbon and nitrogen limitation did not appear to be additive as cultures grown with low carbon followed by nitrogen deprivation showed less PHB than cultures grown only in carbon limited conditions. The data also suggest that carbon limitation is more effective than nitrogen deprivation for increasing PHB accumulation in *T. elongatus*.

When carbon was abundant, cells accumulated large quantities of glycogen (Figure 3. 4) and PHB concentrations were high when carbon was scarce (Figure 3. 5). This inverse relationship between glycogen and PHB has not been previously reported. De Philippis et al [30] found that in *Spirulina maxima*, simultaneous glycogen and PHB accumulation occurred but glycogen was much more heavily accumulated than PHB under all test conditions. However, under varying nitrogen sources PHB levels changed, indicating that competition for reducing equivalents existed between nitrogenase activity and PHB synthesis. Based on these results they proposed that PHB acts as a regulator of intracellular reduction charge [29]. While PHB may act as an internal regulator, the data from *T. elongatus* suggest it may be more a function of carbon availability rather than excess reducing power since carbon limitation led to greater PHB accumulation than nitrogen deprivation did.

Accumulation of PHB has also been attributed to an imbalance in the C/N ratio and NADPH/ATP ratio in some cyanobacteria [29, 141]. De Philippis et al. [29] reported that under phosphate limiting conditions, the ratio of NADPH and ATP formation from photosynthesis could be changed, resulting in an accumulation of reducing power that favored PHB production. It is also known that increased intracellular acetyl-CoA levels favor the synthesis of PHB [29].

Lipid content did not vary substantially at any level of DIC, indicating that, under the conditions of these experiments, it is not significantly affected by availability of inorganic carbon and thus does not play a significant role as a

carbon storage pool. The data indicate that *T. elongatus* may not be a good candidate for lipid production, especially when compared to mesophilic species that can accumulate up to 50% of their dry weight in lipids [33]. Insufficient data is available to make comparisons with many other thermophilic cyanobacteria.

The chlorophyll fluorescence response provided some additional insight into the effect of DIC concentrations on *T. elongatus*. Inorganic carbon accumulation is known to affect chlorophyll fluorescence by stimulating linear electron flow through a mechanism that remains unknown [94]. Several mechanisms have been proposed for this effect. It may be directly related to inorganic carbon uptake, which requires ATP, derived from photosynthesis or it may be a direct effect of carbon accumulation in the cell [7].

In many cyanobacteria, the addition of a photosynthetic electron transport inhibitor is needed to obtain maximum fluorescence (F_m) because of rapid electron removal from PSII due to the high PSI to PSII ratio [7, 17]. However in *T. elongatus* the initial dark-adapted F_m value was higher than F_m after the addition of DCMU, indicating that PSII was completely saturated, therefore F_v/F_m could be accurately calculated.

In cyanobacteria the maximum quantum efficiency of PSII (F_v/F_m) is around 0.4 to 0.6, while in plants it is around 0.8 [17]. This is because PSII represents a relatively small proportion of total chlorophyll in cyanobacteria and therefore the absolute value of F_v/F_m is not a dependable indicator of PSII kinetics [17]. However it remains a valid and commonly used relative indicator of

efficiency between cultures of the same species grown under different conditions provided that chlorophyll content remains consistent between samples. *T. elongatus* had a much lower F_v/F_m with a maximum value of only 0.318 with cells grown on 60 mM DIC. This is somewhat less than the range of 0.4-0.6 observed in other cyanobacteria [17] and suggests that either the cultures where not growing under optimal conditions or that this is the normal range for thermophilic cyanobacteria. However there is a paucity of fluorescence data from thermophilic cyanobacteria and no conclusions can be drawn in regard to the effect of high temperatures on maximum quantum efficiency.

The level of qP remained high and with no statistically significant difference between 5-80 mM, indicating that the cultures were active with most reaction centers open. However, cultures grown on 150 mM DIC had a 23% decrease in qP relative to cells grown on 5 mM DIC. This is consistent with observations in other cyanobacteria [94] and is a reflection of the flexibility of photosynthetic electron transport systems and the high PSI to PSII ratio in cyanobacteria.

No detectable level of NPQ was observed between 5-20 mM DIC. NPQ in cyanobacteria is due primarily to changes in PSII fluorescence yields associated with state transitions [17]. The rise in NPQ and commensurate slight decline of qP in cultures grown with higher DIC concentrations indicates that these cultures were transitioning from state 1 to state 2, thus lowering the rate of PSII photochemistry. State transitions such as these are regulated by either the redox

state of the photosynthetic electron transport chain or by the degree of cyclic electron flow around PSI [102]. The latter explanation seems most likely in *T. elongatus* as the shift to state 2 and the corresponding rise in NPQ was correlated to the DIC concentrations, which would influence the rate of carbon accumulation. Active transport of inorganic carbon is known to drive the transition to state 2, presumably due to the need for cyclic electron flow to produce ATP to provide energy for the carbon concentrating mechanism [112]. Miller et al. [94] proposed that this requirement led to the down regulation of PSII activity to allow high rates of cyclic electron flow for inorganic carbon transport. This would cause a commensurate decrease in quantum yield from PSII and a reciprocal increase in NPQ as was observed in *T. elongatus* at high carbon concentrations. Miller et al. [95] reported that in the absence of inorganic carbon, NPQ could not be observed. It seems reasonable to conclude that the observed non-photochemical fluorescence quenching response at higher DIC levels was due to the ability of the cultures to continue accumulating available carbon. The cultures with 5-20 mM DIC had likely depleted most of the available carbon, while cultures with 40-100 mM DIC still had excess carbon available and were able to continue accumulation as indicated by the NPQ data (Figure 3. 7). The one exception was cultures grown on 150 mM DIC. However, the growth of these cultures was much lower, indicating they were stressed from the high DIC concentration which likely had an effect on their fluorescence response.

Conclusion

The ability of *T. elongatus* to grow under high levels of DIC is significant and indicates that it may be a suitable model organism for developing carbon sequestration strategies. Organisms that can tolerate high concentrations of DIC could be advantageous in industrial CO_2 sequestration where photosynthesis-mediated CO_2 uptake is only functional during the daytime. CO_2 released during the night could be converted to carbonate species and stored for daytime use by microorganisms. The use of an organism such as *T. elongatus* would be advantageous in this situation since only a few species of microalgae can grow well in media with high levels of carbonate salts [152].

When taken together, the growth, carbon storage, and fluorescence data provide a picture of the overall conditions of the cultures. At low DIC concentrations the cells are stressed, as shown by the fluorescence data, and they accumulate PHB either as a stress response or potentially as a way of more efficiently storing carbon. At mid-range DIC levels photosynthetic activity is greatest but neither glycogen nor PHB are accumulated in extremely high concentrations. At this point carbon accumulation is likely not sufficient to induce a state 1 to state 2 transition which would lower overall photosynthetic efficiency. At high DIC concentrations (80-100 mM) photosynthetic activity decreased, as shown by the increase in NPQ (Figure 3. 7), and a corresponding increase in glycogen reserves was observed. Overall, the fluorescence data supported previous reports of fluorescence in cyanobacteria. One notable

exception was that F_m reflected the true maximum fluorescence and the addition of DCMU was not needed to achieve F_m.

Of all the carbon storage compounds with potential as biofuels or biomaterials, only PHB accumulated in significant enough amounts to warrant further consideration. Currently, *Ralstonia eutropha* is widely studied for PHB production and is capable of producing up to 34% dry wt [21]. However *R. eutropha* relies on potentialy expensive feedstocks such as glucose, which limits industrial potential. In contrast, *T. elongatus* is an obligate autotroph and can grow with much lower nutrient inputs. Thus it may provide an alternative for high PHB production with appropriate genetic modification. More work is needed to understand the genetic basis of PHB accumulation in *T. elongatus* and to explore potential modifications that could further increase production. Future work is also needed to determine if similar responses are seen when cultures are grown with high levels of CO_2.

Acknowledgements

This work was supported in part by the Subsurface Biosphere Integrative Graduate Education and Research Traineeship program at Oregon State University, NSF-0114427 and in part by the DOD/ASEE SMART scholarship program. We would also like to thank to David Dickson and Mark Luterra for reviewing this manuscript.

CHAPTER 4: PHOTOSYNTHETIC ACCUMULATION OF CARBON STORAGE COMPOUNDS UNDER CO_2 ENRICHMENT BY THE THERMOPHILIC CYANOBACTERIUM *THERMOSYNECOCCUS ELONGATUS*

Jed. O. Eberly and Roger L. Ely

To be submitted for publication

Abstract

The growth characteristics of *Thermosynechococcus elongatus* on elevated CO_2 were studied in a photobioreactor. Cultures were able to grow on up to 20% CO_2. The maximum productivity and CO_2 fixation rates were 0.09±0.01 mg ml^{-1} d^{-1} and 0.17±0.01 mg ml^{-1} d^{-1} respectively for cultures grown on 20% CO_2. Three major carbon pools; lipids, PHB's, and glycogen, were measured. These carbon stores accounted for 60% of the total biomass carbon in cultures grown on atmospheric CO_2 (no supplemental CO_2) but only accounted for 40% of the total biomass carbon in cultures grown on 5-20% CO_2. Lipid content was around 20% (w/w) under all experimental conditions while PHB content reached 14.5% (w/w) in cultures grown on atmospheric CO_2 and decreased to around 2.0% (w/w) at 5-20% CO_2. Glycogen levels did not vary significantly and remained around 1.4% (w/w) under all test conditions. The maximum amount of CO_2 sequestered over the course of the 9 day chemostat experiment was 1.15 g L^{-1} in cultures grown on 20% CO_2.

Introduction

The past decade has seen a renewed interest in biofuel and biomaterial research corresponding to declining petroleum reserves and the consequent rise in energy costs. Cyanobacteria are ideal organisms for producing biofuels and bioproducts because of their ability to utilize solar energy directly. Cyanobacteria also assimilate CO_2 and thus may also be an effective means of mitigating rising

CO_2 levels while generating biofuels and other valuable bioproducts. Recent reviews have discussed the numerous advantages of combined CO_2 mitigation and biofuels production by microorganisms [2, 133, 137, 152]. This has driven recent efforts in utilizing cyanobacteria and algae for carbon sequestration at power plants and other industrial facilities that produce flue gas which can contain up to 20% CO_2 [56]. The higher CO_2 concentrations found in industrial flue gas could contribute to improved growth rates since the atmosphere contains only 0.03-0.06% CO_2 [152]. Cyanobacteria are also effective at nitrogen and phosphorous removal [85] and aid in metal ion depletion [152], which makes them suitable for wastewater treatment, thereby providing an additional benefit for industrial waste processing.

Using photobioreactors to culture cyanobacteria for CO_2 sequestration offers several advantages. First, increased concentrations of CO_2 can be fed to the cultures, leading to improved productivity. Second, water-use efficiency is greater since evaporation is minimized. And finally, environmental conditions can be carefully controlled, thus minimizing contamination.

There are several obstacles to efficient CO_2 sequestration by cyanobacteria. One key limitation in CO_2 utilization by photosynthetic microbes is the low mass transfer coefficient between CO_2 and water [36]. Even though CO_2 levels may be relatively high, the CO_2 available in solution may limit culture growth.

Another limitation to CO_2 sequestration and biomass production is the elevated temperatures that can be encountered in bioreactors operated in direct sunlight. In a recent review Mata, et al [86] reported that the effect of temperature on biomass production is one important factor that has not yet been sufficiently acknowledged in biomass production and renewable energy research. Part of this limitation is the temperature-dependent solubility of CO_2. As temperature increases, CO_2 solubility decreases, thus lowering the available CO_2. At 30°C, the physiological optima of many cyanobacteria, the solubility constant of CO_2 in water is $2.965x10^{-2}$ mol/L·atm while at 50°C it decreases to $1.817x10^{-2}$ mol/L·atm [32]. Temperatures in photobioreactors can reach 55°C on hot days [86] thus necessitating the use of cooling systems to maintain a constant temperature. Utilizing thermophilic organisms would minimize the amount of energy expended on cooling, thereby contributing to the overall efficiency of the system.

Cyanobacteria store carbon primarily as glycogen [72], while some species of cyanobacteria also accumulate large reserves of lipids and polyhydroxyalkanoates (PHA's) such as polyhydroxybutyrate (PHB) [98, 142], all of which have potential uses as biofuels or biomaterials. Cyanobacteria can also be used as a source of biomass for gasification and pyrolysis for generating fuels [55]. Cyanobacteria are also a source of compounds such as acetylic acids, β-carotene, vitamin B, carotenoids, polyunsaturated fatty acids, lutein, and

cyanophycin that are of value in the health food, pigment, and pharmaceutical industries [48, 52, 76].

Thermophilic cyanobacteria represent a unique subset of phototrophs with characteristics that make them particularly amenable to industrial CO_2 sequestration. The higher optimal growth temperature lowers the likelihood of competing species and may enable them to grow in the high temperature wastewater and flue gas streams emitted from industrial plants. Utilizing thermophilic species could also lower the cooling costs associated with the high temperature waste streams emitted from many industrial facilities [113, 152].

T. elongatus is a unicellular cyanobacterium that grows in hot springs at a temperature of 48-55°C and is an obligate autotroph [108]. The photosystems of *T. elongatus* have served as models for extensive structural studies due to their extraordinary stability [63, 77], however very little is known about the metabolic pathways in this organism. This is due in part to the fact that it is an obligate autotroph and thus is not amenable to significant knockout mutations that are often needed to analyze metabolic pathways.

The aim of this study was to characterize the growth of *T. elongatus* on increasing levels of CO_2 and to determine the carbon uptake rates and maximum productivity in a bioreactor configuration. Accumulation of carbon storage compounds with biofuel and bioproduct potential was also examined.

Materials and Methods

Culturing conditions

Thermosynechococcus elongatus BP-1 was cultured in BG-11 media [20] supplemented with TES-KOH at pH 7.8. Cell growth was monitored by measuring the optical density of the cultures at 730 nm and chlorophyll concentrations were determined using methanol extraction followed by spectrophotometric measurement at 665 nm, with concentrations calculated by the method of Porra, 2002 [119].

Bioreactor Experiments

Bioreactor experiments were carried out in Applikon 3 L water-jacketed glass reactor vessels connected to Applikon ADI 1025 and 1035 Bioconsoles controlled by ADI 1010 and 1020 Biocontrollers (Applikon, Schiedam, Netherlands). Gas flow was controlled using the built in rotameters. Cultures were grown at 50°C, pH 7.8 with a stir speed of 300 rpm. Light was supplied from below at 180 μE m^{-2} s^{-1}. Reactors were bubbled with a mixture of sterile filtered air and CO_2 at a flow rate of 20 ml/min. Cultures were grown under atmospheric, 5, 10, 20, and 30% CO_2. CO_2 concentrations were monitored daily by sterilely removing 100 μl gas samples which were measured by gas chromatography (GC) with a thermal conductivity detector (Agilent Technologies Series 6890N Santa Clara, CA, USA) and GS-CARBONPLOT 30 m x 0.32 mm x 3.0 mm column using argon as the carrier gas with a column flow rate of 1.6 mL min^{-1}. The oven

temperature was 35°C and the detector temperature was 150°C. All bioreactor experiments were run in triplicate. Biomass, OD_{730} and $\%CO_2$ measurements were taken daily over the course of each 9-day experiment. Prior to harvesting the cells, an aliquot was sterilely removed and cultured on BG-11 agar to screen for contamination.

Biomass analysis

The biomass concentration was measured gravimetrically by centrifuging the cells and drying the resultant cell pellet at 60°C for 24 hours. Elemental analysis was done to determine total carbon and nitrogen using a Costech Instruments ECS 4010 System (Costec Analytical Technologies, Valencia, CA USA). The biomass was dried and a <2 mg sample was oxidized at 1000°C and the resulting gasses were measured and compared to an atropene standard.

Carbon storage compounds

Lipids were extracted and quantified following the colorimetric method of Christie [25] modified from the method of Folch et al [41]. Samples were dried, then resuspended in 5 ml $CHCI_3$-MeOH (2:1 v/v) and incubated, shaking overnight at room temperature. Following centrifugation, the supernatant was saved and the pellet extracted twice more with 5 ml $CHCI_3$-MeOH (2:1 v/v). 0.88% KCl was added to the combined supernatant volume, which was then mixed and centrifuged. An aliquot of the bottom fraction containing the lipids was then boiled 45 minutes with potassium dichromate and the absorbance was

measured at 350 nm. A standard curve was generated using palmitic acid. Total carbon in the lipid extracts was determined by elemental analysis.

PHB extraction was done following the method of Law and Slepecky that uses heat and H_2SO_4 to quantitatively convert PHB's to crotonic acid [75]. PHB's were extracted by boiling the samples in chloroform at 60°C for 6 hours. The samples were filtered through a glass filter while hot. A 0.5 ml aliquot was then evaporated, 4 ml H_2SO_4 were added, and the sample was boiled at 100°C for 10 min, and the absorbance was measured at 230 nm. A standard curve was made by dissolving PHB granules (GoodFellow, Oakdale PA, USA) in H_2SO_4.

Glycogen measurements were based on the extraction method of Ernst [40]. Cells were concentrated to an optical density of 600 μg Chl/ml in a final volume of 50 μl. 200 μl of 30% (w/v) KOH was added and the samples were heated at 100°C for 90 minutes. The extracts were then cooled, 600 μl ethanol was added and samples were incubated on ice for 2 hours. The glycogen was collected by centrifugation at 15000 x g for 5 minutes. The pellet was washed twice with ethanol and dried 10 min at 60°C, then resuspended in 300 μl 100 mM sodium acetate (pH 4.75). Following resuspension, 10 μl amyloglucosidase and 10 μl amylase were added and the samples were incubated 1 hour at room temperature to convert the glycogen to glucose. Insoluble fragments were removed by centrifuging at 1500 x g for 10 min and the glucose in the supernatant was quantified using a glucose assay kit (Sigma-Aldrich, St. Louis, MO, USA. product # GAGO20). A glycogen standard was also used to ensure the

enzymatic digest was complete during the incubation time and to correlate glucose concentration to the initial glycogen concentration.

Results

Growth and biomass analysis

T. elongatus was able to grow on up to 20% CO_2 in the photobioreactors. At 30% CO_2 the cultures died and bleached out within 24 hours. Cultures grown on 5-20% CO_2 showed similar growth characteristics as measured by OD_{730} (Figure 4. 1). The average specific first-order growth rate for cultures grown at each CO_2 concentration was calculated by the following equation:

$$\mu = \frac{\mathrm{Ln}(OD_{730}/OD_{730o})}{\Delta t} \tag{4.1}$$

Where μ is the specific first-order growth rate (d^{-1}), OD_{730o} is the initial and OD_{730} is the final optical density at 730 nm, and Δt is the time period in days. Cultures grown with atmospheric CO_2 showed very little growth and achieved a specific first-order growth rate of only 0.10 d^{-1} while a maximum specific first-order growth rate of 0.43 d^{-1} was achieved with cells grown on 20% CO_2 (Table 4. 1).

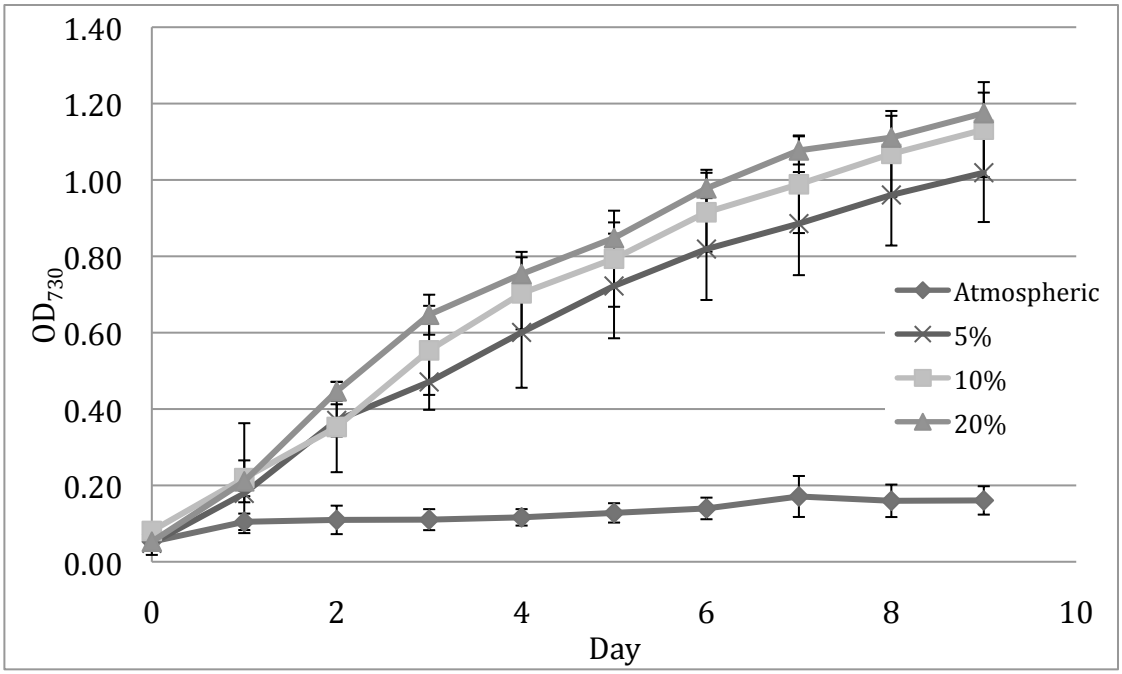

Figure 4. 1. Growth curves of *T. elongatus* with gas bubbling with increasing CO_2 concentrations. Cell density measured as optical density at 730 nm. Data points represent mean (n = 3). Error bars indicate standard deviation from the mean.

Table 4. 1. Specific growth rates, productivity, CO_2 fixation rates, and percent CO_2 utilization of *T. elongatus* under increasing carbon concentrations. Values are the average of three samples ± standard deviation.

Inlet CO_2 Concentration	Specific growth rate (d^{-1})	Productivity (mg ml^{-1} d^{-1})	CO_2 Fixation Rate (mg ml^{-1} d^{-1})	Percent CO_2 used
Atmospheric	0.10±0.04	0.01±0.005	0.01±0.009	54.54±10.26%
5%	0.43±0.03	0.07±0.02	0.14±0.05	5.31±0.01%
10%	0.36±0.01	0.06±0.02	0.11±0.03	1.70±0.35%
20%	0.43±0.02	0.09±0.01	0.17±0.01	1.36±0.17%

Similar culture densities were achieved at 5-20% CO_2 while at atmospheric CO_2 concentrations the maximum cell density was at an OD_{730} of 0.16 (Figure 4. 1). The results of the total carbon and nitrogen analyses showed that the molar ratio

of C:N did not change under the range of CO_2 concentrations tested and remained approximately 5.2:1 (data not shown).

Biomass productivity as a function of substrate concentration was modeled using the Monod expression for the net rate of cell growth:

$$r_{net} = Y\frac{V_{max}S}{K+S}X - bX \tag{4.2}$$

where r_{net} is the net rate of cell growth (mg ml^{-1} d^{-1}) (which is equal to productivity), μ_{max} is the maximum specific first order growth rate (mg ml^{-1} d^{-1}), K is the half-saturation coefficient (%), S is the substrate concentration (%), X is the concentration of active biomass, and b is the endogenous decay coefficient. The initial fitting of the model showed no difference with or without the inclusion of the endogenous decay coefficient. Also, the maximum specific first-order growth rate (μ_{max}) was substituted for YV_{max} thus simplifying equation 4.2 as follows defined in terms of productivity (P):

$$P = \frac{\mu_{max}S}{K+S}X \tag{4.3}$$

K and μ_{max} were determined by nonlinear regression and minimizing the sum of squares. The best-fit estimate of K was 1.37% and μ_{max} was estimated at 0.09 mg ml^{-1} d^{-1}. Results of the model are shown in Figure 4.2. Productivity increased as CO_2 concentration increased from atmospheric to 5%. From 5-20% there was no statistically significant increase in biomass productivity (Figure 4. 2).

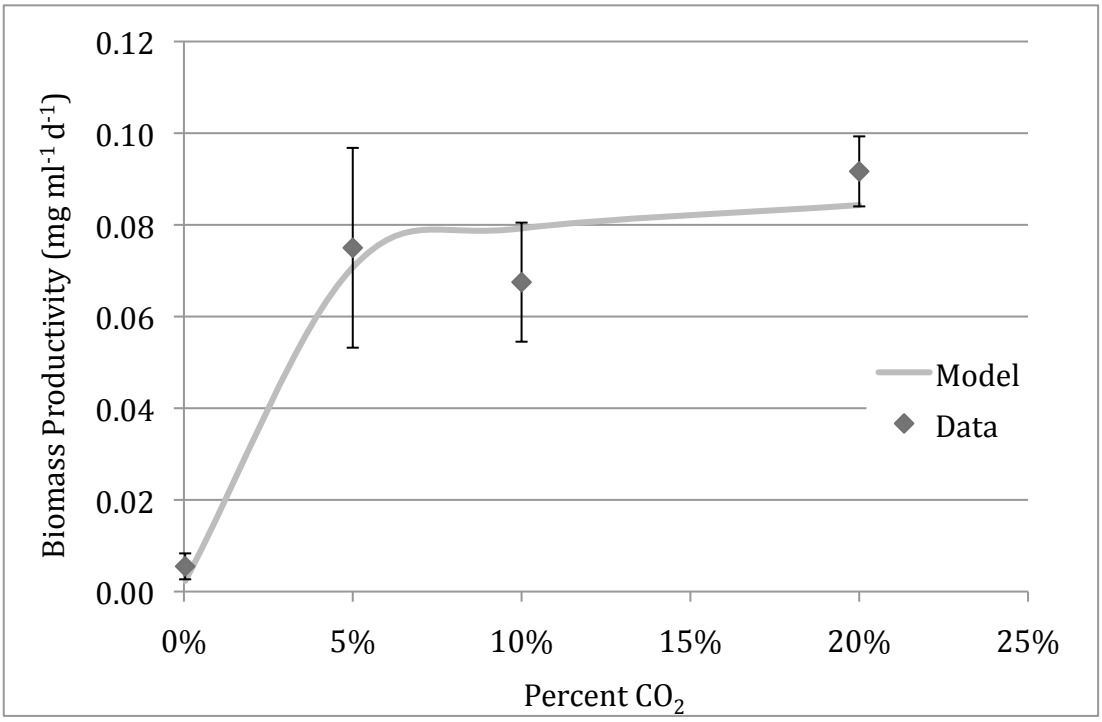

Figure 4. 2. Monod model of maximum biomass accumulation with increasing concentrations of CO_2. Data points represent mean (n = 3). Error bars indicate standard deviation from the mean.

Maximum biomass productivity of *T. elongatus* was 0.09±0.01 mg ml^{-1} d^{-1} with 20% CO_2 while at atmospheric CO_2, productivity was only 0.01±0.003 mg ml^{-1} d^{-1} (Table 4. 1). CO_2 fixation rates were calculated using the following equation from Wang, et al [152]:

$$P_{(CO2)} = 1.88 \times P \qquad (4.4)$$

where P is the biomass productivity (mg ml^{-1} d^{-1}) and $P_{(CO2)}$ is the CO_2 fixation rate (mg ml^{-1} d^{-1}). This equation is derived from the molecular formula for microalgae biomass; $CO_{0.48}H_{1.83}N_{0.11}P_{0.01}$ [24], and has also been applied to

cyanobacteria [152]. CO_2 uptake rate calculations using this method were compared to the method of Kajiwara, et al. [64], which incorporates the measured biomass carbon content, and the results were found to be virtually identical. CO_2 fixation rates reached a maximum of 0.17±0.01 mg ml^{-1} d^{-1} at 20% CO_2 (Table 4. 1). The percent CO_2 utilization was calculated by dividing the amount of CO_2 fixed per day by the CO_2 feed rate per day. The amount of CO_2 utilization decreased with increasing CO_2 concentrations. With no supplemental CO_2 (atmospheric concentrations), 54.54±4.37% of the total CO_2 was used. The percent used decreased with increasing CO_2 concentrations and reached a minimum of 1.36±0.17% with an inlet CO_2 concentration of 20% (Table 4. 1). The maximum amount of CO_2 sequestered over the course of the 9 day bioreactor experiment was 1.15 g L^{-1} in cultures grown on 20% CO_2. The maximum photosynthetic efficiency of CO_2 fixation was around 7.98% at a light intensity of 180 μE m^{-2} s^{-1}. This calculation was based on 48% of the total light being photosynthetically active radiation and the requirement of 8 photons to fix one molecule of CO_2 [133].

Henry's Law was used to determine the solubility of CO_2 in the media under the experimental CO_2 concentrations using the following equation:

$$X_g = \frac{P_T}{H}\rho_g \tag{4.5}$$

Where X_g is the mole fraction of gas in water (mole gas/mole water), P_T is total pressure (1 atm), H is Henry's constant (atm) adjusted for temperature, and ρ_g is

the mole fraction of gas in air (moles gas/moles air). Henry's constant at 50°C is 2971 atm [91]. The mole fraction was then converted to moles of gas per liter of water by multiplying by the formula weight (g/mole) and density of water (g/L). The headspace molar concentration of CO_2 was calculated using the ideal gas law. The solubility of CO_2 was calculated at 30°C and 50°C and the aqueous CO_2 concentration was found to be 38% lower at 50°C. Based on carbonate system equilibrium at pH 7.8, the concentration of HCO_3^- was 0.215 mM with no supplemental CO_2 addition, 30 mM at 5% CO_2, 60 mM at 10% CO_2 and 120 mM at 20% CO_2.

Carbon storage compounds

The concentration of lipids did not vary significantly over the range of test conditions studied here. The average lipid content was approximately 20.0% (w/w) in all samples (Figure 4. 3). In contrast, PHB content varied significantly. Cultures that were not given supplemental CO_2 contained about 14.5% (w/w) PHB while cultures that had 5-20% CO_2 accumulated only about 2.0% PHB (Figure 4. 3). No clear trend could be seen between CO_2 concentration and glycogen content, which remained low (about 1.40% (w/w)) under all test conditions (Figure 4. 3).

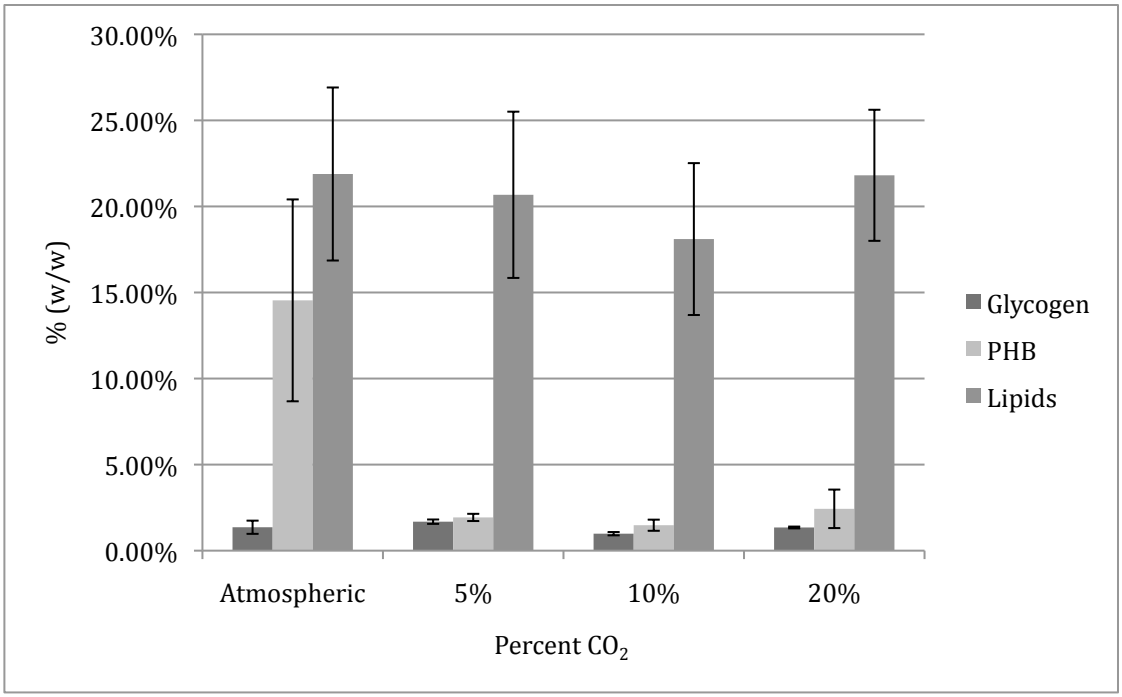

Figure 4. 3. Glycogen, lipid, and PHB content in *T. elongatus* grown over a range of 0-20% CO_2. Data points represent mean (n = 3). Error bars indicate standard deviation from the mean.

The amount of carbon in each storage compound was also determined. Lipids averaged 75.63±1.35% carbon by weight based on elemental analysis. Both PHB and glycogen are polymers of repeating PHB and glucose units, respectively. The percentage of carbon in these compounds on a molar basis was used to calculate the total mass of carbon they contained. Lipids, PHB's, and glycogen accounted for approximately 58% of the total carbon in cells grown on atmospheric CO_2. At 5-20% CO_2 they only accounted for about 40% of the total carbon in the biomass (Figure 4. 4).

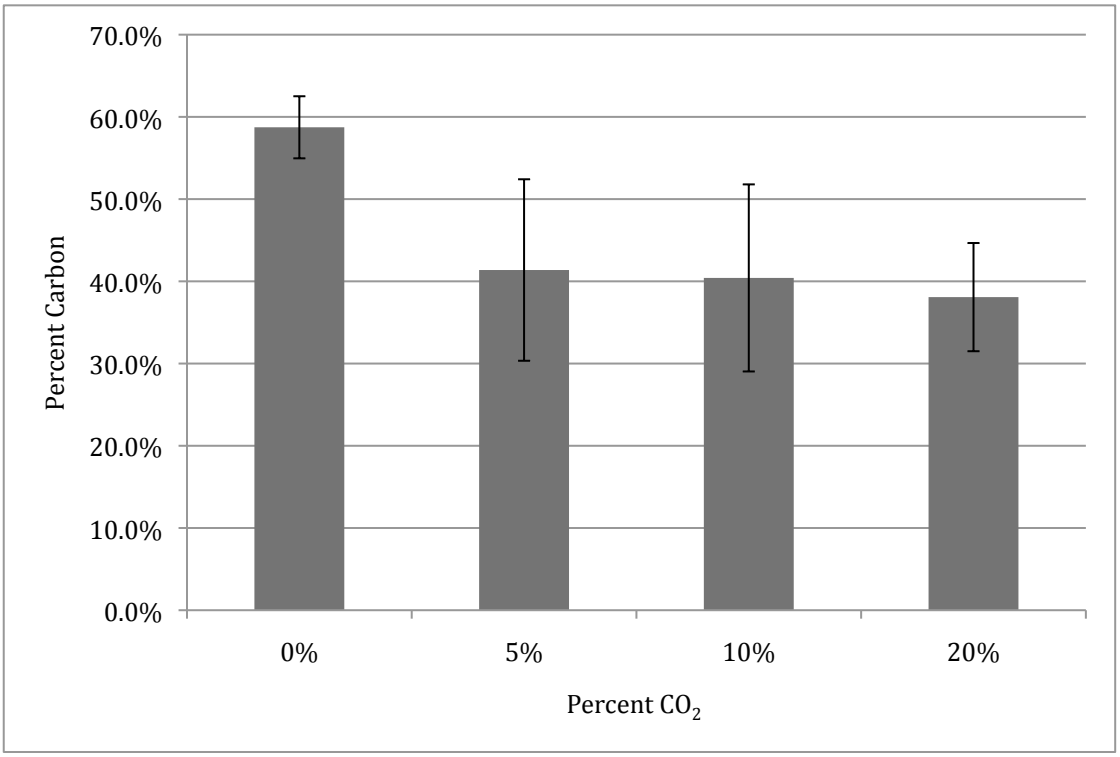

Figure 4. 4. Percent of total biomass carbon in lipids, PHB's, and glycogen. Data points represent mean (n = 3). Error bars indicate standard deviation from the mean.

Discussion

Growth of cyanobacteria on high levels of CO_2 has been described in many mesophilic species [96, 115, 152], however much less is known about the response of thermophilic strains. However, recently the growth of the thermophilic cyanobacterium, *Thermosynechococcus* sp. CL-1, was described on 10 and 20% CO_2 [56]. Saki et al. [124] noted at the time of their work with a thermophilic strain of *Chlorella* that there were very few reports in the literature regarding CO_2 tolerance in thermophilic organisms. Now, 15 years later, little has

changed in that regard. However, several recent reviews have recognized the need for this subject to be addressed, especially in regard to the operation of bioreactors [74, 86]. In addition, data are scarce on the growth and kinetic parameters of thermophilic cyanobacteria in photobioreactors.

Differences in biomass accumulation rates were not statistically significant between 5-20% CO_2, indicating that even though the cells can tolerate higher levels, their ability to take up CO_2 were saturated at 5% under the conditions of the experiments (Figure 4. 2). Growth, productivity, and carbon assimilation rates observed here in *T. elongatus* compared favorably with other thermophilic cyanobacteria. Ono and Cuello [113] found that *Chlorogleopsis* sp. reached a maximum carbon assimilation rate of 0.02054 mg ml^{-1} d^{-1} with 5% CO_2. In contrast *T. elongatus* was able to achieve a carbon fixation rate that was 8 times higher with 20% CO_2 (Table 4. 1). However, the maximum biomass concentration was only 0.833 mg ml^{-1} with 20% CO_2 (Table 4. 1) compared to 1.24 mg ml^{-1} in *Chlorogleopsis* sp. [113]. The lower total biomass may be due in part to shorter culturing times, which were only 9 days compared to 28 days for *Chlorogleopsis* sp., or to light limitation caused by self shading in the bioreactors.

In contrast, several mesophilic species are capable of growth on higher levels of CO_2 and with higher productivity. Recent work with *Spirulina* sp. found a maximum specific growth rate of 0.44 d^{-1}, productivity of 0.22 mg ml^{-1} d^{-1}, maximum biomass concentration of 3.50 mg ml^{-1}, and CO_2 fixation rate of 0.413 mg ml^{-1} d^{-1} when grown on 6 and 12% CO_2 [28]. The specific growth rate of

Spirulina sp. was similar to *T. elongatus* grown on 20% CO_2 but productivity and CO_2 fixation rates were over 2 times higher. Even higher CO_2 fixation rates of up to 1.5 mg ml^{-1} d^{-1} have been achieved with *Synechocystis aquatilis* [103]. The higher CO_2 fixation rates of mesophiles may be due in part to the higher solubility of CO_2 at lower temperatures. At 30°C the soluble concentration of CO_2 is 38% greater than at 50°C for any given headspace CO_2 concentration, therefore the available CO_2 in solution is significantly higher leading to potentially higher uptake rates.

Up to 54.5±4.4% of the CO_2 was utilized by *T. elongatus* when grown with no CO_2 supplementation. The efficiency of CO_2 utilization decreased at higher concentrations reaching a minimum value of 1.3±0.17% at 20% CO_2 (Table 4. 1). The amount of CO_2 utilized at 10-20% was similar to reports for other species. Jacob-Lopes et al., [61] found that *Aphanothece microscopica Nägeli* was able to utilize a maximum of 3.1±0.05% with 15% CO_2.

Average lipid content was around 20%, which is higher than levels reported for the thermophilic cyanobacterium *Thermosynechococcus* sp. CL-1, which contained around 13% (w/w) when grown on 10% CO_2 [56].

The percentage of total biomass carbon in lipids, PHB's, and glycogen was significantly higher in cultures that were grown without supplemental CO_2 (Figure 4. 4). This was primarily due to the concentration of PHB, which was 7 times higher without supplemental CO_2, perhaps due to stress induced by carbon limitation. PHB accumulation is a known stress response under nutrient

deprivation. For example, studies of the thermophilic cyanobacterium, *Synechococcus* sp. MA19, have show PHB accumulation of up to 27% (w/w) under nitrogen-depleted conditions [97], and it appears that carbon limitation may cause a similar stress response in *T. elongatus*. PHB levels in *T. elongatus* grown on atmospheric CO_2 levels were comparable to *Synechococcus* sp. MA19, which has been reported to store up to 20% dry weight using CO_2 as its sole carbon source [97].

PHB content in general appears to be lower in mesophilic cyanobacteria. In *Synechocystis* PCC 6803, PHB concentrations of 7% dry weight have been reported in wild type cells, with mutant strains producing up to 11% dry weight [142]. PHB production has also been studied extensively in several *Spirulina* strains. Reports of PHB concentrations in *Spirulina maxima* vary from 0.1-6%, depending on conditions [5, 30]. The PHB levels were also similar to *T. elongatus* grown in 150 ml shaking flask experiments on 5-150 mM initial dissolved organic carbon (DIC) concentrations. Previous work in our lab has shown that at low levels of DIC (5 mM) cultures accumulated over 10% (w/w) PHB which decreased to around 2% (w/w) in cultures grown on 60-150 mM DIC (see chapter 3).

Glycogen levels averaged approximately 13.5 mg g^{-1} dry cell weight, which is similar to glycogen levels of 10.5 mg g^{-1} reported for *Synechocystis* sp. PCC 6803 [155]. However, when incubated under nitrogen deprived conditions glycogen levels in *Synechocystis* sp. PCC 6803 can be as much as 3 times higher. Currently it

is unknown if *T. elongatus* would produce higher glycogen levels under nitrogen deprived conditions.

The consistency of glycogen production at all CO_2 levels is somewhat surprising (Figure 4. 3). Previous work in our lab demonstrated that the concentration of DIC had a significant effect on the amount of glycogen produced by *T. elongatus* (chapter 3). Cultures grown at 5-60 mM DIC accumulated around 2.5% (w/w) glycogen while at 100 mM DIC the concentration increased to around 8% (w/w) and at 150 mM glycogen content reached 15% (w/w) (Figure 3. 4). The reason for this difference is not clear, especially since at 20% CO_2 and pH 7.8 the effective bicarbonate concentration based on carbonate equilibrium calculations is around 120 mM. Therefore, it would seem likely that the amount of glycogen accumulated should be nearly the same as cultures grown on 100-150 mM DIC. These disparate results may be due in part to the mechanism of CO_2 and HCO_3^- uptake in *T. elongatus*. Maximum culture densities were similar at high CO_2 and HCO_3^- levels which would indicate that growth was not inhibited by any nutrient limitation.

Cultures grown on CO_2 in the bioreactors may have been more limited for light. Although the light intensity was much higher than in the DIC experiments, the bioreactor design was such that they could only be illuminated from the bottom. Self-shading could have been an issue at higher cell densities although the maximum specific growth rates and culture densities were similar to cultures grown on DIC, indicating that their growth was not light limited relative to

cultures grown on DIC. While growth may not have been light limited, the cultures grown on DIC may have had excess energy that could be diverted to sequestering carbon while they were in a carbon rich environment. In contrast, cultures grown on CO_2 may only have received enough light to maintain growth with no extra energy available for building carbon reserves.

The possibility of different carbon uptake mechanisms being activated when grown on CO_2 merits further investigation. *T. elongatus* has homologous sequences for *cmpABCD*, an inducible high-affinity HCO_3^- ATP-dependent transporter, for *ndhF3*, which is involved in inducible high-affinity CO_2 transport, and for *ndhF4* which is involved in low-affinity CO_2 transport. However it has no homologues to the low affinity Na^+ dependent HCO_3^- symporter *sbtA* gene [6]. Due to the apparent absence of a low affinity, constitutively expressed HCO_3^- transporter it is difficult to explain why *T. elongatus* can grow so well and store so much glycogen when grown on high levels of HCO_3^-.

A specialized NDH-1 complex has also been postulated as a mechanism for converting CO_2 to HCO_3^- in cyanobacteria. The proposed system is thought to couple hydration of CO_2^- with photosynthetic electron transport and the translocation of protons across the thylakoid membrane [6]. Such a system would place an additional energy demand of the cell, further limiting glycogen synthesis.

One key issue that this study did not address is the effect of the diurnal cycle on CO_2 sequestration and biomass productivity. Since CO_2 fixation only occurs during daylight, actual productivity and sequestration rates in outdoor

bioreactors will be lower. As a result, in considering industrial CO_2 sequestration, nighttime emissions will not be captured. Other methods would need to be used to temporarily sequester CO_2 as carbonate species at night, which could then be utilized by cyanobacteria during the day. This may well be a viable strategy as previous work has documented the ability of *T. elongatus* to grow on high levels of dissolved inorganic carbon (Chapter 3).

Acknowledgements

We would like to thank Dr. Elizabeth Burrows for her technical assistance in setting up and troubleshooting the bioreactors. This work was supported in part by the DOD/ASEE SMART scholarship program. Special thanks to Markael Luterra for editorial assistance.

CHAPTER 5: GENERAL CONCLUSION

Findings of the research

The research presented in this dissertation contains the first report of H_2 production from *T. elongatus*. The maximum production rate of 188 nmol H_2 mg Chl a^{-1} hr^{-1} is much lower than the reported values for many other thermophilic organisms [35] but comparable to some mesophilic cyanobacteria, such as *Anabaena* sp. 7120, which produce around 260 nmol H_2 mg Chl a^{-1} hr^{-1} [118, 132]. Responses to inhibitors and inability to catalyze deuterium exchange indicate that the process of H_2 production may be distinct from that associated with a typical bidirectional H_2ase.

T. elongatus was able to grow well on up to 20% CO_2 (120 mM DIC) without any prior acclimatization to high carbon levels. Significant differences were observed between cultures grown in flasks and in the bioreactors even though similar initial equilibrium bicarbonate concentrations were present. Dissolved carbon concentrations were constant throughout the bioreactor experiments due to the continuous gas flow, while in the flask experiments DIC gradually decreased over time, which may have caused differences in the amount of carbon stored. In addition, the bioreactors likely experienced self-shading as the cell density increased, thus limiting the amount of energy they received. Maximum biomass accumulation occurred in the bioreactors with cells grown on 20% CO_2, and were about 34% higher than in cultures grown in flasks even though culture densities were similar. This is consistent with reports of biomass accumulation in *Thermosynechococcus* sp. CL-1 that also showed higher biomass accumulation in cultures grown on CO_2 [56].

Lipid concentrations were not significantly affected by the source or concentration of inorganic carbon. In contrast, low levels of inorganic carbon caused a significant increase in PHB accumulation that appeared to be stress induced. Glycogen content was affected by the concentration of inorganic carbon with the greatest accumulation occurring when grown on 150 mM DIC. In contrast, the level of CO_2 in the bioreactors had no effect on glycogen accumulation even though equilibrium HCO_3^- concentrations were similar.

Impact of the research

This work provides the first report of H_2 production from a thermophilic cyanobacterium. It is also the first reported analysis of *T. elongatus* for H_2 production and is interesting in light of the fact that this organism contains no sequences homologous to any known H_2ases.

This research also represents the first time a thermophilic cyanobacterium has been characterized for the purpose of both CO_2 sequestration and biofuels and bioproducts production. While a few studies in recent years have looked at dissolved inorganic carbon assimilation in thermophilic cyanobacteria [56, 113], they have not correlated carbon uptake to the accumulation of compounds with potential use as biofuels or biomaterials.

One of the most significant findings of this research was the difference in glycogen accumulation between the flask and bioreactor experiments even though inorganic carbon concentrations were similar. The relationship between

the concentration of inorganic carbon and the carbon storage compounds, particularly PHB and glycogen, merits further consideration. The high level of glycogen accumulation in cells that were grown under high DIC was also significant and this may prove to be the biopolymer with the most potential in *T. elongatus*, particularly if used for ethanol and butanol production through fermentation [52, 79] or as a feedstock for the production of other valuable compounds. Glucose has also proven to be a superior feedstock for H_2 production by gasification [51].

Engineering implications

Several engineering challenges remain in the development of a biobased system for CO_2 sequestration. The operation of bioreactors at higher temperatures adds one significant challenge that must be considered in future bioreactor and experimental design. Specifically, evaporation rates are much higher, especially when high gas flow rates are used. The reactors used in these experiments had reflux columns that were connected to a circulating water bath. However, even with this in place, condensation was observed in the exhaust vent. Actual evaporative loss for this system could not be calculated because of the lack of the necessary instrumentation for measuring relative humidity. A larger condenser is needed to reduce the evaporative loss. Operating bioreactors in continuous flow rather than batch mode would also minimize the effect of

evaporative loss since the amount of evaporation would be negligible compared to the rate of fluid flow through.

T. elongatus could potentially be used at any location that has a constant supply of high temperature, CO_2 rich, flue gas. Power plant flue gas temperatures can be as high as 40°C even after desulfurization and removal of nitrous oxides [122] and *T. elongatus* is well suited for tolerating the high concentrations of CO_2 as well as the high temperatures that would be encountered in such an environment. The high temperatures in particular are advantageous for minimizing contamination since fewer organisms are capable of living at these temperatures. The resulting biomass produced from such a system has many potential uses, both as fuel and other bioproducts (Figure 1.1). Pyrolysis or gasification can be used to produce gas and oils [81], or the entire biomass could be used for feed or fertilizer. Production of specific products, such as lipids or PHB's may also be feasible, provided that the concentrations can be improved through genetic or metabolic engineering strategies.

Future direction

The mechanism of H_2 production from *T. elongatus* remains unknown and more work is needed to identify the responsible pathway. Several approaches could be taken to identify the genetic basis for H_2 production. One approach would be to generate a mutant library using error-prone PCR and then screen for

mutants that are unable to produce H_2. Another approach would be to target potential genes that may be associated with H_2 production.

One potential candidate for the source of H_2 is a formate hydrogen lyase (FHL) complex. In this system, pyruvate formate lyase (PFL) is used to split pyruvate to acetyl-CoA and formate, and FHL then catalyzes the subsequent conversion of formate to CO_2 and H_2 [70]. Although no gene sequence homologous to FHL has been annotated in *T. elongatus*, one sequence (tlr0226) has been annotated as a pyruvate formate lyase-activating enzyme and another one (tlr0227) is annotated as a pyruvate-formate-lyase deactivase. Multiple BLAST searches identified similar sequences in other thermophilic organisms but not in mesophilic cyanobacteria, which suggests the possibility that H_2 production in *T. elongatus* is through an enzyme unique to thermophiles.

The presence of an unknown mechanism of H_2 production highlights the need for continued efforts in analyzing novel species for H_2 production and also indicates that traditional screening methods, such as sequence analyses, are not comprehensive enough. Additional high-throughput methods, such as the assay described in chapter 2, must also be employed to screen for H_2 production even when gene analyses would indicate no H_2ases are present. The research outlined in this dissertation raises the need for further exploration in a number of areas. To achieve the goal of photobiological CO_2 sequestration, biofuel and biomaterials production, future work is needed in the following areas:

- Perform pilot scale bioreactor experiments with *T. elongatus* using industrial flue gas and water supply to determine how robust the cultures are when exposed to potentially toxic contaminants in these waste streams. A pilot scale project would also provide a way of determining the effect of natural light intensities and photoperiods on the growth and carbon sequestration rates.
- Investigate the production of additional value-added byproducts such as carotenoids, vitamins, omega-3 fatty acids, lutein, acetylic acids, cyanophycin, acetate, butanol, ethylene, and isoprene [52].
- Prospect for novel thermophilic organisms with high growth rates, a tolerance for high CO_2 levels, and the ability to produce high levels of H_2, PHB's, lipids, or other valuable byproducts.
- Improve bioreactor designs. As the size of a bioreactor increases, the culture can become light-limited due to self-shading. Approaches to this problem include designing tubular reactors or incorporating fiber optics to channel light into the center of the reactor. Basic process engineering principles involving mass transfer and hydrodynamics must also be improved in current reactor designs.
- An efficient method of harvesting biomass still remains elusive and more work is needed to develop mechanisms that work well on a large scale. Current methods include centrifugation, flocculation, gravity

sedimentation, and filtration [22]. However, all of these suffer from a variety of scale-up limitations.

- A detailed cost, efficiency, and life cycle analysis is also needed. Estimated costs of producing biodiesel range from $1.40-4.40 per gallon for systems currently under development [134] and DOE estimates of the cost of biological H_2 production is about \$30 kg^{-1} at 10% solar energy to H_2 conversion efficiency [122] with a price goal of \$1-3 kg^{-1} [146]. In addition, many value-added bioproducts have not had a detailed cost analysis.
- Coordinate with industry to ensure system design considerations are within the necessary structural, operational, and safety specifications.

BIBLIOGRAPHY

[1] Ananyev G. Carrieri D, Dismukes G. Optimization of Metabolic Capacity and Flux through Environmental Cues To Maximize Hydrogen Production by the Cyanobacterium *Arthrospira (Spirulina) maxima*. Appl Environ Microbiol 2008;74:6102-6113.

[2] Antoni D. Zverlov VV, Schwarz WH. Biofuels from microbes. Appl Microbiol Biotechnol 2007;77:23-35.

[3] Appel J, Phunpruch, S., Steinmuller, C., Schulz, R. Bi-directional hydrogenase of Synechocystis sp. PCC 6803 works as an electron valve during photosynthesis. Arch Microbiol 2000;173:333-338.

[4] Apt K, Behrens P. Commercial developments in microalgal biotechnology. J Phycol 1999;35:215-226.

[5] Asada Y. Miyake M. Miyake J. Kurane R, Tokiwa Y. Photosynthetic accumulation of poly-(hydroxybutyrate) by cyanobacteria--the metabolism and potential for CO2 recycling. International journal of Biological Macromolocules 1999;25:37-42.

[6] Badger M, Price G. CO2 concentrating mechanisms in cyanobacteria: molecular components, their diversity and evolution. J Exp Bot 2003;54:609-622.

[7] Badger M, Schreiber U. Effects of inorganic carbon accumulation on photosynthetic oxygen reduction and cyclic electron flow in the cyanobacterium Synechococcus PCC7942. Photosynth Res 1993;37:177-191.

[8] Badura A. Esper B. Ataka K. Grunwald C. Woll C. Kuhlmann J. Heberle J, Rogner M. Light-driven water splitting for (bio-)hydrogen production: photosystem 2 as the central part of a bioelectrochemical device. Photochem Photobiol 2006;82:1385-1390.

[9] Battchikova N, Aro E. Cyanobacterial NDH-1 complexes: multiplicity in function and subunit composition. Physiol Plant 2007;131:22-32.

[10] Beeby M. O'Connor BD. Ryttersgaard C. Boutz DR. Perry LJ, Yeates TO. The Genomics of disulfide bonding and protein stabilization in thermophiles. PLoS Biol 2005;3:1549-1558.

[11] Benemann J. Hydrogen production by microalgae. J Appl Phycol 2000;12:291-300.

[12] Borowitzka MA. Commercial production of microalgae: ponds, tanks, tubes and fermenters. J Biotechnol 1999;70:313-321.

[13] Bruins ME. Janssen AEM, Boom RM. Thermozymes and their applications - A review of recent literature and patents. Appl Biochem Biotechnol 2001;90:155-186.

[14] Brune D, Novak J. The use of carbonate equilibrium chemistry in quantifying algal carbon uptake kinetics. Appl Microbiol Biotechnol 1981;13:71-76.

[15] Burrows E. Chaplen F, Ely R. Effects of Selected Electron Transport Chain Inhibitors on 24-hour Hydrogen Production by Synechocystis sp. PCC 6803. Bioresour Technol 2010; In Press. doi:10.1016/j.biortech.2010.10.042

[16] Burrows EH. Wong WK. Fern X. Chaplen FW, Ely RL. Optimization of pH and nitrogen for enhanced hydrogen production by Synechocystis sp. PCC 6803 via statistical and machine learning methods. Biotechnol Prog 2009;25:1009-1017.

[17] Campbell D. Hurry V. Clarke A, Gustafsson P. Chlorophyll fluorescence analysis of cyanobacterial photosynthesis and acclimation. Microbiol Mol Biol Rev 1998;62:667-683.

[18] Carpenter R, Mimeault M. The Photosynthetic Partial Reactions Involved in Photoelectrochemical Current Generation by Thylakoid Membranes. Biotechnol Lett 1987;9:111-116.

[19] Castenholz R. Thermophilic blue-green algae and the thermal environment. Microbiol Mol Biol Rev 1969;33:476-504.

[20] Castenholz RW, 1988. Thermophilic Cyanobacteria: Special Problems, Methods Enzymol. Academic Press, Inc., San Diego, pp. 96-100.

[21] Chai F. Cao F. Zhai F. Chen Y. Wang X, Su Z. Transesterification of Vegetable Oil to Biodiesel using a Heteropolyacid Solid Catalyst. Adv. Synth. Catal. 2007;349:1057-1065.

[22] Chen C. Yeh K. Aisyah R. Lee D, Chang J. Cultivation, photobioreactor design and harvesting of microalgae for biodiesel production: A critical review. Bioresour Technol 2010;102:71-81.

[23] Chen G. A microbial polyhydroxyalkanoates (PHA) based bio-and materials industry. Chem Soc Rev 2009.

[24] Chisti Y. Biodiesel from microalgae. Biotechnol Adv 2007;25:294-306.

[25] Christie W, 1973. Lipid analysis: isolation, separation, identification, and structural analysis of lipids. Pergamon Press.

[26] Cooley JW, Vermaas WFJ. Succinate Dehydrogenase and Other Respiratory Pathways in Thylakoid Membranes of Synechocystis sp. Strain PCC 6803: Capacity Comparisons and Physiological Function. J Bacteriol 2001;183:4251-4258.

[27] Cournac L. Guedeney G. Peltier G, Vignais PM. Sustained Photoevolution of Molecular Hydrogen in a Mutant of Synechocystis sp. Strain PCC 6803 Deficient in the Type I NADPH-Dehydrogenase Complex. J Bacteriol 2004;186:1737-1746.

[28] de Morais M, Costa J. Biofixation of carbon dioxide by Spirulina sp. and Scenedesmus obliquus cultivated in a three-stage serial tubular photobioreactor. J Biotechnol 2007;129:439-445.

[29] De Philippis R. Ena A. Guastiini M, Sili C. Factors affecting poly-[beta]-hydroxybutyrate accumulation in cyanobacteria and in purple non-sulfur bacteria. FEMS Microbiol Rev 1992;103:187-194.

[30] De Philippis R. Sili C, VINCENZINI M. Glycogen and poly-{beta}-hydroxybutyrate synthesis in Spirulina maxima. Microbiology 1992;138:1623-1628.

[31] Del Campo J. García-González M, Guerrero M. Outdoor cultivation of microalgae for carotenoid production: current state and perspectives. Appl Microbiol Biotechnol 2007;74:1163-1174.

[32] Diamond L, Akinfiev N. Solubility of CO2 in water from-1.5 to 100 C and from 0.1 to 100 MPa: evaluation of literature data and thermodynamic modelling. Fluid phase equilibria 2003;208:265-290.

[33] Dismukes G. Carrieri D. Bennette N, Ananyev G. Aquatic phototrophs: efficient alternatives to land-based crops for biofuels. Curr Opin Biotechnol 2008;19:235-240.

[34] Dutta D. De D. Chaudhuri S, Bhattacharya SK. Hydrogen production by Cyanobacteria. Microb Cell Fact 2005;4:1-11.

[35] Eberly JO, Ely RL. Thermotolerant Hydrogenases: Biological Diversity, Properties, and Biotechnological Applications. Crit Rev Microbiol 2008;34:1 - 14.

[36] Eckert JS. Foote EH. Rollison LR, Walter LF. ABSORPTION PROCESSES UTILIZING PACKED TOWERS. Industrial & Engineering Chemistry 1967;59:41-47.

[37] Egorova K, Antranikian G. Industrial relevance of thermophilic Archaea. Curr Opin Microbiol 2005;8:649-655.

[38] Eguchi S. Takano H. Ono K, Takio S. Photosynthetic Electron Transport Regulates the Stability of the Transcript for the Protochlorophyllide Oxidoreductase Gene in the Liverwort, Marchantia paleacea var. diptera. Plant Cell Physiol 2002;43:573-577.

[39] Eriksen N. Riisgård F, Gunther W. On-line estimation of O 2 production, CO 2 uptake, and growth kinetics of microalgal cultures in a gas-tight photobioreactor. J Appl Phycol 2007;19:161-174.

[40] Ernst A. Kirschenlohr H. Diez J, Böger P. Glycogen content and nitrogenase activity in Anabaena variabilis. Arch Microbiol 1984;140:120-125.

[41] Folch J. Lees M, Stanley G. A simple method for the isolation and purification of total lipides from animal tissues. J Biol Chem 1957;226:497.

[42] Ghirardi ML. Posewitz MC. Maness PC. Dubini A. Yu J, Seibert M. Hydrogenases and Hydrogen Photoproduction in Oxygenic Photosynthetic Organisms. Annu Rev Plant Biol 2007;58:71-91.

[43] Gibbons B, Edsall J. Rate of hydration of carbon dioxide and dehydration of carbonic acid at 25. J Biol Chem 1963;238:3502-3507.

[44] Gromiha MM. Oobatake M, Sarai A. Important amino acid properties for enhanced thermostability from mesophilic to thermophilic proteins. Biophys Chem 1999;82:51-67.
[45] Gutthann F. Egert M. Marques A, Appel J. Inhibition of respiration and nitrate assimilation enhances photohydrogen evolution under low oxygen concentrations in Synechocystis sp. PCC 6803. Biochimica et Biophysica Acta (BBA) - Bioenergetics 2007;1767:161-169.
[46] H A, A SXFC. Triacylglycerols in prokaryotic microorganisms. Appl Microbiol Biotechnol 2002;60:367-376.
[47] Haehnel W, Hochheimer A. On the current generated by a galvanic cell driven by electron transport. Bioelectrochemistry and Bioenergetics 1979;6:563-574.
[48] Hai T, Oppermann-Sanio F. Purification and characterization of cyanophycin and cyanophycin synthetase from the thermophilic Synechococcus sp. MA19. FEMS Microbiol Lett 1999;181:229-236.
[49] Hallenbeck P. Fermentative hydrogen production: principles, progress, and prognosis. International Journal of Hydrogen Energy 2009.
[50] Hankamer B. Lehr F. Rupprecht J. Mussgnug JH. Posten C, Kruse O. Photosynthetic biomass and H 2production by green algae: from bioengineering to bioreactor scale-up. Physiol Plant 2007;131:10-21.
[51] Hao X. Guo L. Mao X. Zhang X, Chen X. Hydrogen production from glucose used as a model compound of biomass gasified in supercritical water. International Journal of Hydrogen Energy 2003;28:55-64.
[52] Harun R. Singh M. Forde G, Danquah M. Bioprocess engineering of microalgae to produce a variety of consumer products. Renewable and Sustainable Energy Reviews 2010;14:1037-1047.
[53] Hei DJ, Clark DS. Pressure Stabilization of Proteins from Extreme Thermophiles. Appl Environ Microbiol 1994;60:932-939.
[54] Hodges M, Barber J. State 1-State 2 Transitions in a Unicellular Green Algae: . Plant physiology 1983;72:1119-1122.
[55] Holladay J. White J. Bozell J, Johnson D, 2007. Top Value-Added Chemicals from Biomass-Volume II—Results of Screening for Potential Candidates from Biorefinery Lignin, in: Energy, D.o. (Ed.).
[56] Hsueh H. Li W. Chen H, Chu H. Carbon bio-fixation by photosynthesis of Thermosynechococcus sp. CL-1 and Nannochloropsis oculta. Journal of Photochemistry & Photobiology, B: Biology 2009;95:33-39.
[57] Hu Q. Sommerfeld M. Jarvis E, Ghirardi M. Microalgal triacylglycerols as feedstocks for biofuel production: perspectives and advances. The Plant … 2008.
[58] Huertas I. Colman B, Espie G. Active transport of CO2 by three species of marine microalgae. J Phycol 2000;36:314-320.
[59] Ihara M. Nishihara H. Yoon K-S. Lenz O. Friedrich B. Nakamoto H. Kojima K. Honma D. Kamachi T, Okura I. Light-driven Hydrogen Production by a

Hybrid Complex of a [NiFe]-Hydrogenase and the Cyanobacterial Photosystem I. Photochem Photobiol 2006;82:676.

[60] Inoue N. Taira Y. Emi T. Yamane Y. Kashino Y. Koike H, Satoh K. Acclimation to the growth temperature and the high-temperature effects on photosystem II and plasma membranes in a mesophilic cyanobacterium, Synechocystis sp. PCC6803. Plant Cell Physiol 2001;42:1140-1148.

[61] Jacob-Lopes E, Gimenes Scoparo C. Biotransformations of carbon dioxide in photobioreactors. Energy Conversion and Management 2010;51:894-900.

[62] Jacob-Lopes E. Scoparo C, Franco T. Rates of CO2 removal by Aphanothece microscopica Nägeli in tubular photobioreactors. Chemical Engineering and Processing: Process Intensification 2008;47:1365-1373.

[63] Jordan P. Fromme P. Witt HT. Klukas O. Saenger W, Krauss N. Three-dimensional structure of cyanobacterial photosystem I at 2.5 A resolution. Nature 2001;411:909-917.

[64] Kajiwara S. Yamada H, Ohkuni N. Design of the bioreactor for carbon dioxide fixation by Synechococcus PCC7942. Energy Conversion and Management 1997;38:S529-S532.

[65] Kalaitzis JA. Lauro FM, Neilan BA. Mining cyanobacterial genomes for genes encoding complex biosynthetic pathways. Nat Prod Rep 2009;26:1447.

[66] Kanai T. Ito S, Imanaka T. Characterization of a cytosolic NiFe-hydrogenase from the hyperthermophilic archaeon Thermococcus kodakaraensis KOD1. J Bacteriol 2003;185:1705-1711.

[67] Kaplan A, Reinhold L. CO2 concentrating mechanisms in photosynthetic microorganisms. Annu Rev Plant Biol 1999;50:539-570.

[68] Kaplan A. Schwartz R. Lieman-Hurwitz J. Ronen-Tarazi M, Reinhold L, 1994. Physiological and Molecular Studies on the Response of Cyanobacteria to Changes in the Ambient Inorganic Carbon Concentration, in: Bryant, D.O. (Ed.), The Molecular Biology of Cyanobacteria. Kluwer Academic Publishers, pp. 469-485.

[69] Kautsky H. Appel W, Amann H. Chlorophyll fluorescence and carbon assimilation. Part XIII. The fluorescence and the photochemistry of plants. Biochemische Zeitschrift 1960;332:277-292.

[70] Kim S. Seol E. Mohan Raj S. Park S, Oh Y. Various hydrogenases and formate-dependent hydrogen production in Citrobacter amalonaticus Y19. International Journal of Hydrogen Energy 2008;33:1509-1515.

[71] Kooten O, Snel J. The use of chlorophyll fluorescence nomenclature in plant stress physiology. Photosynth Res 1990;25:147-150.

[72] Kromkamp J. Formation and functional significance of storage products in cyanobacteria. N Z J Mar Freshw Res 1987;21:457-465.

[73] Kumar S, Nussinov R. How do thermophilic proteins deal with heat? Cell. Mol. Life Sci. 2001;58:1216-1233.
[74] Kunjapur A, Eldridge R. Photobioreactor Design for Commercial Biofuel Production from Microalgae. Ind. Eng. Chem. Res 2010;49:3516-3526.
[75] Law J, Slepecky R. ASSAY OF POLY-B-HYDROXYBUTYRIC ACID. J Bacteriol 1961;82:33-36.
[76] Li Y. Horsman M. Wu N. Lan C, Dubois-Calero N. Biofuels from microalgae. Biotechnol Prog 2008;24.
[77] Loll B. Kern J. Saenger W. Zouni A, Biesiadka J. Towards complete cofactor arrangement in the 3.0 A resolution structure of photosystem II. Nature 2005;438:1040-1044.
[78] Lopes Pinto F. Troshina O, Lindblad P. A brief look at three decades of research on cyanobacterial hydrogen evolution. International Journal of Hydrogen Energy 2002;27:1209-1215.
[79] Lu X. A perspective: Photosynthetic production of fatty acid-based biofuels in genetically engineered cyanobacteria. Biotechnol Adv 2010;28:742-746.
[80] Lucia L, Argyropoulos D. Chemicals and energy from biomass. Canadian Journal of Chemistry 2006;84:960-970.
[81] Luengo J. García B. Sandoval A, Naharro G. Bioplastics from microorganisms. Curr Opin Microbiol 2003;6:251-260.
[82] Lütke-Eversloh T. Fischer A, Remminghorst U. Biosynthesis of novel thermoplastic polythioesters by engineered Escherichia coli. Nat Mater 2002;1:236-240.
[83] Lv P. Yuan Z. Wu C. Ma L. Chen Y, Tsubaki N. Bio-syngas production from biomass catalytic gasification. Energy Conversion and Management 2007;48:1132-1139.
[84] Malik AQ, Damit SJBH. Outdoor testing of single crystal silicon solar cells. Renewable Energy 2003;28:1433-1445.
[85] Mallick N. Biotechnological potential of immobilized algae for wastewater N, P and metal removal: a review. Biometals 2002;15:377-390.
[86] Mata T. Martins A, Caetano N. Microalgae for biodiesel production and other applications: A review. Renewable and Sustainable Energy Reviews 2010;14:217-232.
[87] Maxwell K, Johnson G. Chlorophyll fluorescence--a practical guide. J Exp Bot 2000.
[88] Maxwell K, Johnson GN. Chlorophyll fluorescence--a practical guide. J Exp Bot 2000;51:659-668.
[89] Merrett M. Nimer N, Dong L. The utilization of bicarbonate ions by the marine microalga Nannochloropsis oculata (Droop) Hibberd. Plant, Cell & Environment 1996;19:478-484.
[90] Mertens R, Liese A. Biotechnological applications of hydrogenases. Current Opinion in Biotechnology 2004;15:343-348.

[91] Metcalf. Eddy. Tchobanoglous G. Burton FL, Stensel HD, 2004. Wastewater engineering : treatment and reuse, 4th ed. McGraw-Hill, Boston.

[92] Metz JG. Pakrasi HB. Seibert M, Arntzer CJ. Evidence for a dual function of the herbicide-binding D1 protein in photosystem II. FEBS Lett 1986;205:269-274.

[93] Miller A, Canvin D. The quenching of chlorophyll a fluorescence as a consequence of the transport of inorganic carbon by the cyanobacterium Synechococcus UTEX 625. Biochimica et Biophysica Acta (BBA)-Bioenergetics 1987;894:407-413.

[94] Miller A. Espie G, Bruce D. Characterization of the non-photochemical quenching of chlorophyll fluorescence that occurs during the active accumulation of inorganic carbon in the cyanobacterium Synechococcus PCC 7942. Photosynth Res 1996;49:251-262.

[95] Miller A. Espie G, Canvin D. The effects of inorganic carbon and oxygen on fluorescence in the cyanobacterium Synechococcus UTEX 625. Can J Bot 1991;69:1151-1160.

[96] Miyachi S. Iwasaki I, Shiraiwa Y. Historical perspective on microalgal and cyanobacterial acclimation to low-and extremely high-CO 2 conditions. Photosynth Res 2003;77:139-153.

[97] Miyake M. Erata M, Asada Y. A thermophilic cyanobacterium, Synechococcus sp. MA19, capable of accumulating poly-[beta]-hydroxybutyrate. Journal of Fermentation and Bioengineering 1996;82:512-514.

[98] Miyake M. Takase K. Narato M. Khatipov E. Schnackenberg J. Shirai M. Kurane R, Asada Y. Polyhydroxybutyrate production from carbon dioxide by cyanobacteria. Appl Biochem Biotechnol 2000;84-6:991-1002.

[99] Miyamoto K. Hallenbeck PC, Benemann JR. Hydrogen Production by the Thermophilic Alga Mastigocladus laminosus: Effects of Nitrogen, Temperature, and Inhibition of Photosynthesis. Appl Environ Microbiol 1979;38:440-446.

[100] Molina Grima E. Belarbi E. Acien Fernandez F. Robles Medina A, Chisti Y. Recovery of microalgal biomass and metabolites: process options and economics. Biotechnol Adv 2003;20:491-515.

[101] Mooibroek H. Oosterhuis N. Giuseppin M. Toonen M. Franssen H. Scott E. Sanders J, Steinbüchel A. Assessment of technological options and economical feasibility for cyanophycin biopolymer and high-value amino acid production. Appl Microbiol Biotechnol 2007;77:257-267.

[102] Mullineaux C, Allen J. State 1-state 2 transitions in the cyanobacterium Synechococcus 6301 are controlled by the redox state of electron carriers between photosystems I and II. Photosynth Res 1990;23:297-311.

[103] Murakami M, Ikenouchi M. The biological CO2 fixation and utilization project by rite (2) Screening and breeding of microalgae with high

capability in fixing CO2. Energy Conversion and Management 1997;38:S493-S497.
[104] Myers J. Graham J, Wang R. Light harvesting in Anacystis nidulans studied in pigment mutants. Plant Physiology 1980;66:1144-1149.
[105] Naik S. Gopal SKV, Somal P. Bioproduction of polyhydroxyalkanoates from bacteria: a metabolic approach. World J Microbiol Biotechnol 2008;24:2307-2314.
[106] Nakajima M. Sakamoto T, Wada K. The Complete Purification and Characterization of Three Forms of Ferredoxin-NADP+ Oxidoreductase from a Thermophilic Cyanobacterium Synechococcuselongatus. Plant Cell Physiol 2002;43:484-493.
[107] Nakamura Y. Kaneko T. Sato S, Ikeuchi M. Complete genome structure of the thermophilic cyanobacterium Thermosynechococcus elongatus BP-1. DNA … 2002.
[108] Nakamura Y. Kaneko T. Sato S. Ikeuchi M. Katoh H. Sasamoto S. Watanabe A. Iriguchi M. Kawashima K. Kimura T. Kishida Y. Kiyokawa C. Kohara M. Matsumoto M. Matsuno A. Nakazaki N. Shimpo S. Sugimoto M. Takeuchi C. Yamada M, Tabata S. Complete genome structure of the thermophilic cyanobacterium Thermosynechococcus elongatus BP-1 (supplement). DNA Research 2002;9:135-148.
[109] Obst M, Steinbüchel A. Cyanophycin—an ideal bacterial nitrogen storage material with unique chemical properties. Inclusions in prokaryotes Microbiology Monographs 2006;1:167-193.
[110] Odom JM, Peck HD. Hydrogen cycling as a general mechanism for energy coupling in the sulfate-reducing bacteria, Desulfovibrio sp. FEMS Microbiol Lett 1981;12.
[111] Ogawa T, Kaplan A. Inorganic carbon acquisition systems in cyanobacteria. Photosynth Res 2003;77:105-115.
[112] Ogawa T. Miyano A, Inoue Y. Photosystem-I-driven inorganic carbon transport in the cyanobacterium, Anacystis nidulans. Biochimica et Biophysica Acta (BBA) - Bioenergetics 1985;808:77-84.
[113] Ono E, Cuello J. Carbon dioxide mitigation using thermophilic cyanobacteria. Biosyst Eng 2007;96:129-134.
[114] Ozaki H. Ikeuchi M. Ogawa T. Fukuzawa H, Sonoike K. Large-scale analysis of chlorophyll fluorescence kinetics in Synechocystis sp. PCC 6803: identification of the factors involved in the modulation of photosystem stoichiometry. Plant Cell Physiol 2007;48:451-458.
[115] Papazi A. Makridis P, Divanach P. Bioenergetic changes in the microalgal photosynthetic apparatus by extremely high CO2 concentrations induce an intense biomass production. Physiol Plant 2008;132:338-349.
[116] Patnaik PR. Perspectives in the Modeling and Optimization of PHB Production by Pure and Mixed Cultures. Crit Rev Biotechnol 2005;25:153-171.

[117] Pfannschmidt T. Schutze K. Brost M, Oelmuller R. A Novel Mechanism of Nuclear Photosynthesis Gene Regulation by Redox Signals from the Chloroplast during Photosystem Stoichiometry Adjustment. J Biol Chem 2001;276:36125-36130.

[118] Pinto FAL. Troshina O, Lindblad P. A brief look at three decades of research on cyanobacterial hydrogen evolution. International Journal of Hydrogen Energy 2002;27:1209-1215.

[119] Porra R. The chequered history of the development and use of simultaneous equations for the accurate determination of chlorophylls a and b. Photosynth Res 2002;73:149-156.

[120] Price G. Sültemeyer D, Klughammer B. The functioning of the CO 2 concentrating mechanism in several cyanobacterial strains: a review of general physiological characteristics, genes, proteins, and recent advances. Can J Bot 1998;76:973-1002.

[121] Prince R, Kheshgi H. … photobiological production of hydrogen: potential efficiency and effectiveness as a renewable fuel. Critical Revs. in Microbiology 2005.

[122] Prince RC, Kheshgi HS. The photobiological production of hydrogen: potential efficiency and effectiveness as a renewable fuel. Crit Rev Microbiol 2005;31:19-31.

[123] Rehm B. Bacterial polymers: biosynthesis, modifications and applications. Nat Rev Microbiol 2010;8:578-592.

[124] Sakai N. Sakamoto Y. Kishimoto N, Chihara M. Chlorella strains from hot springs tolerant to high temperature and high CO2. Energy Conversion and Management 1995;36:693-696.

[125] Sakurai H, Masukawa H. Promoting R & d in photobiological hydrogen production utilizing mariculture-raised cyanobacteria. Marine Biotechnology 2007;9:128-145.

[126] Salem K, van Waasbergen LG. Photosynthetic Electron Transport Controls Expression of the High Light Inducible Gene in the Cyanobacterium Synechococcus elongatus Strain PCC 7942. Plant Cell Physiol 2004;45:651-658.

[127] Schicho RN. Ma K. Adams MW, Kelly RM. Bioenergetics of sulfur reduction in the hyperthermophilic archaeon Pyrococcus furiosus. J Bacteriol 1993;175:1823-1830.

[128] Schmitz O, G. Boison, R. Hilscher, B. Hundeshagen, W. Zimmer, F., Lottspeich HB. Molecular biological analysis of a bidirectional hydrogenase from cyanobacteria. Eur J Biochem 1995;233:266-276.

[129] Schörken U, Kempers P. Lipid biotechnology: Industrially relevant production processes. Eur J Lipid Sci Technol 2009;111:627-645.

[130] Schrader PS. Burrows EH, Ely RL. High-throughput screening assay for biological hydrogen production. Anal Chem 2008;80:4014-4019.

[131] Schriek S. Ruckert C. Staiger D. Pistorius E, Michel K-P. Bioinformatic evaluation of L-arginine catabolic pathways in 24 cyanobacteria and transcriptional analysis of genes encoding enzymes of L-arginine catabolism in the cyanobacterium Synechocystis sp. PCC 6803. BMC Genomics 2007;8:437.

[132] Schutz K. Happe T. Troshina O. Lindblad P. Leitao E. Oliveira P, Tamagnini P. Cyanobacterial H2 production , a comparative analysis. Planta 2004;218:350-359.

[133] Scott S. Davey M. Dennis J, Horst I. Biodiesel from algae: challenges and prospects. Curr Opin Biotechnol 2010;21:277-286.

[134] Sheehan J. Dunahay T. Benemann J, Roessler P. A look back at the US Department of Energy's aquatic species program—biodiesel from algae. National Renewable Energy Laboratory 1998;296.

[135] Shibata M. Ohkawa H. Katoh H. Shimoyama M, Ogawa T. Two CO~ 2 uptake systems in cyanobacteria: four systems for inorganic carbon acquisition in Synechocystis sp. strain PCC6803. Funct Plant Biol 2002;29:123-129.

[136] Shima S, Thauer RK. A third type of hydrogenase catalyzing H2 activation. Chemical Record (New York, N.Y) 2007;7:37-46.

[137] Singh J, Gu S. Commercialization potential of microalgae for biofuels production. Renewable and Sustainable Energy Reviews 2010;14:2596-2610.

[138] Singh S. Kate B, Banerjee U. Bioactive compounds from cyanobacteria and microalgae: an overview. Crit Rev Biotechnol 2005;25:73-95.

[139] Skjånes K. Lindblad P, Muller J. BioCO2–A multidisciplinary, biological approach using solar energy to capture CO2 while producing H2 and high value products. Biomol Eng 2007;24:405-413.

[140] Smith L. McCarty P, Kitanidis P. Spreadsheet method for evaluation of biochemical reaction rate coefficients and their uncertainties by weighted nonlinear least-squares analysis of the integrated Monod equation. Appl Environ Microbiol 1998;64:2044.

[141] Stal L. Poly (hydroxyalkanoate) in cyanobacteria: an overview. FEMS Microbiol Lett 1992;103:169-180.

[142] Sudesh K, Iwata T. Sustainability of biobased and biodegradable plastics. Clean 2008;36:433-442.

[143] Survase S, Bajaj I. Biotechnological production of vitamins. Food Technol Biotechnol 2006;44:381-396.

[144] Tamagnini P. Axelsson R. Lindberg P. Oxelfelt F. Wunschiers R, Lindblad P. Hydrogenases and Hydrogen Metabolism of Cyanobacteria. Microbiol Mol Biol Rev 2002;66:1-20.

[145] Ting C, Owens T. Limitations of the pulse-modulated technique for measuring the fluorescence characteristics of algae. Plant physiology 1992;100.

[146] Turner J. Sverdrup G, Mann M. Renewable hydrogen production. International Journal of Energy Research 2008;32:379-407.
[147] Turner P. Mamo G, Karlsson EN. Potential and utilization of thermophiles and thermostable enzymes in biorefining. Microb Cell Fact 2007;6:9.
[148] Vieille C, Zeikus G. Hyperthermophilic enzymes: sources, uses, and molecular mechanisms for thermostability. Microbiol Mol Biol Rev 2001;65:1-43.
[149] Vieille C, Zeikus JG. Thermozymes: identifying molecular determinants of protein structural and functional stability. Trends Biotechnol 1996;14:183-190.
[150] Vignais PM. Billoud B, Meyer J. Classification and phylogeny of hydrogenases. FEMS Microbiol Rev 2001;25:455-501.
[151] Vignais PM, Colbeau A. Molecular biology of microbial hydrogenases. Curr Issues Mol Biol 2004;6:159-188.
[152] Wang B. Li Y. Wu N, Lan C. CO 2 bio-mitigation using microalgae. Appl Microbiol Biotechnol 2008;79:707-718.
[153] Weast R, 1986. CRC handbook of chemistry and physics.
[154] Werpy T. Petersen G. Aden A. Bozell J, Holladay J. Top Value Added Chemicals From Biomass. Volume 1-Results of Screening for Potential Candidates From Sugars and Synthesis Gas. oai.dtic.mil 2004.
[155] Yoo S. Keppel C. Spalding M, Jane J. Effects of growth condition on the structure of glycogen produced in cyanobacterium Synechocystis sp. PCC6803. Int J Biol Macromol 2007;40:498-504.
[156] Zhang K. Kurano N, Miyachi S. Outdoor culture of a cyanobacterium with a vertical flat-plate photobioreactor: effects on productivity of the reactor orientation, distance setting between the plates, and culture temperature. Appl Microbiol Biotechnol 1999;52:781-786.

APPENDIX

Appendix A

Calculations

Headspace and aqueous CO_2 concentrations

Headspace CO_2 concentrations were calculated from the ideal gas law. Headspace volume of the reactors was 1.1 L, the temperature was 50°C (323.15K), pressure: 1 atm, r: 0.08206 L·atm/K·mol.

$$\frac{PV}{rt} = n \tag{1}$$

From this equation, n = 0.04148 moles of gas in the headspace. Moles of CO_2 are total moles of gas (n) multiplied by the percentage of CO_2 in the inlet gas flow. Data are shown in Table A.1. The aqueous concentration of CO_2 was calculated using the following equation:

$$x_g = \frac{P_T}{H}\rho_g \tag{3}$$

Where x_g is the mole fraction of gas in water (mole gas/mole water), P_T is total pressure (1 atm), H is Henry's constant (atm) adjusted for temperature, and ρ_g is the mole fraction of gas in air (moles gas/moles air). Henry's constant at 30°C and 50°C is 1846 atm and 2971 atm respectively [91]. The mole fraction was then converted to moles of gas per liter of water by multiplying by the formula weight (g/mole) and density of water (g/L) yielding the following concentrations (Table A.1). The following table shows the decrease in CO_2 solubility as temperature increases. The solubility at 50°C is about 38% lower than at 30°C.

Table A. 1: Comparison of aqueous CO_2 concentrations at 30°C and 50°C at given headspace CO_2 concentrations.

Temp (°C)	Headspace CO_2 concentration (%)	Headspace CO_2 concentration (moles)	Aqueous CO_2 concentration (mol/L)
50	0.036%	1.493×10^{-4}	6.73×10^{-6}
50	5.00%	2.07×10^{-3}	9.35×10^{-4}
50	10.00%	4.15×10^{-3}	1.87×10^{-3}
50	20.00%	8.30×10^{-3}	3.74×10^{-3}
30	0.036%	1.49×10^{-4}	1.08×10^{-5}
30	5.00%	2.07×10^{-3}	1.50×10^{-3}
30	10.00%	4.15×10^{-3}	3.01×10^{-3}
30	20.00%	8.30×10^{-3}	6.02×10^{-3}

Carbonate equilibrium calculations

The carbonate system includes the following species in equilibrium:

$$CO_{2(aq)} + H_2O <-> H_2CO_3 <-> H^+ + HCO_3^- <-> 2H^+ + CO_3^{2-} \quad (4)$$

This equilibrium is primarily controlled by pH. At pH 7.8 HCO_3^- is the predominant carbonate species. The hydration rate constant (K_h) at pH 7.85 is 0.0356 [43], and the equilibrium can then be defined as:

$$K_h = \frac{[H_2CO_3]}{[CO_2]} \quad (5)$$

Given K_h is 0.0356 and known aqueous CO_2 concentrations, the concentration of H_2CO_3 can be determined as follows: $[H_2CO_3] = [CO_2] \times 0.0356$. H_2CO_3 concentrations were calculated using this relationship to verify that the amount was small enough to be considered insignificant. The concentrations are shown in Table A.2.

Table A. 2. Equilibrium concentration of carbonate species

CO_2 (%)	CO_2 in headspace (moles)	Aqueous CO_2 (mol/L)	H_2CO_3 (mol/L)	HCO_3 (mol/L)	CO_3^{2-} (mol/L)
0%	$1.493x10^{-4}$	6.73×10^{-6}	2.33×10^{-7}	2.15×10^{-4}	7.63×10^{-7}
5%	2.074×10^{-3}	9.35×10^{-4}	3.24×10^{-5}	2.99×10^{-2}	1.06×10^{-4}
10%	$4.148x10^{-3}$	1.87×10^{-3}	6.47×10^{-5}	5.97×10^{-2}	2.12×10^{-4}
20%	$8.296x10^{-3}$	3.74×10^{-3}	1.29×10^{-4}	1.19×10^{-1}	4.24×10^{-4}

H_2CO_3 is diprotic and thus has two dissociation constants and forms two products according to the following reactions:

$$H_2CO_3 \longleftrightarrow HCO_3^- + H^+ \quad K_{a1} = 2.5 \times 10^{-4} \; pK_{a1}=3.45 \tag{6}$$

$$HCO_3^- \longleftrightarrow CO_3^{2-} + H^+ \quad K_{a2} = 5.61 \times 10^{-11} \; pK_{a2}=10.25 \tag{7}$$

However, as stated previously, very little H_2CO_3 exists in solution at pH 7.8, therefore the equation can be rewritten as:

$$CO_2 + H_2O \longleftrightarrow HCO_3^- + H^+ \tag{8}$$

This K_a is $5.19x\ 10^{-7}$ at 50°C (The above K_a and pK_a values are taken from the CRC Handbook of Chemistry and Physics, 66th edition, 1986 [153]) From this equation and K_a value, the equilibrium relationship can be defined as:

$$K_a = \frac{[HCO_3^-][H^+]}{[CO_{2(aq)}]} \tag{9}$$

Given K_a = 5.19 x 10^{-7}, $[H^+]$ = 1.58 x 10^{-8} at pH 7.8, and the concentration of CO_2 dissolved in the media, the above relationship can be used to determine the concentration of HCO_3^- (see Table A. 2).

Carbon assimilation rates

Biomass productivity was calculated by subtracting the initial dry weight from the final dry, divided by the number of days the cultures were grown. Sample calculation for 20% CO_2:

$$\frac{0.740\,{}^{mg}/_{ml} - 0.020\,{}^{mg}/_{ml}}{8d} = 0.090 mg \cdot ml^{-1} \cdot d^{-1} \quad (10)$$

The CO_2 fixation rate (P_{CO2}) is 1.88 x biomass productivity (P). This equation is derived from the molecular formula for microalgae biomass [152]. For the above biomass productivity, the CO_2 fixation rate is 0.169 mg ml^{-1} d^{-1}. Data for all conditions are shown in Table 3.2.

Modeling productivity

The productivity was modeled based on the following expression for the net rate of cell growth, which is equal to the biomass productivity:

$$P = \frac{\mu_{max} S}{K + S} X - bX \quad (11)$$

where P is the productivity (mg ml^{-1} d^{-1}), μ_{max} is the maximum biomass productivity (mg ml^{-1} d^{-1}), K is the half-saturation coefficient (%), S is the substrate concentration (%), X is the concentration of active biomass, and b is the

endogenous decay coefficient. Analysis of the model with decay coefficients ranging from 0.01-1 made no difference in the model fit and therefore the decay term was not included in the final model (Figure 3.3) and the equation can be simplified to:

$$P = \frac{\mu_{max} S}{K + S} X \quad (12)$$

Photosynthetic efficiency

Light was supplied from full spectrum compact fluorescent bulbs (Sylvania, Danvers, MA USA) at an intensity of 180 μmol m^{-2} s^{-1}. With PAR accounting for about 48% of total radiation [133], the photon flux density is 86 μmol photons m^{-2} s^{-1}. The total μmol m^{-2} s^{-1} of photons was converted to moles of photons m^{-2} s^{-1} and multiplied by Avogadro's number and by the illuminated surface area of the reactor (0.000123 m^2) to yield a total of 6.332 x 10^{16} photons s^{-1}. Over the course of the 9-day experiment the total was 4.23 x 10^{24} photons. With 20% CO_2 a maximum of 3.096 g of CO_2 was fixed which contains 4.22 x 10^{22} molecules of CO_2 based on Avogadro's number. 8 photons are required to fix one CO_2 [133] thus yielding an overall efficiency of 7.98%.

Bioreactor mass balance

The overall bioreactor carbon balance was described by the following equation:

$$V\frac{dC}{dt} = C_{in}Q - C_{out}Q - X_aV - r_cV = 0 \quad (13)$$

Where V is the reactor volume, C is the carbon concentration (mg ml^{-1}) in CO_2 stream, Q is the gas flow rate (mg min^{-1}), X_a is the substrate dependent biomass accumulation (mg ml^{-1} min^{-1}), and r_c is carbon accumulation in the media due to carbonate equilibrium (mg ml^{-1}). There was no inlet or outlet biomass flow so the biomass accumulation can be defined by equation 12. At steady state the mass balance equation simplifies to:

$$C_{in}\frac{Q}{V} - X_a - r_c = C_{out}\frac{Q}{V} \quad (14)$$

This equation was multiplied by the total amount of time (9 days) to obtain the total amount of CO_2 (mg ml^{-1}) in each component. The amount of CO_2 in the media was calculated based on the carbonate equilibrium (see table A.1). The amount of carbon from CO_2 sequestered in the biomass and media was calculated by two different approaches. The first approach was based on the total carbon analysis of the biomass and media. The amount of carbon in the biomass and media determined by total carbon analysis was subtracted from the total amount

of CO_2 entering the reactor over the 9-day experiment to determine the amount of carbon exiting the bioreactor.

The second approach was to calculate the total amount of carbon fixed based on the CO_2 fixation rate (equation 3.4) and the carbon in the media from the carbonate equilibrium calculations (Table 3.2). These values were then subtracted from the total carbon entering the bioreactor to determine the total amount of CO_2 out. The calculated CO_2 out values compared favorably with the average GC measurements (Table A. 3). The calculations based on the total carbon analysis were closest with a difference of only 0.63-1.32% from the GC measurements (Table A. 4). However, the standard deviations of the GC measurements were large enough that the differences between the inlet and outlet are not statistically significant (Table A. 2).

Table A. 3: Comparison of mass balance calculations based on total carbon analysis with calculations based on CO_2 fixation rates and carbonate equilibrium. Note that atmospheric levels were not calculated because outlet CO_2 concentrations were below the detection limit of the GC.

	From total C analysis				From CO_2 fixation rate and carbonate equilibrium			
Percent CO_2	CO_2 in (mg/ml)	CO_2 in biomass mg/ml	CO_2 in media mg/ml	CO_2 out (mg/ml)	CO_2 in biomass mg/ml	CO_2 in media mg/ml	CO_2 out (mg/ml)	Difference in CO_2 out between methods (mg/ml)
5%	31.34±9.88	0.93±0.04	1.36±0.00	29.05±9.88	1.05±0.43	1.360	28.71±9.89	0.337
10%	60.61±11.94	1.19±0.07	2.14±0.45	57.28±11.95	1.13±0.20	2.718	56.75±11.95	0.527
20%	101.50±5.08	1.29±0.05	1.64±0.32	98.57±5.09	1.43±0.11	5.437	94.51±5.08	4.061

Table A. 4: Difference in CO_2 outlet concentrations based on GC measurements and calculated concentrations. *Based on total carbon analysis.

Percent CO_2	Measured % CO_2 in	Calculated % CO_2 out	Average GC measurements	Difference between calculated and measured	CO_2 Consumed*
5%	4.89±0.42%	4.63±0.02%	4.37±0.29%	0.63±0.51%	0.37±1.62%
10%	10.45±0.39%	9.45±0.02%	8.68±1.24%	1.32±1.30%	0.55±2.05%
20%	20.31±0.51%	19.42±0.01%	19.05±2.00%	0.95±2.06%	0.58±1.00%